SUPPORTING INFORMATION

^{109}Ag NMR Chemical Shift as a Descriptor for Brønsted Acidity from Molecules to Materials

Colin Hansen[‡, a], Scott R. Docherty[‡, a], Weicheng Cao[a], Alexander V. Yakimov[a] and Christophe Copéret[*, a]

[a]ETH Zürich, Department of Chemistry and Applied Biosciences, Vladimir Prelog Weg 1-5, ETH Zürich, CH-8093 Zurich, Switzerland

---

Contents

S1 General Considerations

Materials

All operations were performed under an argon atmosphere in an M. Braun glove box or using standard Schlenk techniques. Tetrahydrofuran (THF) was dried via distillation from purple Na^0/benzophenone. Dry deuterated Benzene (C_6D_6) was obtained via vacuum distillation from purple Na^0/benzophenone. Dry deuterated Chloroform ($CDCl_3$) was obtained via vacuum distillation from CaH_2. Dichloromethane (CH_2Cl_2) was dried using a MB SPS 800 solvent purification system where columns used for purification were packed with activated alumina. Pentane and Toluene (C_7H_8) were dried using a MB SPS 800 solvent purification system where columns used for purification were packed with activated alumina. Diethyl ether was dried using a MB SPS 800 solvent purification system where columns used for purification were packed with activated alumina. Dioxane ($C_4H_8O_2$) was vacuum transferred from purple Na^0/benzophenone. Hexamethyldisiloxane (HMDSO) was vacuum transferred from CaH_2. All solvents were further degassed via three freeze-pump-thaw cycles and stored over 4 Å molecular sieves after being transferred to a glove box. Ag_2O was purchased from Sigma Aldrich (≥99.99% trace metal basis) and used as received. $MgMes_2(thf)_2$, IMesHCl (*1,3-Bis(2,4,6-trimethylphenyl)imidazolium chloride*) and $NaOSi(O^tBu)_3$ were prepared according to literature procedures. [1-3] SIMesHCl (*1,3-Bis(2,4,6-trimethylphenyl)imidazolinium chloride*) was purchased from Sigma Aldrich (95%) and used as received. BHT (Butylated hydroxytoluene, 2,6-di-*tert*-butyl-4-methylphenol, > 99.0 %) was purchased from Fluka-Chemie AG, and was sublimed (ca. 10^{-3} mbar, 65 °C) prior to use. Lithium bis(trimethylsilyl)amide (Li(HMDS), 97%) was purchased from Sigma Aldrich, and used after recrystallisation from pentane. Methylmagnesium bromide (MeMgBr, 3.0 M in diethyl ether) was purchased from Acros organics and used as received. Sodium *tert*-butoxide (NaO^tBu, 98 %) was purchased from Acros Scientific and used as received. ^{15}N-labelled pyridine (^{15}N-Py), purchased from CortecNet, was dried over CaH_2 for at least 72 h prior to use. Ferrocene was purchased from Sigma Aldrich and sublimed prior to use.

Silica (Aerosil Degussa, 200 $m^2 g^{-1}$) was compacted with deionized water, dried at 100 °C for 7 days, crushed and sieved (250−400 µm) for easier handling. γ-Al_2O_3 (SASOL® Puralox SBa-200, 216 $m^2 g^{-1}$) was compacted with deionized water, dried at 100 °C for 7 days, crushed and sieved (250−400 µm) for

easier handling. Quantification of the –OH density of the oxide supports was performed through reaction of $[Mg(CH_2Ph)_2(THF)_2]$ with a known amount of the oxide. The amount of toluene liberated was quantified by NMR in C_6D_6 using ferrocene as an internal standard. For this purpose, a recycle delay (D_1) of 58 seconds was used.

Characterization

Solution NMR spectra were recorded at room temperature (298 K) on either a Bruker 500 MHz solution state spectrometer equipped with a broadband probe or a broadband cryoprobe (^{13}C, ^{1}H). ^{1}H and ^{13}C chemical shifts are referenced relative to residual solvent peaks.[4] Chemical shifts are reported in parts per million (ppm). Where appropriate, signal multiplicity has been condensed to a single letter format, i.e.: s=singlet, d=doublet, t=triplet, q=quartet, m=multiplet. Solvent signals are denoted accordingly. Unless otherwise specified, ^{13}C spectra were recorded using 2048 scans, and ^{1}H spectra were acquired using 64 scans.

The Small Molecule Crystallography Center (SMoCC) of ETH Zürich provided the equipment for single crystal structure determination. XRD data was recorded on either a Rigaku XtaLAB Synergy-S single crystal diffractometer or a Bruker APEX-II CCD diffractometer. Suitable crystals were selected and tip-mounted on a MiTeGen Pin covered with Paratone Oil. Using Olex2[5], the structure was solved with the SHELXT[6] structure solution program and refined with the SHELXL[7] refinement package using CGLS minimization. Elemental Analysis was provided by the in-house Molecular and Biomolecular Analysis Service (MoBiAS) of ETH Zürich and Analytisches Labor Pascher in Remagen, Germany. DFT calculations were performed on the ETH Euler cluster using Gaussian 09.[8] Nitrogen physisorption isotherms were measured on a on a BEL JAPAN BELSORP-mini apparatus. The specific surface area of the oxide supports were determined from nitrogen (N_2) physisorption isotherms (−196 °C) and application of the Brunauer−Emmett−Teller (BET) method.[9]

Infrared (IR) spectra of the molecular compounds were collected under inert atmosphere using a Bruker Alpha spectrometer in attenuated total reflectance (ATR) mode, equipped with a diamond ATR module (deuterated triglycine sulfate (DTGS) detector, 2 cm^{-1} spectral resolution, 4000-400 cm^{-1}, average of 32 scans). Transmission-IR were recorded on Bruker FT-IR Alpha spectrometer equipped with RockSolid interferometer, DTGS (deuterated triglycine sulfate) detector, SiC globar source; solid samples were mounted on a magnetic pellet holder. A typical experiment consisted of the measurement of transmission in 16 scans in the region from 4000 to 400 cm^{-1}. Spectra were analyzed using ThermoScientific™ OMNIC™ 8 Software. Spectra of silica-supported samples are normalized to the Si-O-Si overtone peak maximum at 1868 cm^{-1}.

General procedure treatment of oxide with ^{15}N pyridine.

Prior to dosing, ^{15}N-py was degassed using 3 successive freeze-pump-thaw cycles. In a typical ^{15}N-Py dosing experiment, the vessel containing the material was evacuated to 10^{-5} mbar, after which the material was exposed for 20 min at room temperature to a saturated vapor pressure of ^{15}N-Py, followed by evacuation at room temperature at ca. 10^{-5} mbar for 15 min. After dosing, the material was stored in an argon-filled glovebox prior to further analysis.

Solid state NMR:

Solid State ^{13}C-^{1}H cross-polarization magic-angle spinning (CP-MAS) NMR experiments were carried out on a Bruker 600 MHz (14.1 T) spectrometer using a 3.2 mm low-temperature HX probe at 100 K. For these experiments, samples were packed in 3.2 mm sapphire rotors, and spinning speeds of either 7 kHz or 8 kHz were used. For DNP experiments, all samples were prepared in an argon-filled glove box by incipient wetness impregnation with 16 mM TEKPol solution in d_3/d_8-toluene (10:90 vol%, ca. 40 µL for 30 mg sample). For DNP, the probe was coupled to a 395 GHz gyrotron microwave source with an output power of 6−10 W. The reference used for the static magnetic field was set by the ^{1}H resonance of toluene at 2.3 ppm.[4] A ^{1}H saturation-recovery experiment with the microwave irradiation turned on was used to measure the DNP buildup time (T_{DNP}). DNP Enhancements were measured using the ^{1}H resonance of the solvent. ^{13}C-^{1}H CP-MAS experiments were recorded by setting the recycle delay to 1.3(T_{DNP}) and the ^{1}H excitation and decoupling radio-frequency (RF) fields to 100 kHz. A contact pulse of 3 ms was used. All cross-polarization parameters were optimized to fulfil the Hartmann−Hahn condition under MAS to obtain the optimal experimental efficiency. For ^{13}C NMR experiments, processing was performed in TopSpin®.[10, 11]

Solid State ^{15}N-^{1}H cross-polarization magic-angle spinning (CP-MAS) NMR experiments were carried out on a Bruker 600 MHz (14.1 T) spectrometer using a 3.2 mm low-temperature HX probe at 100 K. For these experiments, samples were packed in 3.2 mm sapphire rotors, and spinning speeds of either 8 kHz or 11 kHz were used. For DNP experiments, all samples were prepared in an argon-filled glove box by incipient wetness impregnation with either 16 mM TEKPol solution in 1,1,2,2-tetrachloroethane (TCE, ca. 40 µL for 30 mg sample), or 16 mM TEKPol solution in d_3/d_8-toluene (10:90 vol%, ca. 40 µL for 30 mg sample). For DNP experiments, the probe was coupled to a 395 GHz gyrotron microwave source with an output power of 6−10 W. The reference used for the static magnetic field was set by the ^{1}H resonance of TCE at 6.9 ppm[12] or toluene (Ar-CH_3) at 2.3 ppm.[4] A ^{1}H saturation-recovery experiment with the microwave irradiation turned on was used to measure the DNP buildup time (T_{DNP}). DNP Enhancements (ε_H) were measured using the ^{1}H resonance of the solvent. ^{15}N-^{1}H CP-MAS

experiments were recorded by setting the recycle delay to 1.3(T_{DNP}) and the ^{1}H excitation and decoupling radio-frequency (RF) fields to 100 kHz. A contact pulse of 3 ms was used. All cross-polarization parameters were optimized to fulfil the Hartmann−Hahn condition under MAS to obtain the optimal experimental efficiency. For ^{15}N NMR experiments, processing was performed in TopSpin® and fitting was subsequently performed in DMfit.[6] Fitting of spectra was performed over the entire manifold of spinning sidebands.[13-15]

DNP-enhanced solid State ^{29}Si-^{1}H cross-polarization magic-angle spinning (CP-MAS) NMR experiments were carried out on a Bruker 600 MHz (14.1 T) spectrometer using a 3.2 mm low-temperature HX probe at 100 K. For these experiments, the sample was packed in a 3.2 mm sapphire rotor, and a spinning speed of 10 kHz was used. The sample was prepared in an argon-filled glove box by impregnation with 16 mM TEKPol solution in 1,1,2,2-tetrachloroethane (TCE, ca. 40 µL for 30 mg sample). The probe was coupled to a 395 GHz gyrotron microwave source with an output power of 6−10 W. The reference used for the static magnetic field was set by the ^{1}H resonance of TCE at 6.9 ppm.[12] A ^{1}H saturation-recovery experiment with the microwave irradiation turned on was used to measure the DNP buildup time (T_{DNP}). DNP Enhancements (ε_H) were measured using the ^{1}H resonance of the solvent. ^{29}Si-^{1}H CP-MAS experiments were recorded by setting the recycle delay to 1.3(T_{DNP}) and the ^{1}H excitation and decoupling radio-frequency (RF) fields to 100 kHz. A contact pulse of 2 ms was used. All cross-polarization parameters were optimized to fulfil the Hartmann−Hahn condition under MAS to obtain the optimal experimental efficiency. For ^{29}Si NMR experiments, processing was performed in TopSpin® and fitting was subsequently performed in DMfit.[6] Fitting of individual peaks was performed using Gaussian-Lorentzian peak shape on the isotropic peaks.[10, 11]

DNP-enhanced solid state ^{109}Ag NMR experiments were carried out at ≈100 K on a Bruker Avance III spectrometer operating at 9.4 T and a 263 GHz Klystron microwave source with an output power of approximately 10 W. The 3.2 mm HX low temperature MAS probe was used with sapphire rotors. For the ^{1}H-^{109}Ag CPECHO (CP-t-180pulse-t-acquire) experiments, the CP contact time was 25 ms and the ^{1}H decoupling power was 0. Delay times were set to be 1.3 times the T_1 obtained from saturation recovery experiments of the protons of the solvent. The ^{109}Ag chemical shift is referenced to $AgSO_3CH_3$ (87.2 ppm) which is, in turn, referenced with respect to a 9 M aqueous solution of $AgNO_3$ (0 ppm).[16] DNP Enhancements (ε_H) were measured using the ^{1}H resonance of the solvent. The processing of ^{109}Ag NMR spectra was performed in TopSpin® and fitting was subsequently performed in DMfit.[6] Fitting of spectra was performed over the entire manifold of spinning sidebands.[10, 11]

S2 Synthetic Methods

Synthesis of SIMesAgCl (A-Cl)

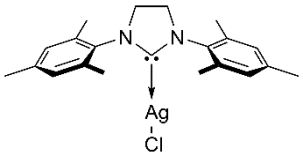

The Synthesis was adapted from literature procedures.[17-20] To a 250 ml round bottom flask was added SIMesCl (1,3-Bis(2,4,6-trimethylphenyl)imidazolinium chloride) (2.0 g, 5.84 mmol) followed by Dichloromethane (ca. 50 mL). To the solution was added Ag_2O (0.68 g, 2.95 mmol). The mixture was stirred at reflux for 22 h. After filtering the reaction mixture through Celite® the clear light-yellow solution was taken to dryness. The crude product was dissolved in Dichloromethane and layered with double the amount of Pentane for recrystallization in the freezer (-35°C) from which white needle-like crystals were obtained in a yield of 50% (1.32 g, 2.93 mmol). **^{1}H-NMR** (25°C, 500 MHz, $CDCl_3$): δ 6.94 (s, 4H, Ar-*H*), δ 4.00 (s, 4H, backbone C_2H_4), δ 2.30 (s, 6H, p-CH_3), δ 2.29 (s, 12H, o-CH_3). (25°C, 500 MHz, C_6D_6): δ 6.64 (s, 4H, Ar-*H*), δ 2.93 (s, 4H, backbone C_2H_4), δ 2.05 (s, 6H, p-CH_3), δ 1.98 (s, 12H, o-CH_3). **^{13}C-NMR** (25°C, 125.7 MHz, C_6D_6):138.4, 135.0, 129.7, 50.2, 20.7, 17.4.

Synthesis of SIMesAgMes (A-Mes)

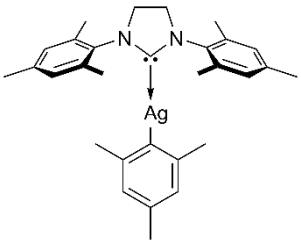

To an amber vial was added SIMesAgCl (**A-Cl**) (52.9 mg, 0.12 mmol) followed by THF (ca. 5 mL). To the suspension was added $Mes_2Mg(THF)_2$ (23.2 mg, 0.06 mmol) in THF (ca. 3 mL). The mixture was stirred for 24 h before 3 drops of Dioxane were added to precipitate $[MgX_2(C_4H_8O_2)]_n$. After filtering the reaction mixture through Celite® the solution was taken to dryness. The crude product was dissolved in toluene (ca. 5 mL) for recrystallization in the freezer (-35°C) from which colorless/transparent cubic crystals were obtained in a yield of 64% (40.0 mg, 0.075 mmol). XRD quality crystals (cubes) were obtained from recrystallisation in toluene. **^{1}H-NMR** (25°C, 500 MHz, C_6D_6): δ 6.99 (s, 2H, Ar-*H (Ag-Mesityl)*), δ 6.76 (s, 4H, Ar-*H (NHC-Mes)*), δ 3.05 (s, 4H, backbone C_2H_4), δ 2.33 (s, 9H, Ar-CH_3 (4-position)), δ 2.16 (s, 12H, o-CH_3 (2,6-position) *(NHC)*), δ 2.11 (s, 6H, o-CH_3 (2,6–position) *Ag-Mesityl)*). **^{13}C-NMR** (25°C, 125.7MHz, C_6D_6): 213.8 (N-*C*-N, pseudo-*dd* ($^1J_{^{13}C-^{109}Ag}$ = 130 Hz; $^1J_{^{13}C-^{107}Ag}$ = 113 Hz)), 146.0, 138.0, 135.9, 135.6, 132.6, 129.3, 124.2, 50.1, 29.3, 21.3, 20.6, 17.7. **IR** (ATR-IR) [cm^{-1}] 3050-2800 (m, C-H str.), 2727 (w, Mes C-H str.), 1607 (w, arom. C-C str.), 1484/1443 (m, arom. C-C str.), 1259 (m, C-N str.), 1010 (s, C-N str.), 844/614/571/530 (m). **Elemental Analysis** C: 67.53% H: 6.93% N: 5.28% (Calc.: 67.54% / 6.99% / 5.25%).

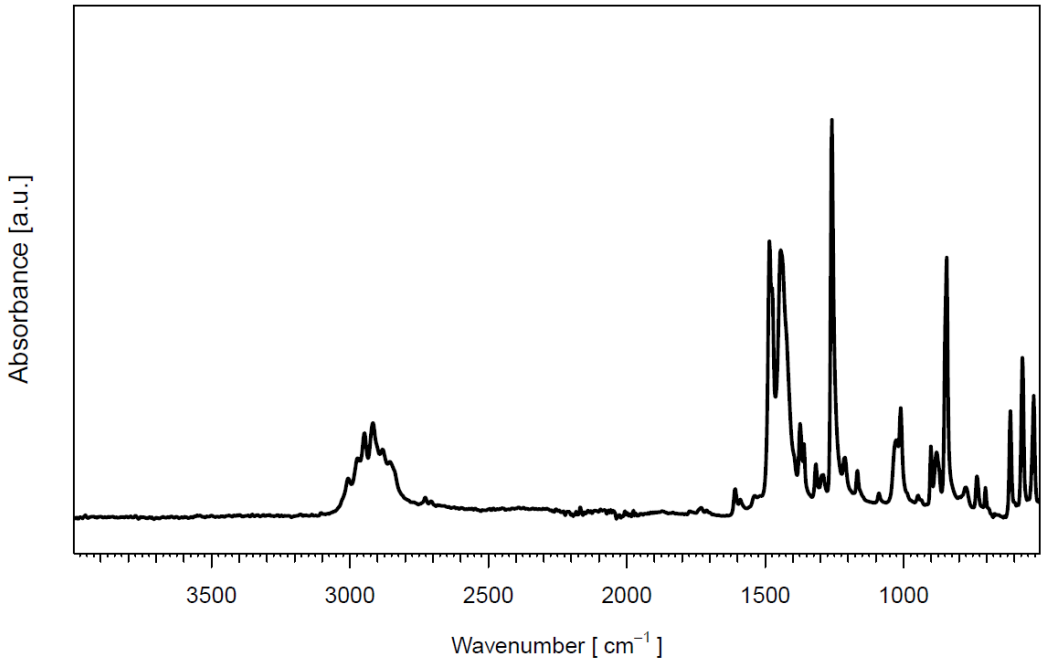

Figure S 1. ATR-IR spectrum of SIMesAgMes (**A-Mes**) (264 scans)

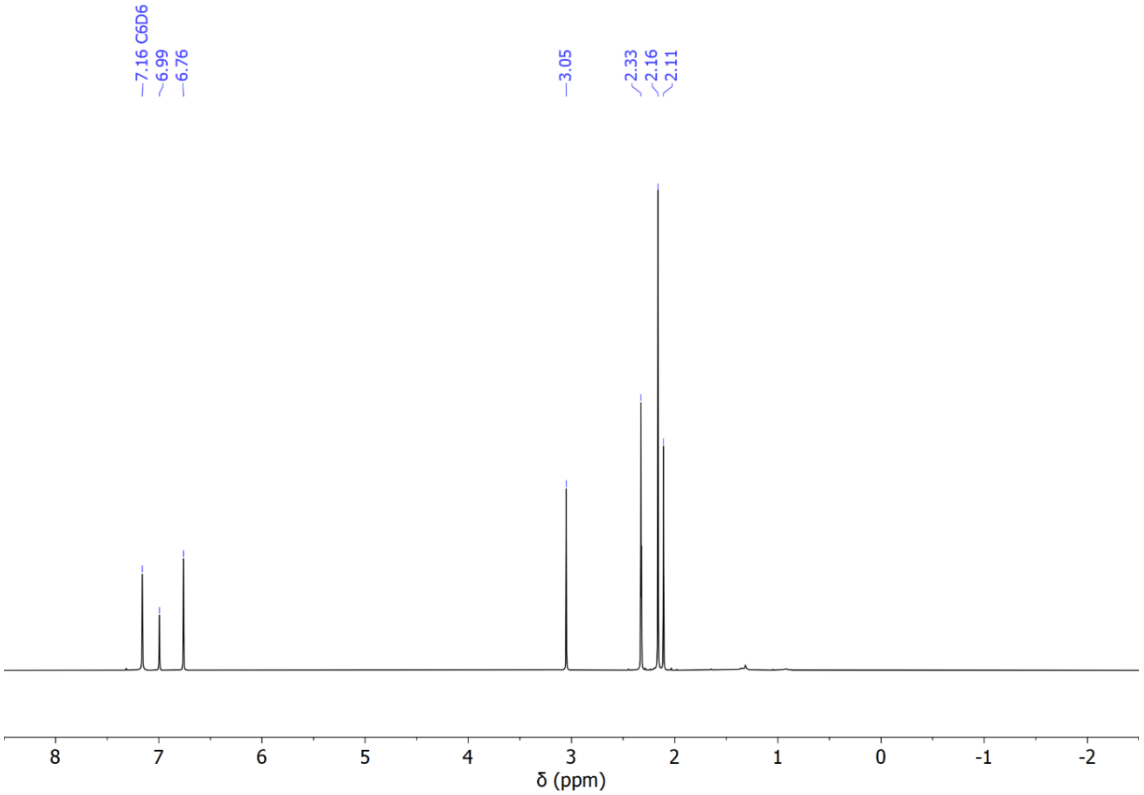

Figure S 2. ^{1}H NMR spectrum of SIMesAgMes (**A-Mes**) recorded in C_6D_6 (500 MHz, 25°C).

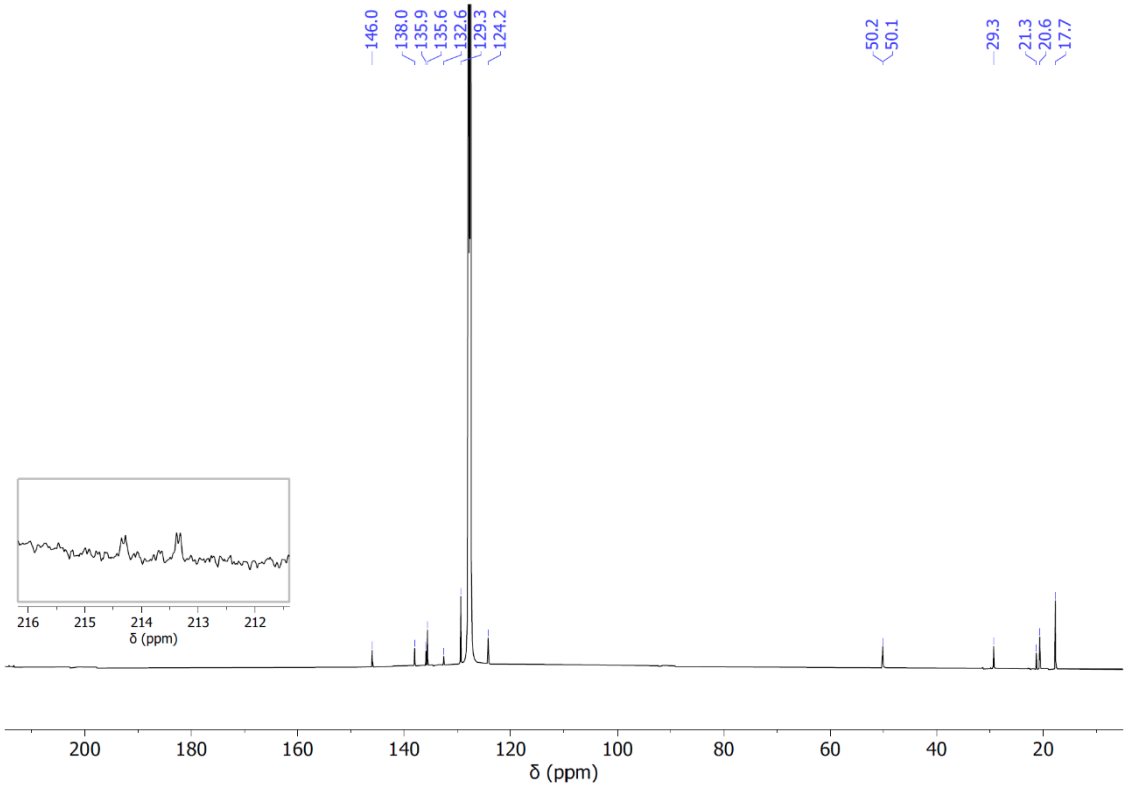

Figure S 3. ^{13}C NMR spectrum of SIMesAgMes (**A-Mes**) recorded in C_6D_6 (125.7 MHz, 25°C). Zoomed region shown in inset shows coupling of carbene carbon to both isotopes of silver ($^{1}J_{^{13}C\text{-}^{109}Ag}$ = 130 Hz; $^{1}J_{^{13}C\text{-}^{107}Ag}$ = 113 Hz)

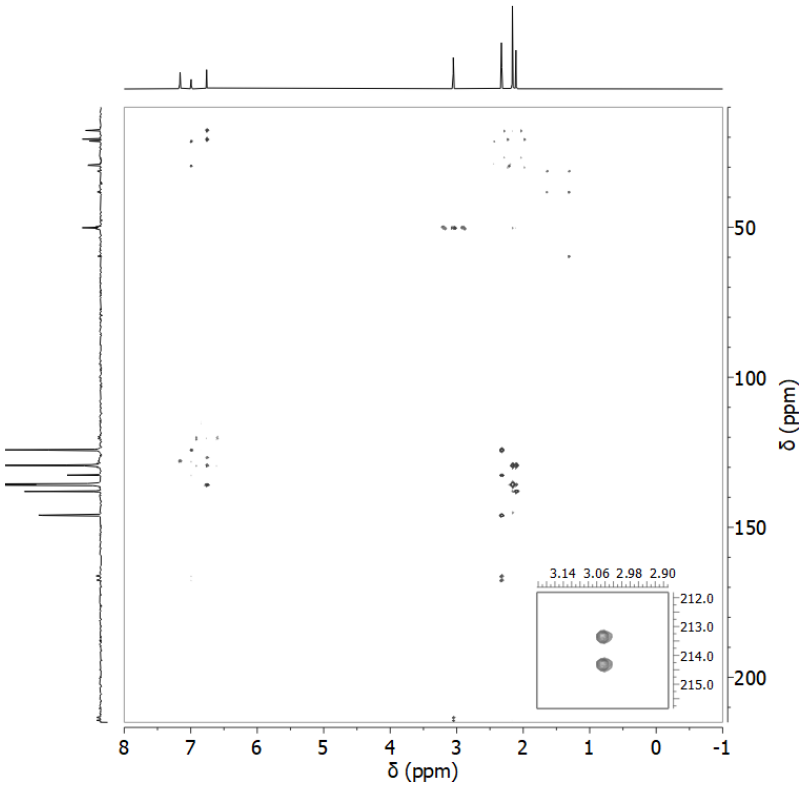

Figure S 4. SIMesAgMes (**A-Mes**) ^{1}H-^{13}C HMBC (^{1}H: 500 MHz, ^{13}C: 125.7 MHz, C_6D_6, 298 K), inset shows region of interest containing carbene splitting.

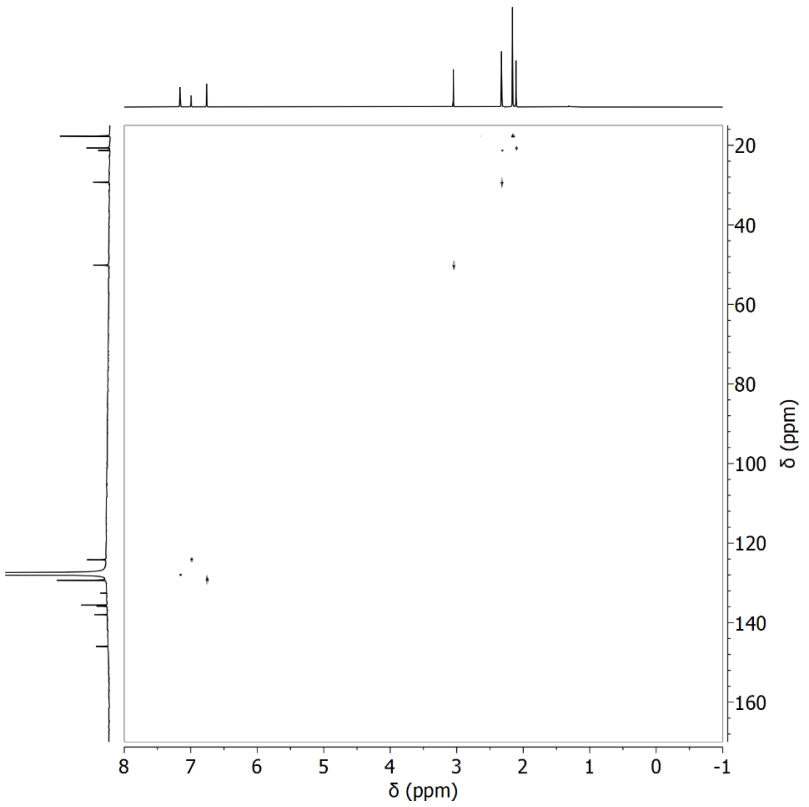

Figure S 5. SIMesAgMes (**A-Mes**) ^{1}H-^{13}C HSQC (^{1}H: 500 MHz, ^{13}C: 125.7 MHz, C_6D_6, 298 K)

Synthesis of SIMesAgO^{t}Bu (A-OtBu)

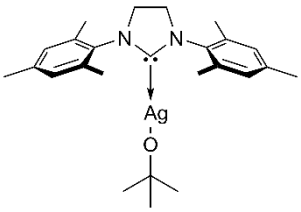

To an amber vial was added SIMesAgCl (**A-Cl**) (100.2 mg, 0.22 mmol) followed by THF (ca. 5 mL). To the suspension was added NaO^{t}Bu (21.5 mg, 0.22 mmol) in THF (ca. 3 mL). The mixture was stirred for 2h. After filtering the reaction mixture through Celite® the solution was taken to dryness, leaving a glass like substance on the walls of the vial. The crude product was dissolved in toluene, filtered, dried, and finally washed with pentane to obtain a yield of 53% (57 mg, 0.12 mmol). Despite trying different solvents/techniques, XRD-quality crystals of SIMesAgO^{t}Bu have not been obtained (The powdered product nevertheless fulfilled purity requirements for further use in ^{109}Ag NMR). **^{1}H-NMR** (25°C, 500 MHz, C_6D_6): δ 6.70 (s, 4H, Ar-*H*), δ 2.97 (s, 4H, backbone C_2H_4), δ 2.09 (s, 6H, p-CH_3), δ 2.03 (s, 12H, o-CH_3), δ 1.35 (s, 9H, -CH_3). **^{13}C-NMR** (25°C, 125.7 MHz, C_6D_6): 208.2 (N-*C*-N, *d* ($^1J_{^{13}C-^{109/107}Ag}$ = 217 Hz), 138.2, 135.3, 129.6, 67.9, 50.1, 34.9, 20.7, 17.5, 13.9. **IR** (ATR-IR) [cm^{-1}] 3050-2800 (m, C-H str.), 2733 (w, Mes C-H str.), 1607 (w, arom. C-C str.), 1489/1452 (s, arom. C-C str.), 1269 (s, C-O str.), 1187 (s, C-N str.), 1012/957/848/571(m). **Elemental Analysis** C: 60.87% H: 7.34% N: 5.65% (Calc.: 61.60% / 7.24% / 5.75%).

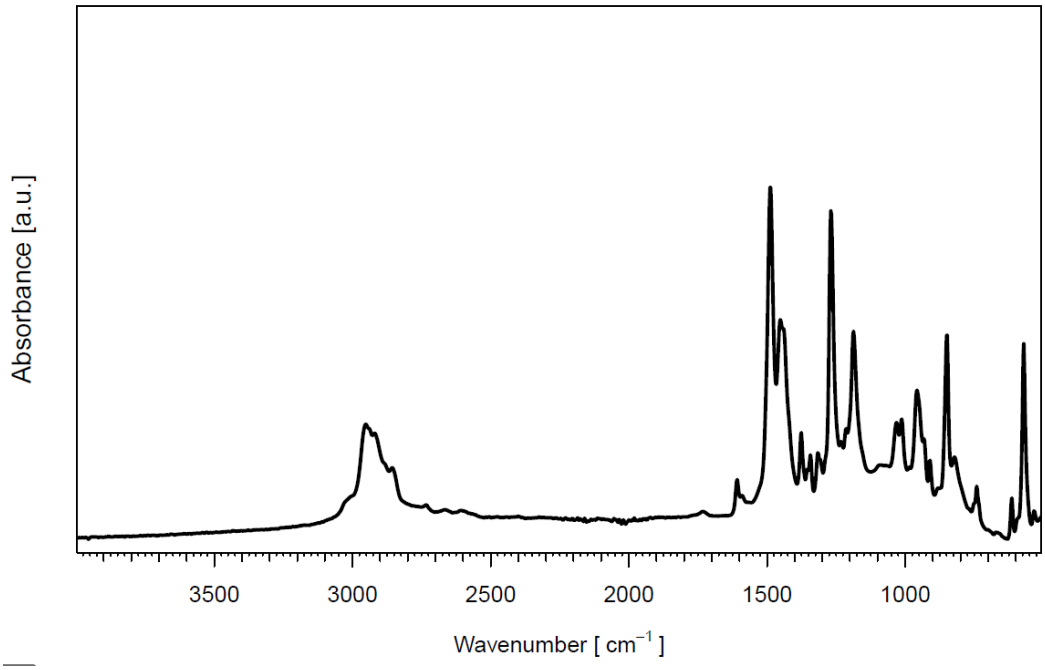

Figure S 6. ATR-IR spectrum of SIMesAgO^{t}Bu (**A-OtBu**) (264 scans)

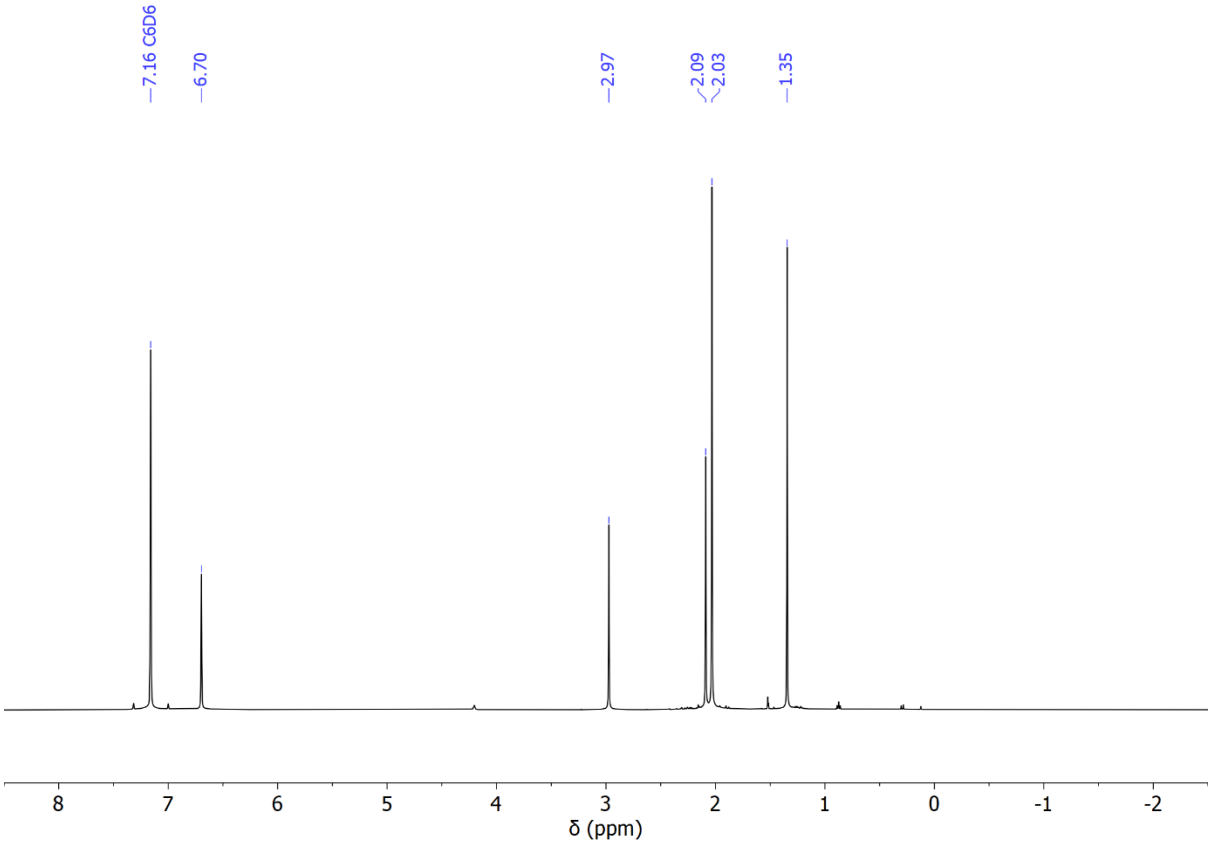

Figure S 7. ^{1}H NMR spectrum of SIMesAgO^{t}Bu (**A-OtBu**) recorded in C_6D_6 (500 MHz, 25°C).

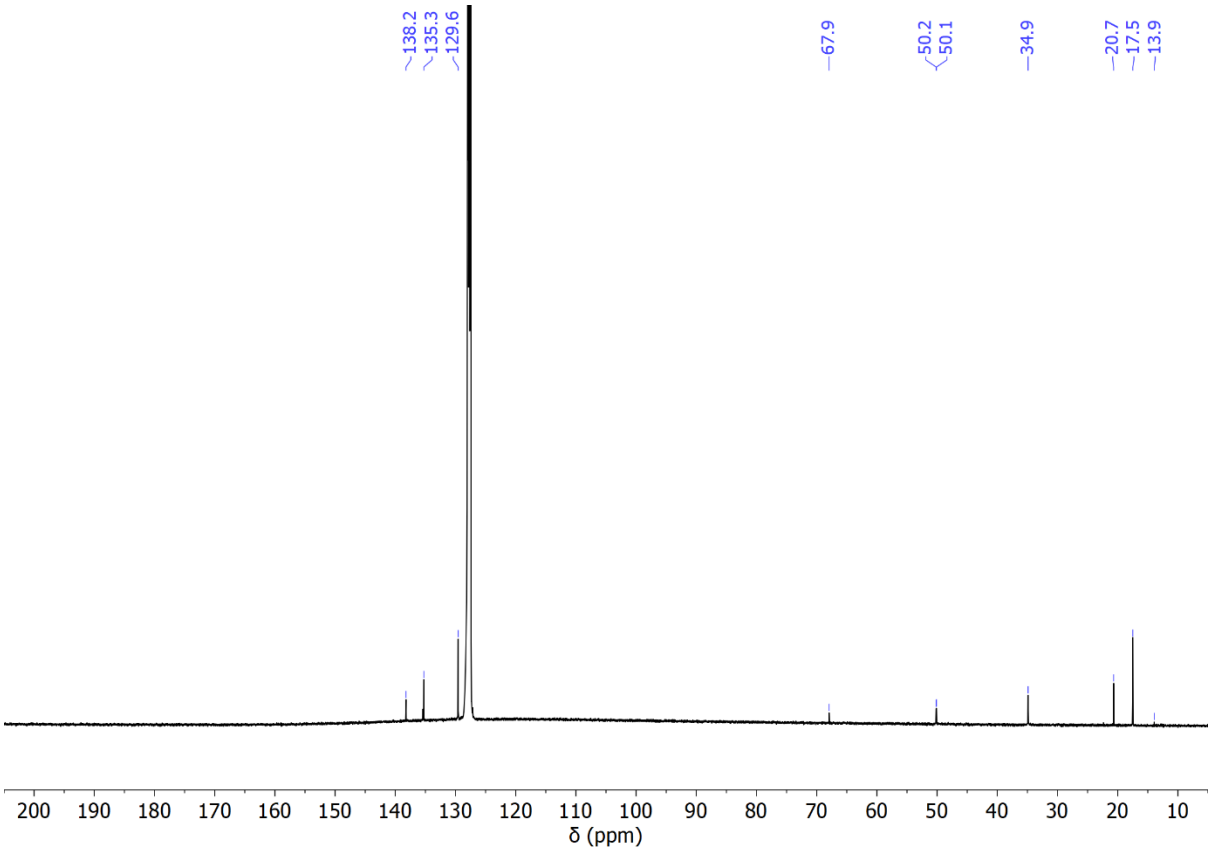

Figure S 8. ^{13}C NMR spectrum of SIMesAgO^{t}Bu (**A-OtBu**) recorded in C_6D_6 (125.7 MHz, 25°C).

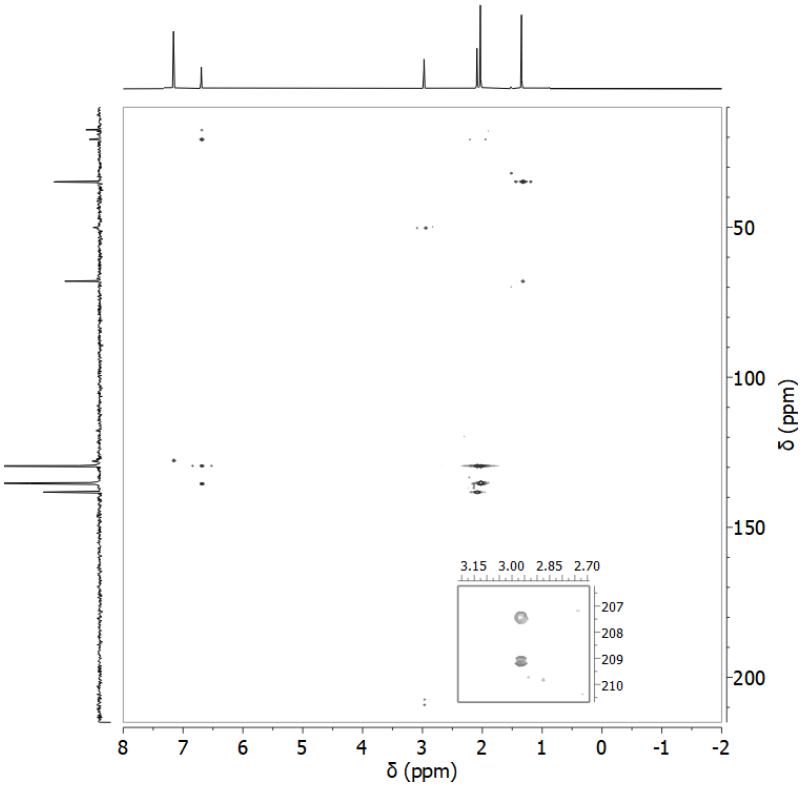

Figure S 9. SIMesAgO^{t}Bu (**A-OtBu**) ^{1}H-^{13}C HMBC (^{1}H: 500 MHz, ^{13}C: 125.7 MHz, C_6D_6, 298 K), inset shows region of interest containing carbene splitting.

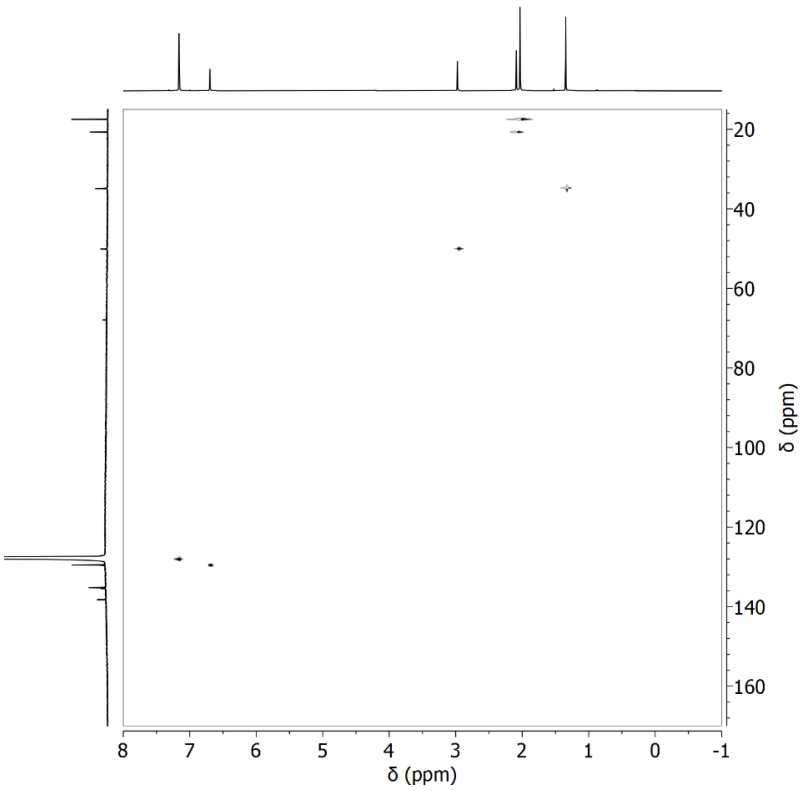

Figure S 10. SIMesAgO^{t}Bu (**A-OtBu**) ^{1}H-^{13}C HSQC (^{1}H: 500 MHz, ^{13}C: 125.7 MHz, C_6D_6, 298 K)

Synthesis of SIMesAgOSi(O^{t}Bu)$_3$ (SIMesAgOTBOS) (A-TBOS)

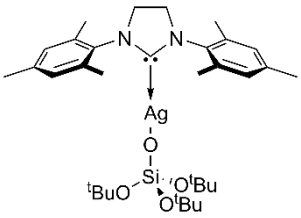

To an amber vial was added SIMesAgCl (**A-Cl**) (100.3 mg, 0.22 mmol) followed by THF (ca. 5 mL). To the suspension was added NaOSi(O^{t}Bu)$_3$ (63.7 mg, 0.22 mmol) in THF (ca. 3 mL). The mixture was stirred for 2h. After filtering the reaction mixture through Celite® the solution was taken to dryness. The crude product was dissolved in toluene (ca. 5 mL) for recrystallization in the freezer (-35°C) from which colorless cubic crystals were obtained in a yield of 50% (74.8 mg, 0.11 mmol). XRD quality crystals(cubic/colorless/transparent) were obtained from recrystallisation in toluene. **^{1}H-NMR** (25°C, 500 MHz, C_6D_6): δ 6.69 (s, 4H, Ar-*H*), δ 2.94 (s, 4H, backbone C_2H_4), δ 2.09 (s, 6H, p-CH_3), δ 2.03 (s, 12H, o-CH_3), δ 1.53 (s, 27H, -CH_3). **^{13}C-NMR** (25°C, 125.7 MHz, C_6D_6): 207.8 (N-*C*-N, *d* ($^1J_{^{13}C\text{-}^{109/107}Ag}$ = 214 Hz), 138.2, 135.4, 135.1, 129.7, 69.8, 50.1, 32.1, 20.7, 17.5. **IR** (ATR-IR) [cm^{-1}] 3050-2800 (m, C-H str.), 2729 (w, Mes C-H str.), 1608 (w, arom. C-C str.), 1489/1357 (s, arom. C-C str.), 1271 (s, C-O str.), 1193 (s, C-N str.), 1061/1002 (s, Si-O-C str.), 817/692(m). **Elemental Analysis** C: 57.70% H: 7.68% N: 4.35% (Calc.: 58.48% / 7.88% / 4.13%).

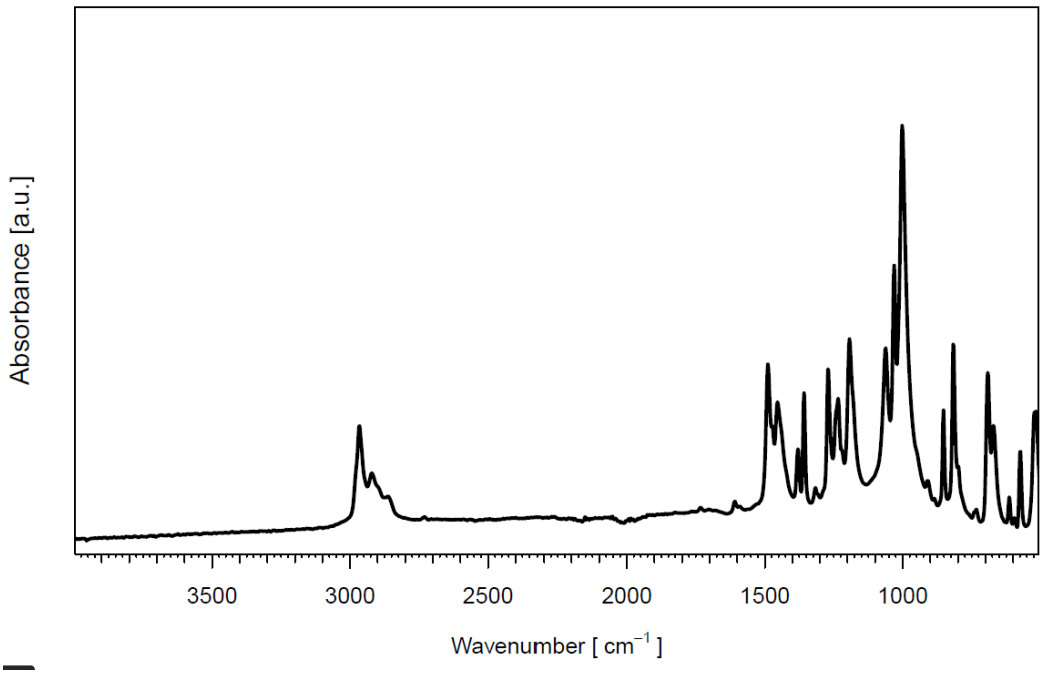

Figure S 11. ATR-IR spectrum of SIMesAgOTBOS (**A-TBOS**) (264 scans)

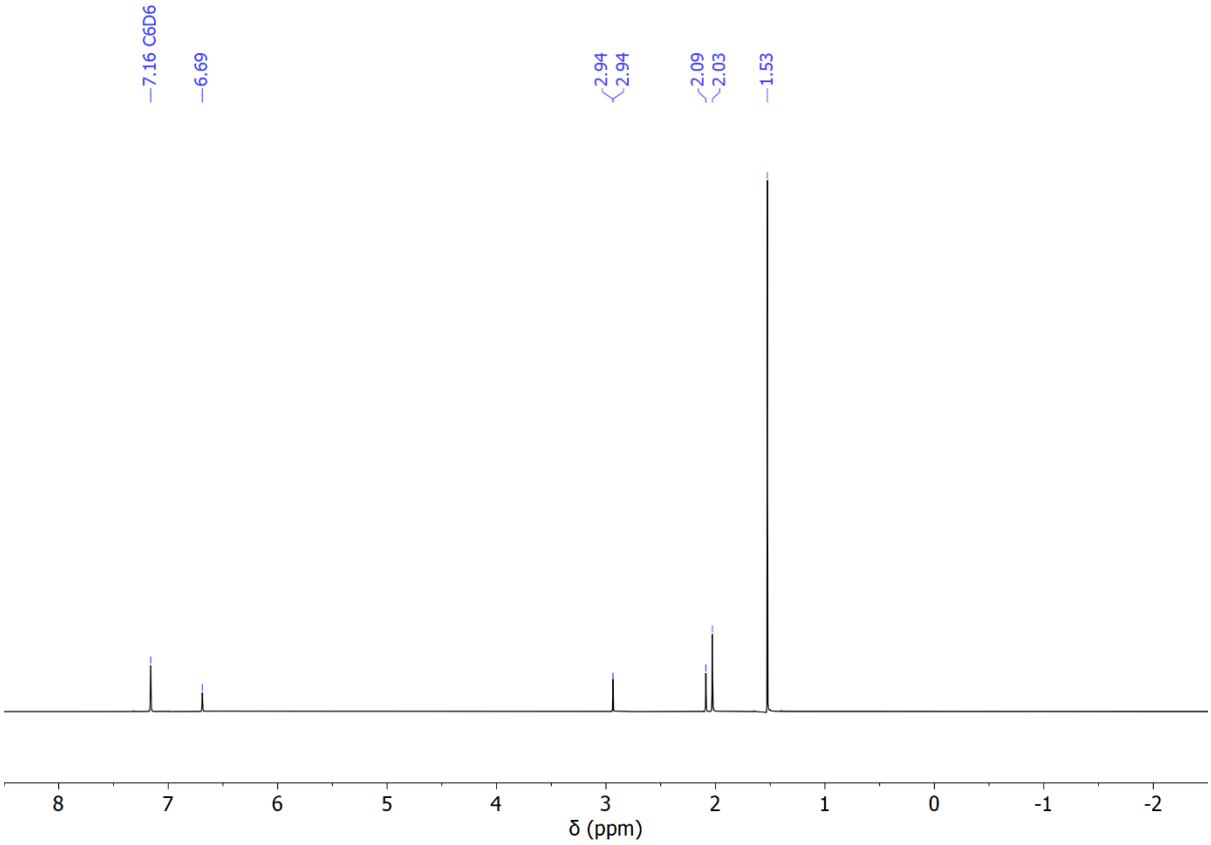

Figure S 12. ^{1}H NMR spectrum of SIMesAgOTBOS (**A-TBOS**) recorded in C_6D_6 (500 MHz, 25°C).

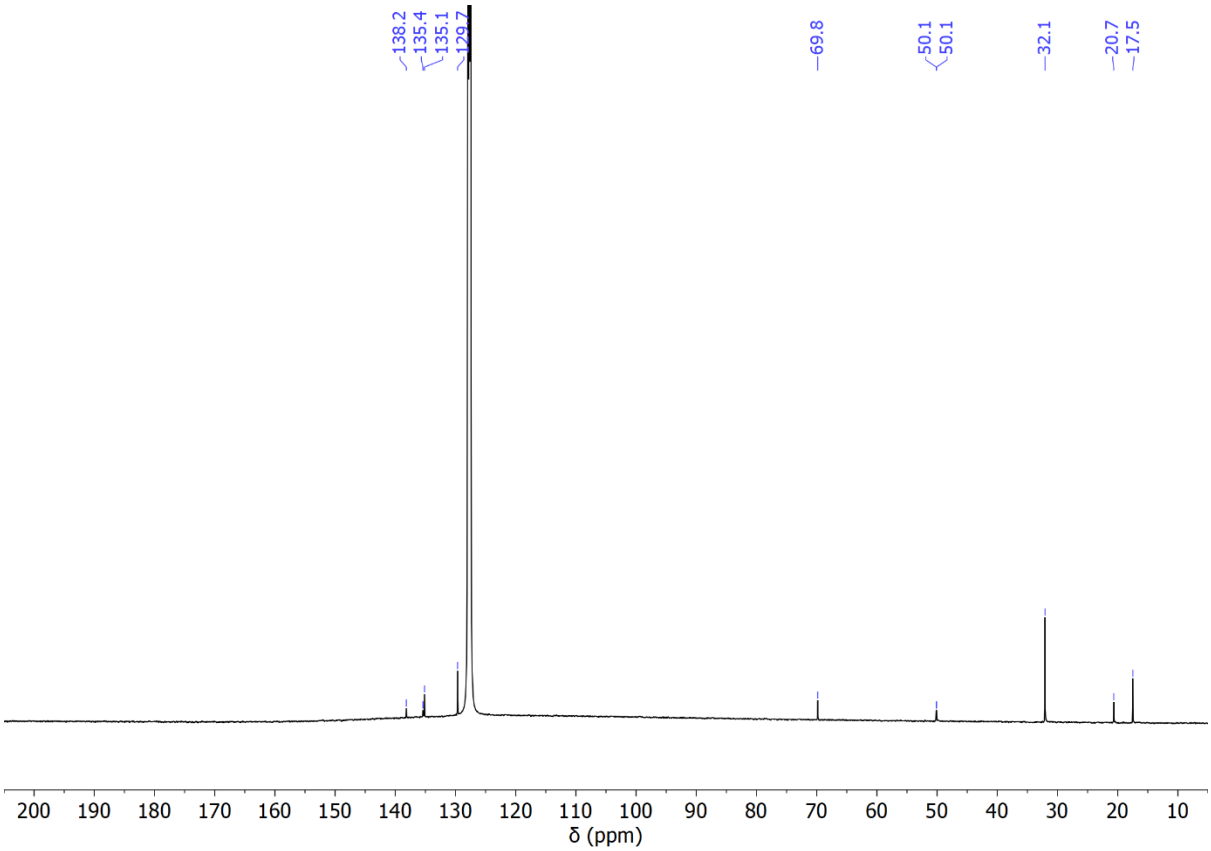

Figure S 13. ^{13}C NMR spectrum of SIMesAgOTBOS (**A-TBOS**) recorded in C_6D_6 (125.7 MHz, 25°C).

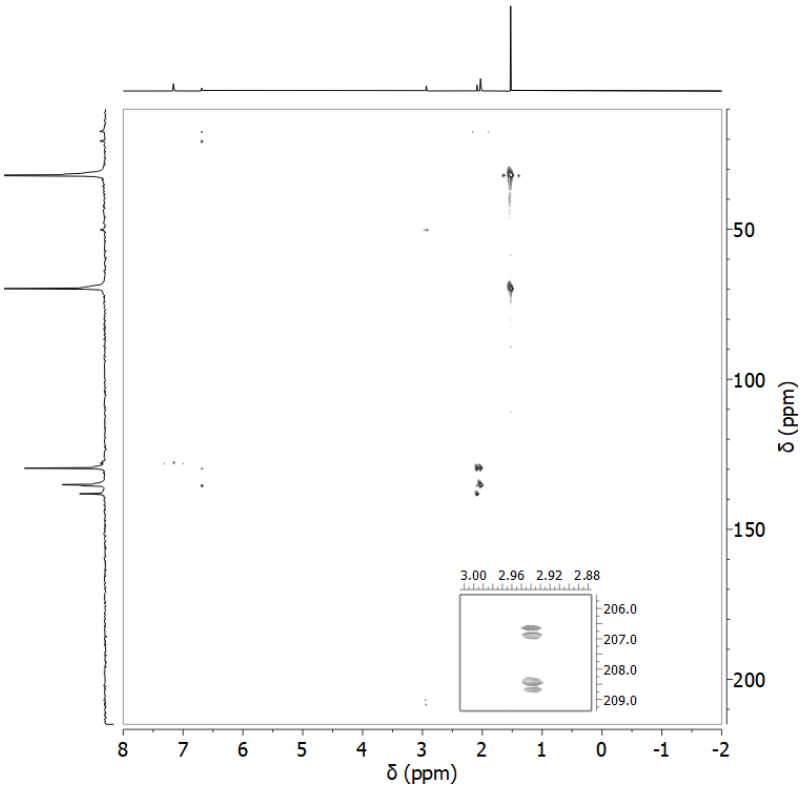

Figure S 14. SIMesAgOTBOS (**A-TBOS**) ^{1}H-^{13}C HMBC (^{1}H: 500 MHz, ^{13}C: 125.7 MHz, C_6D_6, 298 K), inset shows region of interest containing carbene splitting.

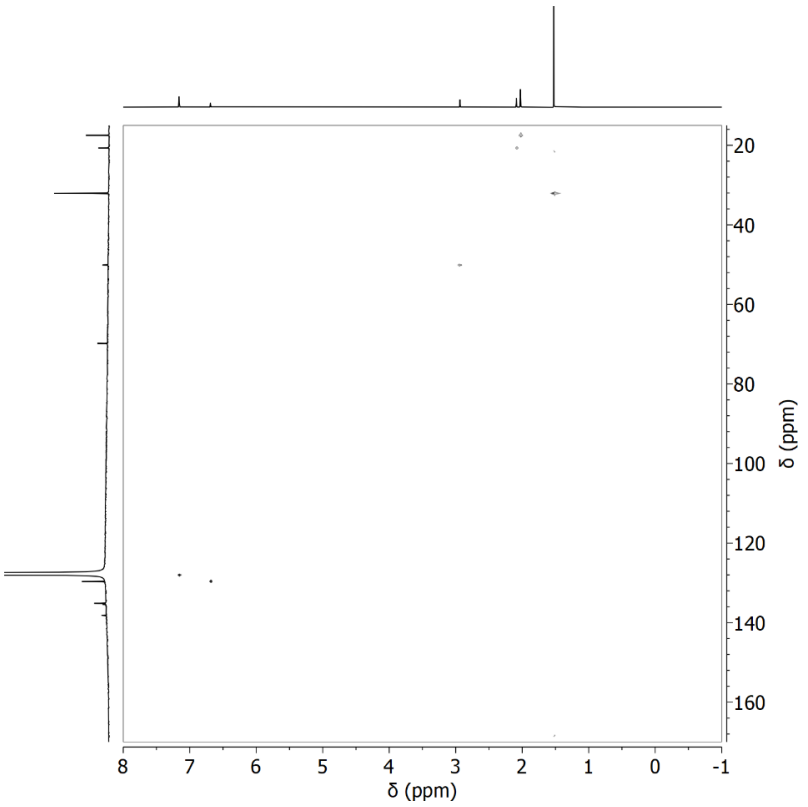

Figure S 15. SIMesAgOTBOS (**A-TBOS**) ^{1}H-^{13}C HSQC (^{1}H: 500 MHz, ^{13}C: 125.7 MHz, C_6D_6, 298 K)

Synthesis of SIMesAgN(SiMe$_3$)$_2$ (SIMesAgHMDS) (A-HMDS)

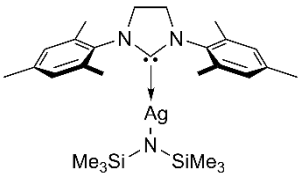

To an amber vial was added SIMesAgCl (**A-Cl**) (100.0 mg, 0.22 mmol) followed by THF (ca. 5 mL). To the suspension was added LiHMDS (39.1 mg, 0.23 mmol) in THF (ca. 3 mL). The mixture was stirred for 6h. After filtering the reaction mixture through Celite® the solution was taken to dryness. The crude product was dissolved in toluene (ca. 5 mL), concentrated and pentane was added to precipitate a white product. Recrystallization was performed in HMDSO (ca. 7 mL) in the freezer (-35°C) from which colorless crystals were obtained in a yield of 34% (43 mg, 0.075 mmol). XRD quality crystals were obtained from recrystallisation in HMDSO. **^{1}H-NMR** (25°C, 500 MHz, C_6D_6): δ 6.76 (s, 4H, Ar-*H*), δ 2.96 (s, 4H, backbone C_2H_4), δ 2.12 (s, 6H, p-CH_3), δ 2.09 (s, 12H, o-CH_3), δ 0.17 (s, 18H, Si-CH_3). **^{13}C-NMR** (25°C, 125.7 MHz, C_6D_6): 209.0 (N-*C*-N, *d* ($^1J_{^{13}C-^{109/107}Ag}$ = 187 Hz), 138.4, 135.4, 129.6, 50.0, 20.6, 17.5, 6.4. **IR** (ATR-IR) [cm^{-1}] 3050-2800 (m, C-H str.), 2733 (w, Mes C-H str.), 1608 (w, arom. C-C str.), 1485 (s, arom. C-C str.), 1267/1232 (s, C-N str.), 1037/813 (s, C-Si-N str.), 659/573(m). **Elemental Analysis** C: 55.78% H: 7.62% N: 7.01% (Calc.: 56.43% / 7.72% / 7.31%).

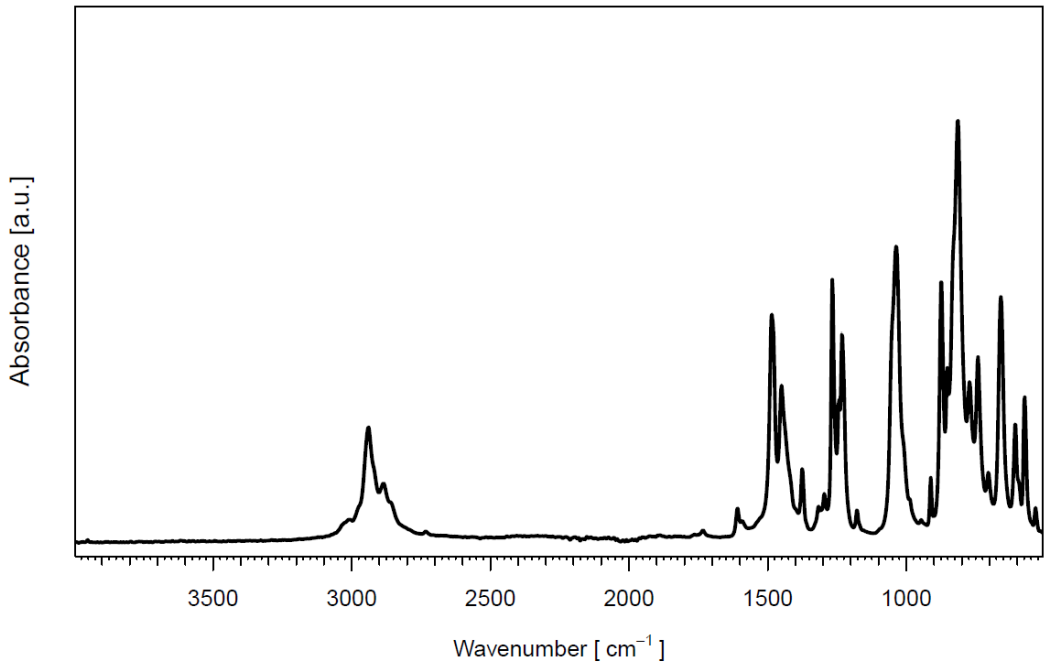

Figure S 16. ATR-IR spectrum of SIMesAgHMDS (**A-HMDS**) (264 scans)

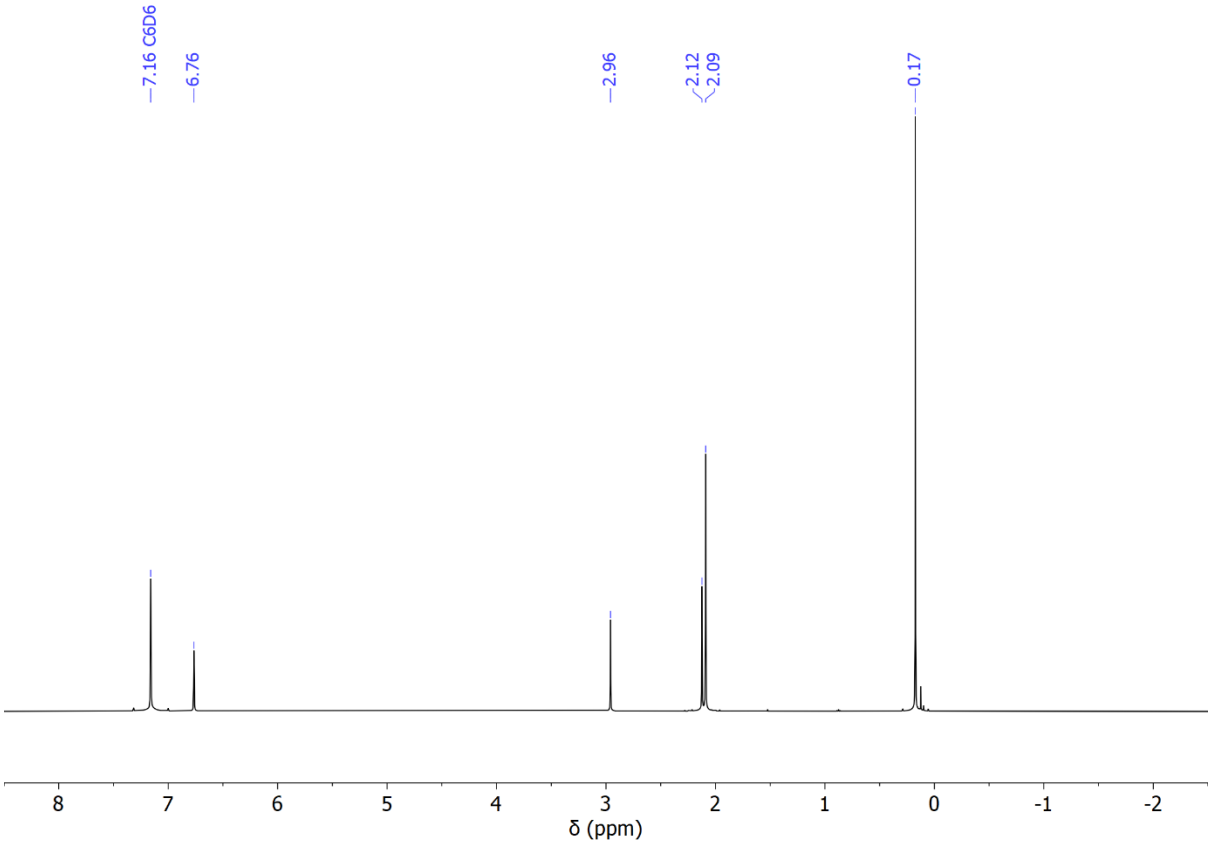

Figure S 17. ^{1}H NMR spectrum of SIMesAgHMDS (**A-HMDS**) recorded in C_6D_6 (500 MHz, 25°C).

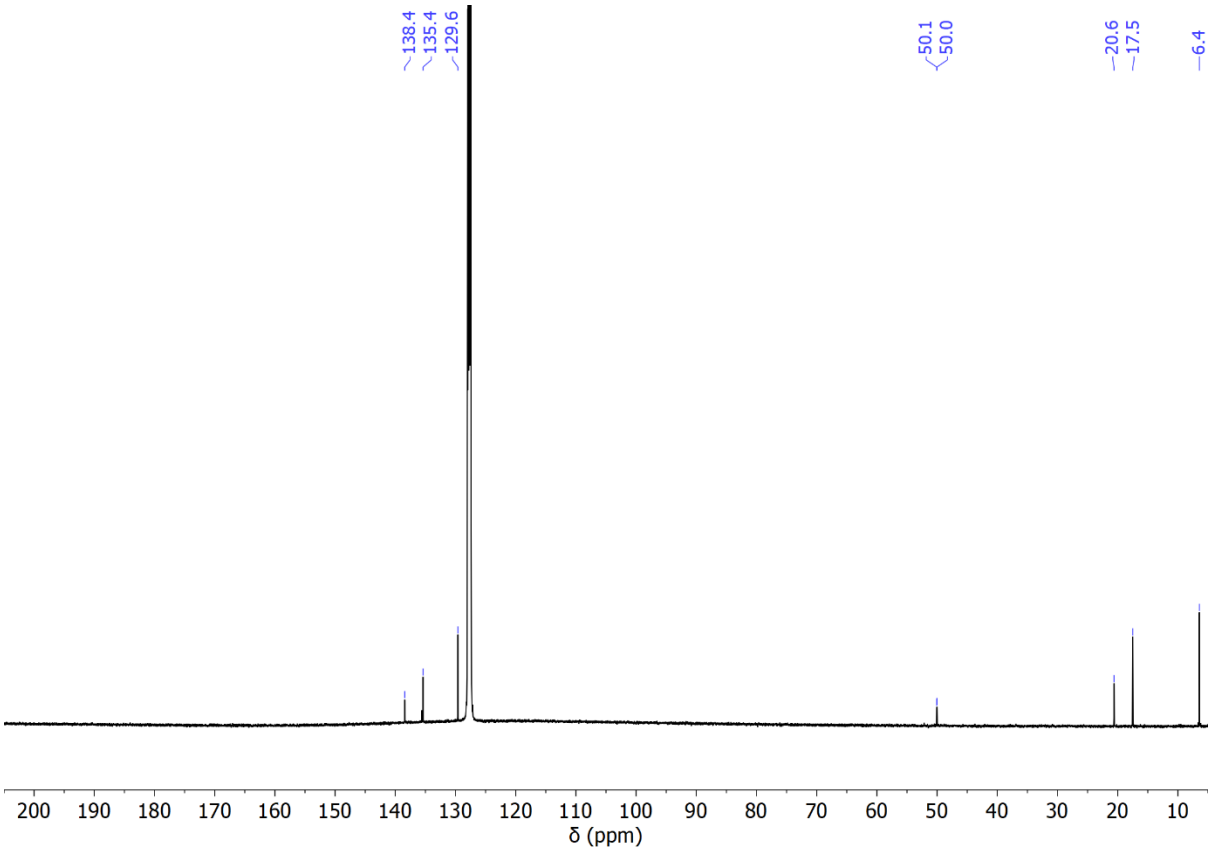

Figure S 18. ^{13}C NMR spectrum of SIMesAgHMDS (**A-HMDS**) recorded in C_6D_6 (125.7 MHz, 25°C).

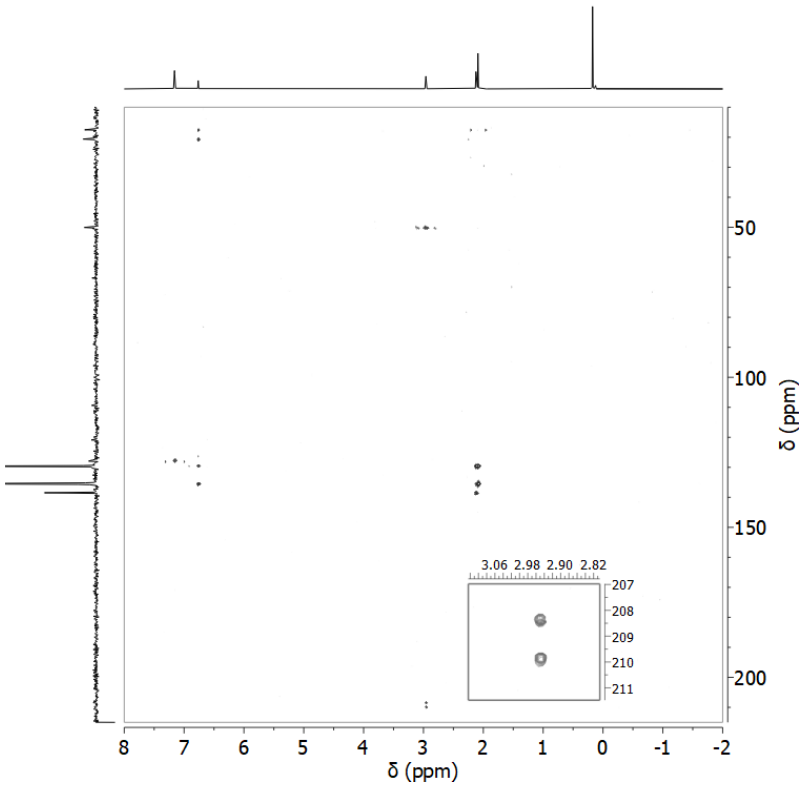

Figure S 19. SIMesAgHMDS (**A-HMDS**) ^{1}H-^{13}C HMBC (^{1}H: 500 MHz, ^{13}C: 125.7 MHz, C_6D_6, 298 K), inset shows region of interest containing carbene splitting.

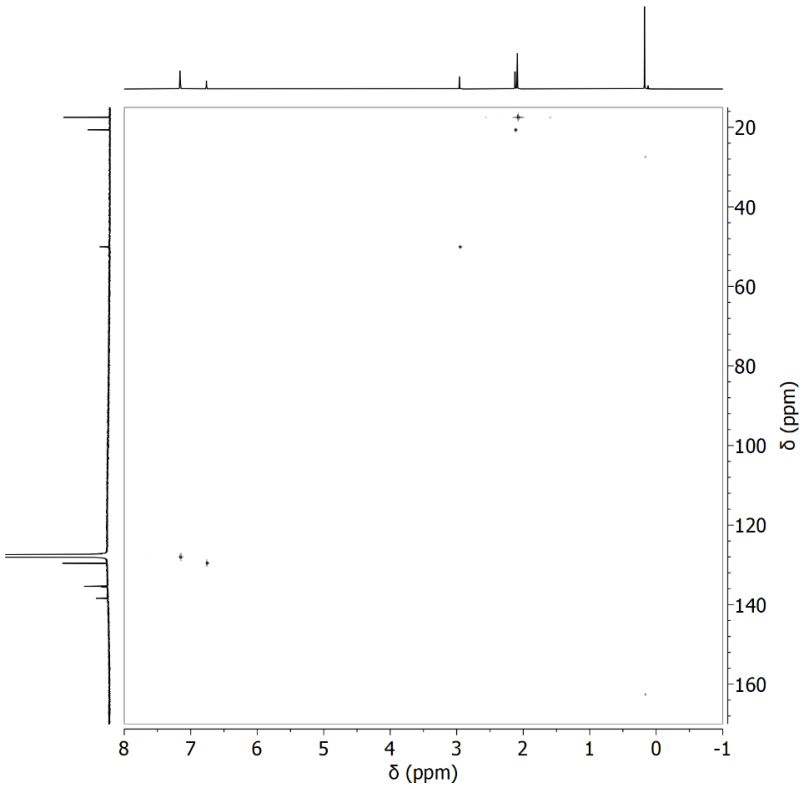

Figure S 20. SIMesAgHMDS (**A-HMDS**) ^{1}H-^{13}C HSQC (^{1}H: 500 MHz, ^{13}C: 125.7 MHz, C_6D_6, 298 K)

Synthesis of SIMesAgMe (A-Me)

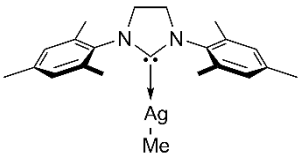

The Synthesis was adapted from Literature procedure.[21] To an amber Schlenk was added SIMesAgCl (**A-Cl**) (196.0 mg, 0.44 mmol) followed by THF (ca. 8 mL). To the suspension was added a 3M solution of MeMgBr in Et_2O (0.2 ml, 0.6 mmol). The mixture turned dark immediately and was stirred for 10 minutes before dioxane (10 mL) was added to precipitate $[MgX_2(C_4H_8O_2)]_n$. The reaction was then stirred for 12 h. After filtering the reaction mixture through Celite® the solution was taken to dryness. The crude product was dissolved in toluene (ca. 8 mL) for recrystallization in the freezer from which colorless/cubic crystals were obtained in a yield of 39% (74.1 mg, 0.17 mmol). XRD quality crystals were obtained from recrystallisation in toluene. **^{1}H-NMR** (25°C, 500 MHz, C_6D_6): δ 6.70 (s, 4H, Ar-*H*), δ 3.02 (s, 4H, backbone C_2H_4), δ 2.17 (s, 6H, p-CH_3), δ 2.05 (s, 12H, o-CH_3), δ -0.13/-0.15 (dd, 3H, -CH_3). **^{13}C-NMR** (25°C, 125.7 MHz, C_6D_6): 213.7 (N-*C*-N, *d* ($^1J_{^{13}C-^{109/107}Ag}$ = 117 Hz), 137.7, 135.3, 129.5, 50.2, 20.7, 17.7, -13.8- ($^1J_{^{13}C-^{109}Ag}$ = 139 Hz, $^1J_{^{13}C-^{107}Ag}$ = 120 Hz). **IR** (ATR-IR) [cm^{-1}] 3050-2800 (m, C-H str.), 2731 (w, Mes C-H str.), 1608 (w, arom. C-C str.), 1483/1438 (s, arom. C-C str.), 1261/1171 (s, C-N str.), 1033/848/624/571 (m). **Elemental Analysis** C: 62.18% H: 6.97% N: 6.22% (Calc.: 61.54% / 6.81% / 6.52%) (Instability of the compound (rapid decomposition) makes elemental analysis challenging)

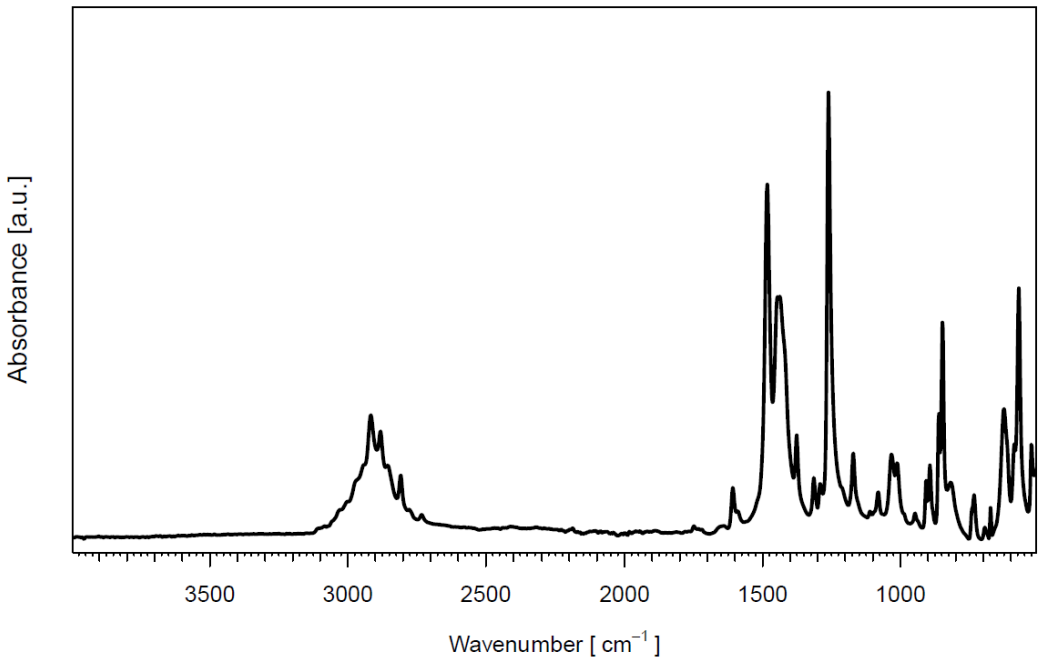

Figure S 21. ATR-IR spectrum of SIMesAgMe (**A-Me**) (264 scans)

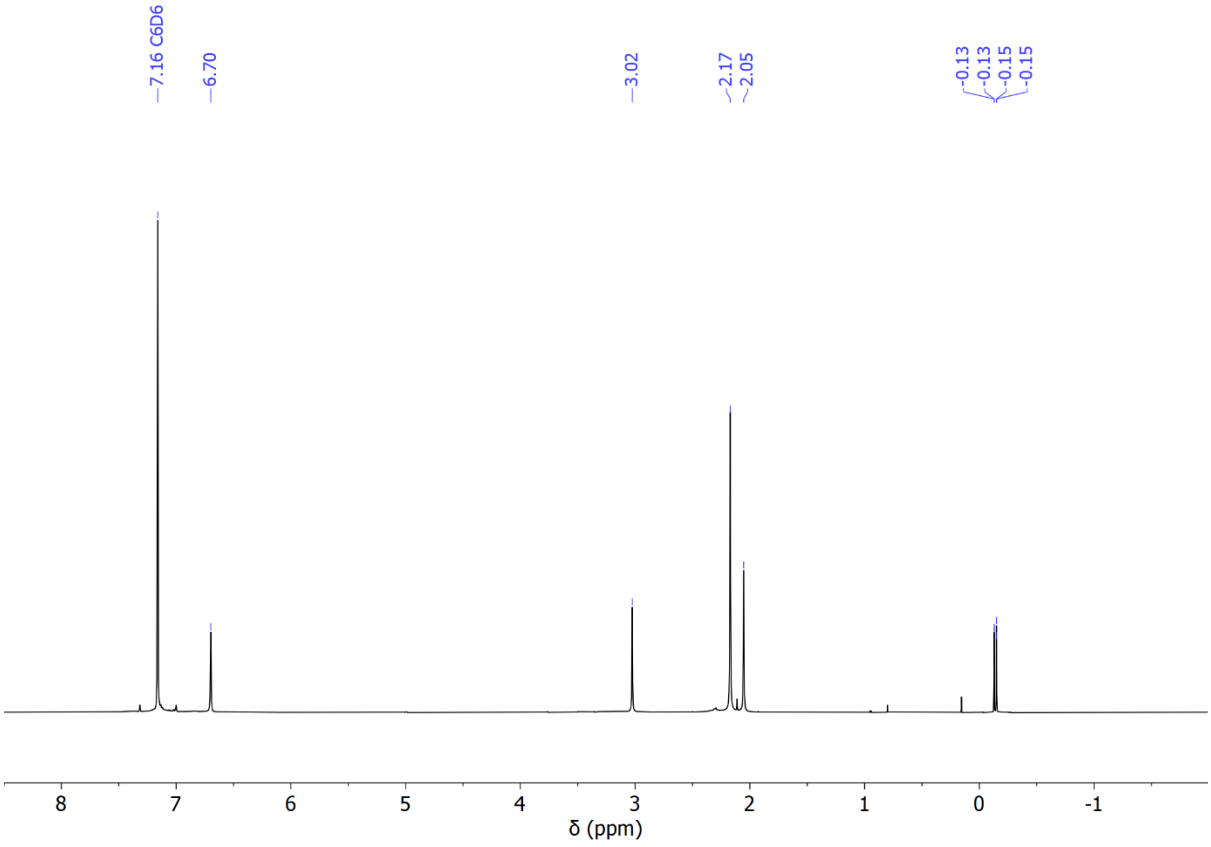

Figure S 22. ^{1}H NMR spectrum of SIMesAgMe (**A-Me**) recorded in C_6D_6 (500 MHz, 25°C).

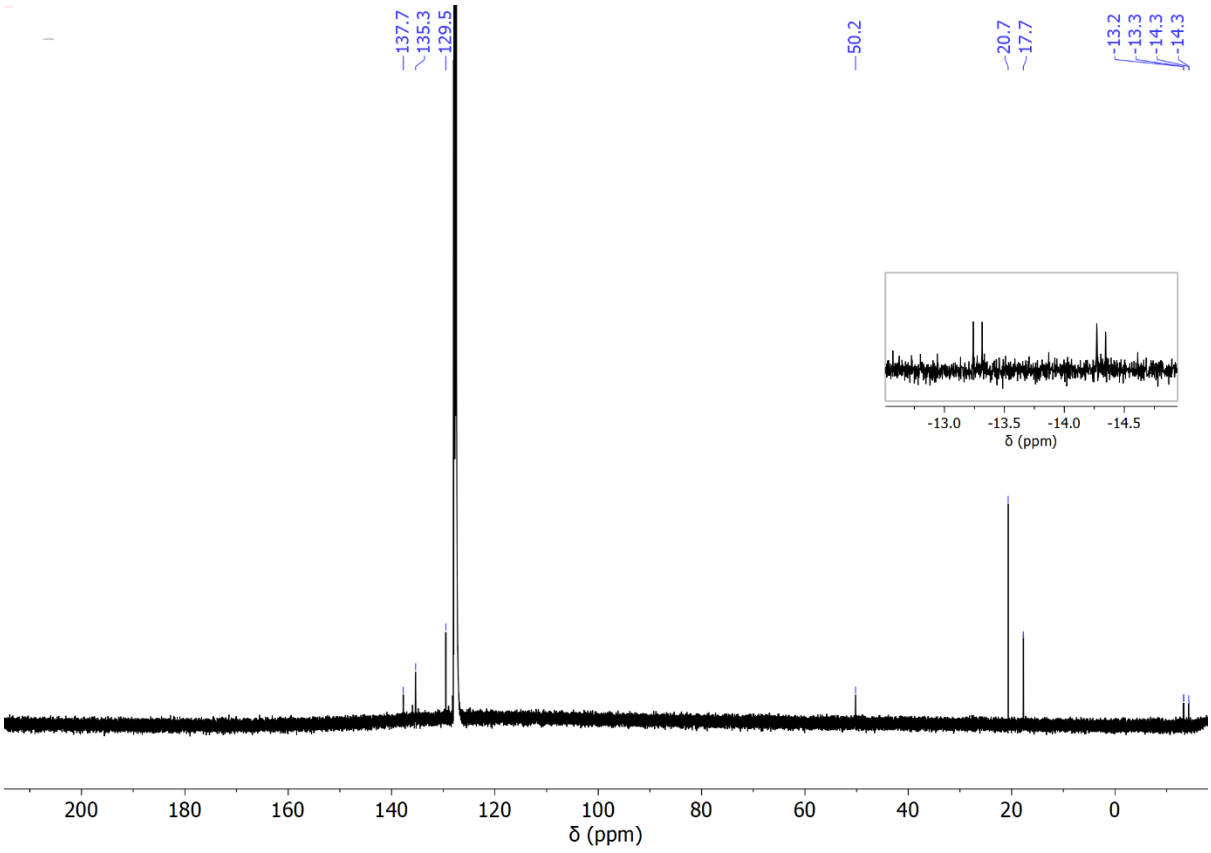

Figure S 23 ^{13}C NMR spectrum of SIMesAgMe (**A-Me**) recorded in C_6D_6 (125.7 MHz, 25°C).

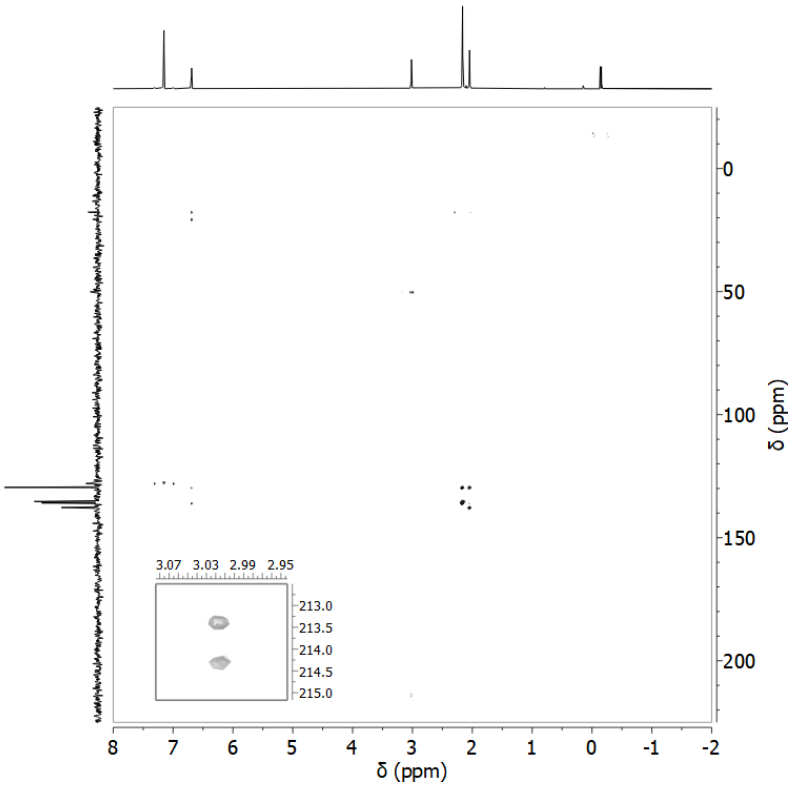

Figure S 24 SIMesAgMe (**A-Me**) ^{1}H-^{13}C HMBC (^{1}H: 500 MHz, ^{13}C: 125.7 MHz, C_6D_6, 298 K), inset shows region of interest containing carbene splitting.

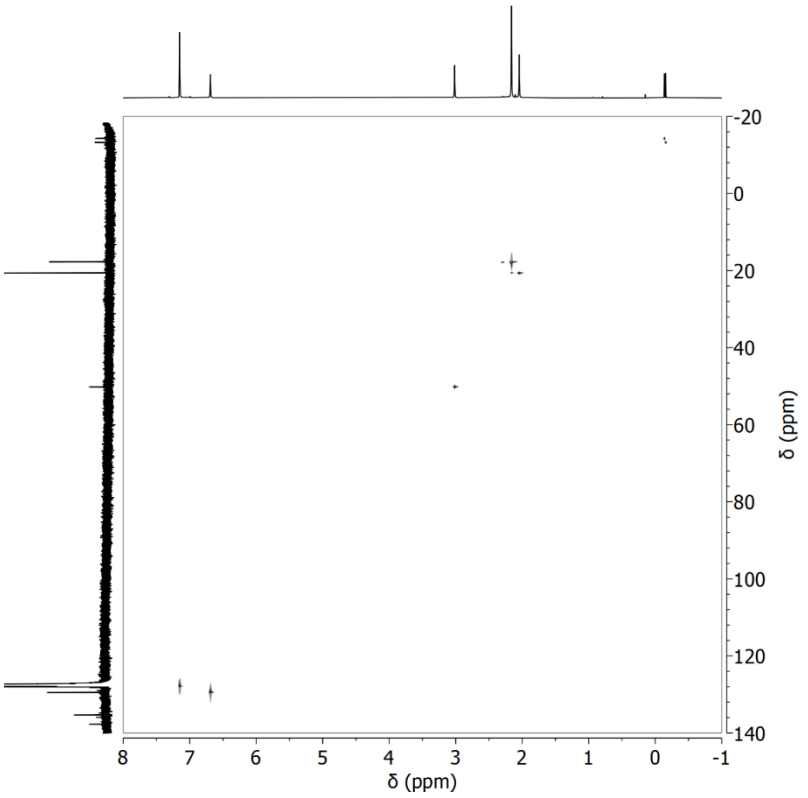

Figure S 25 SIMesAgMe (**A-Me**) ^{1}H-^{13}C HSQC (^{1}H: 500 MHz, ^{13}C: 125.7 MHz, C_6D_6, 298 K)

Synthesis of SIMesAgOAr (A-BHT)

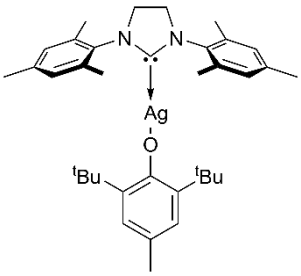

To an amber vial was added SIMesAgMes (**A-Mes**) (35.4 mg, 0.066 mmol) followed by THF (ca. 5 mL). To the suspension was added 2,6-Bis(1,1-dimethylethyl)-4-methylphenol (BHT) (15.1 mg, 0.068 mmol) in THF (ca. 3 mL). The mixture was stirred for 6 h. After filtering the reaction mixture through Celite® the solution was taken to dryness yielding a white powder in a yield of 69% (29 mg, 0.046 mmol). XRD quality crystals (transparent) were obtained from recrystallisation in cold diethyl ether (freezer: -35°C). **^{1}H-NMR** (25°C, 500 MHz, C_6D_6): δ 7.20 (s, 2H, Ar-*H (Ag-Mesityl)*), δ 6.70 (s, 4H, Ar-*H (NHC-Mes)*), δ 2.94 (s, 4H, backbone C_2H_4), δ 2.45 (s, 3H, -C*H*$_3$ (4-position)), δ 2.12 (s, 6H, -C*H*$_3$ (4-position) *(NHC)*), δ 1.97 (s, 12H, -C*H*$_3$ (2,6-position) *(NHC)*), δ 1.62 (s, 18H, -CC*H*$_3$ (2,6-position)). **^{13}C-NMR** (25°C, 125.7 MHz, C_6D_6): 207.2 (N-*C*-N, pseudo-*dd* ($^{1}J_{^{13}C\text{-}^{109}Ag}$ = 253 Hz; $^{1}J_{^{13}C\text{-}^{107}Ag}$ = 219 Hz)), 138.4, 135.2, 129.6, 125.1, 50.0, 35.2, 31.1, 21.6, 20.6, 17.4. **IR** (ATR-IR) [cm^{-1}] 3050-2800 (m, C-H str.), 2729 (w, Mes C-H str.), 1610 (w, arom. C-C str.), 1487/1454/1415/1378 (s, arom. C-C str.), 1267 (s, C-N str.), 1025/850/571 (m). **Elemental Analysis** C: 68.55% H: 7.91% N: 4.32% (Calc.: 68.24% / 7.79% / 4.42%).

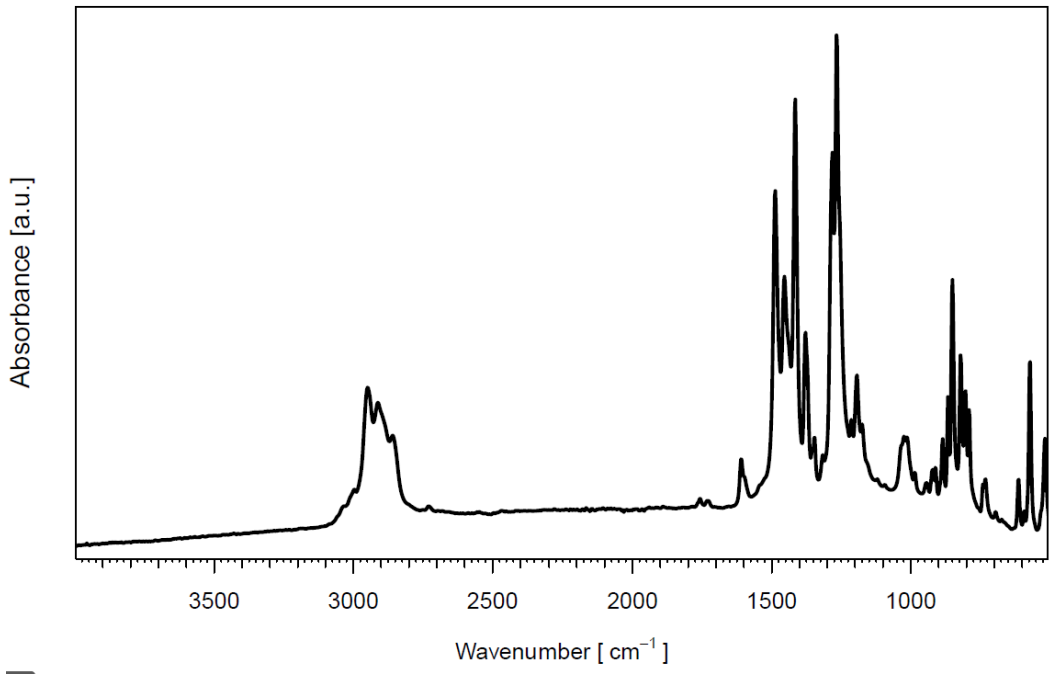

Figure S 26. ATR-IR spectrum of SIMesAgOAr (**A-BHT**) (264 scans)

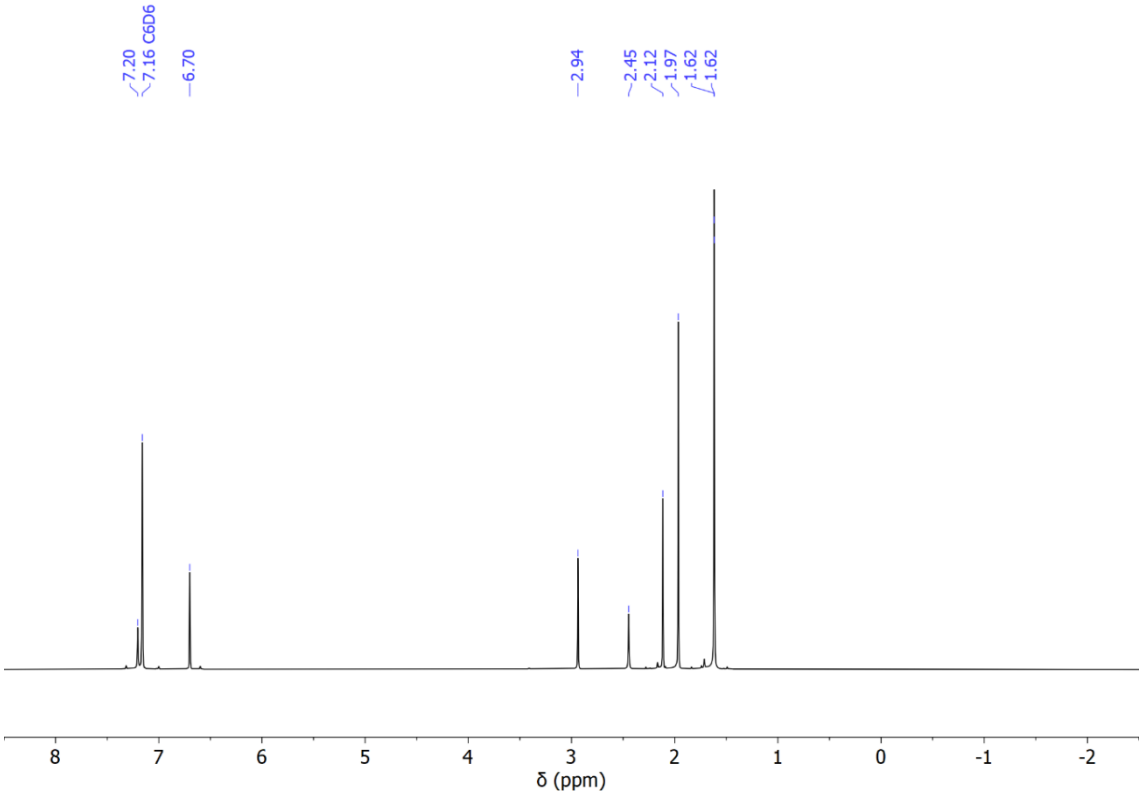

Figure S 27. ^{1}H NMR spectrum of SIMesAgOAr (**A-BHT**) recorded in C_6D_6 (500 MHz, 25°C).

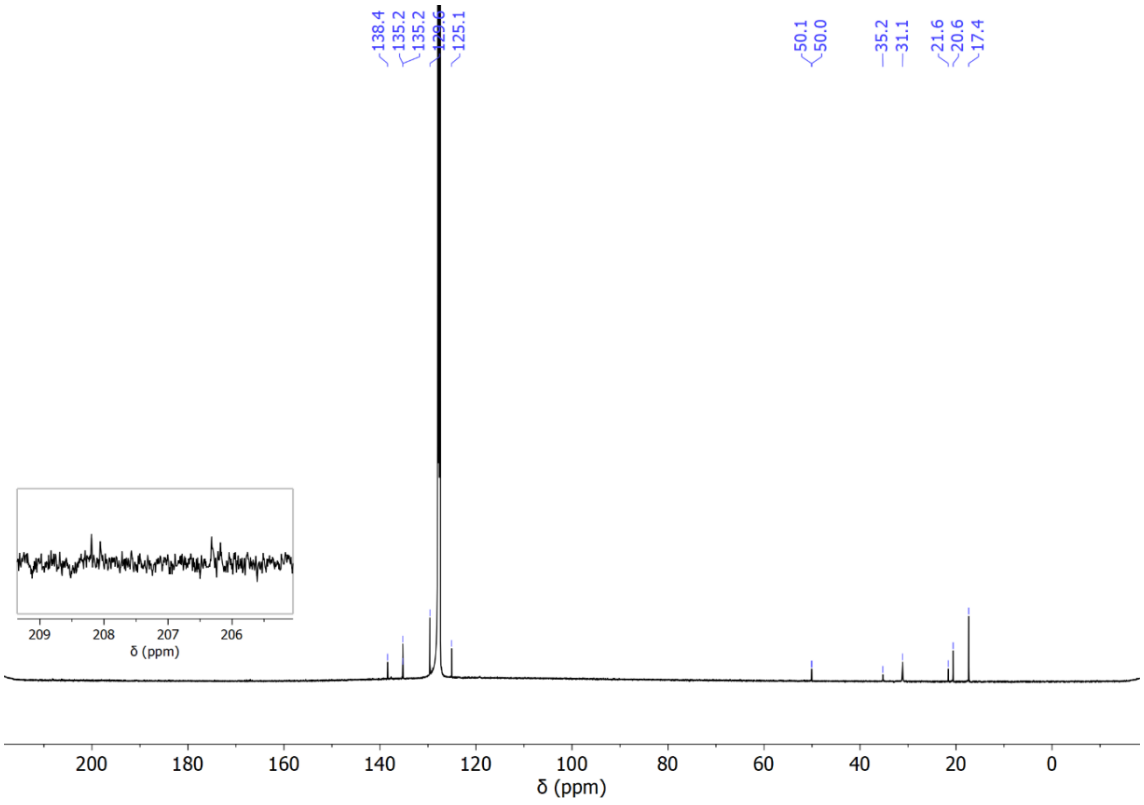

Figure S 28. ^{13}C NMR spectrum of SIMesAgOAr (**A-BHT**) recorded in C_6D_6 (125.7 MHz, 25°C). Zoomed region shown in inset shows coupling of carbene carbon to both isotopes of silver ($^{1}J_{^{13}C\text{-}^{109}Ag}$ = 253 Hz; $^{1}J_{^{13}C\text{-}^{107}Ag}$ = 219 Hz)

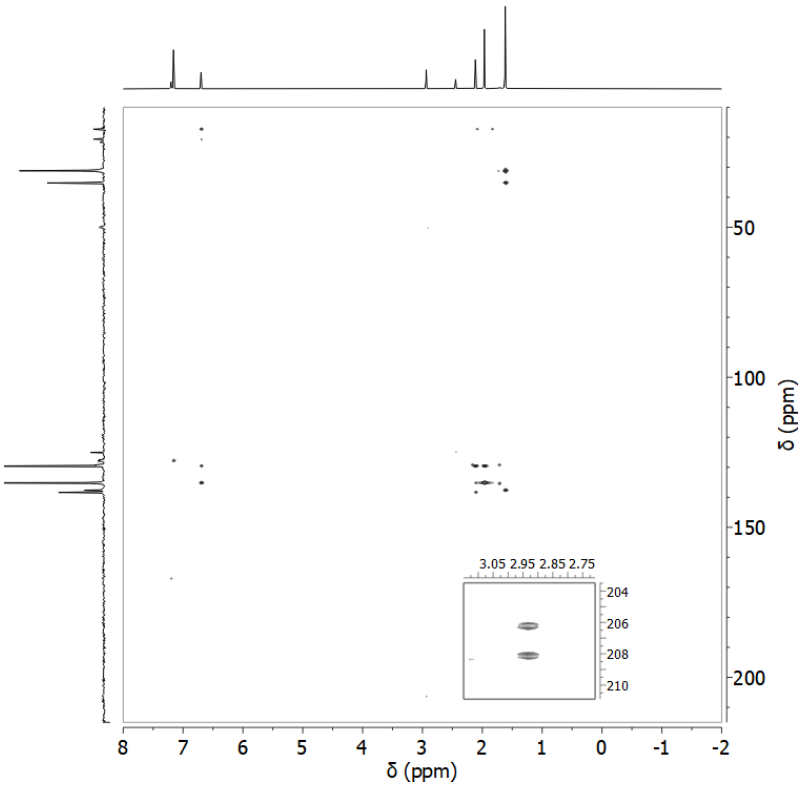

Figure S 29. SIMesAgOAr (**A-BHT**) ^{1}H-^{13}C HMBC (^{1}H: 500 MHz, ^{13}C: 125.7 MHz, C_6D_6, 298 K), inset shows region of interest containing carbene splitting.

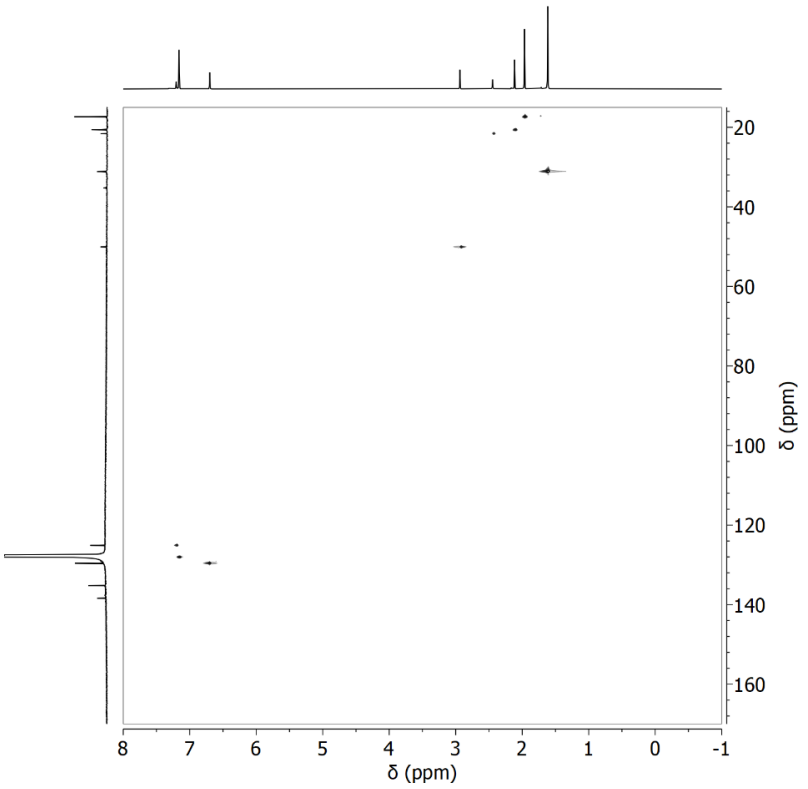

Figure S 30. SIMesAgOAr (**A-BHT**) ^{1}H-^{13}C HSQC (^{1}H: 500 MHz, ^{13}C: 125.7 MHz, C_6D_6, 298 K)

Synthesis of IMesAgCl (B-Cl)

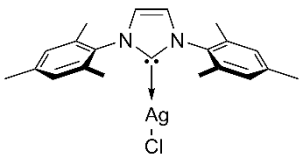

The Synthesis was adapted from literature procedures.[17-20] To a 250 ml round bottom flask was added IMesCl (*1,3-Bis(2,4,6-trimethylphenyl)imid-azolium chloride*) (1.8 g, 5.26 mmol) followed by Dichloromethane (ca. 50 mL). To the solution was added Ag_2O (1.5 g, 6.47 mmol). The mixture was stirred at reflux for 20 h. After filtering the reaction mixture through Celite® the clear light-yellow solution was taken to dryness. The crude product was dissolved in THF for recrystallization in the freezer (-35°C) and pale-yellow platelets were obtained in a yield of 23% (0.53 g, 1.18 mmol). **^{1}H-NMR** (25°C, 500 MHz, $CDCl_3$): δ 7.13 (s, 2H, backbone C_2H_2), δ 7.00 (s, 4H, Ar-*H*), δ 2.35 (s, 6H, *p*-CH_3), δ 2.07 (s, 12H, *o*-CH_3). (25°C, 500 MHz, C_6D_6): δ 6.61 (s, 4H, Ar-*H*), δ 5.94 (s, 2H, backbone C_2H_2), δ 2.05 (s, 6H, *p*-CH_3), δ 1.79 (s, 12H, *o*-CH_3). **^{13}C-NMR** (25°C, 125.7 MHz, C_6D_6): 139.2, 135.2, 134.2, 129.3, 121.6, 20.7, 17.2.

Synthesis of IMesAgMes (B-Mes)

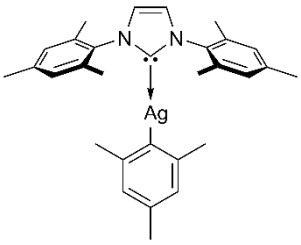

To an amber vial was added IMesAgCl (**B-Cl**) (100.6 mg, 0.22 mmol) followed by THF (ca. 5 mL). To the suspension was added dropwise a solution of $Mes_2Mg(THF)_2$ (50.2 mg, 0.12 mmol) in THF (ca. 3 mL). The mixture was stirred for 22 h before 2 drops of dioxane were added to precipitate $[MgX_2(C_4H_8O_2)]_n$. After filtering the reaction mixture through Celite® solvent was removed under reduced pressure to yield a white product. The crude product was dissolved in toluene (5 mL) and cooled to -35 °C for 24 hours. Colorless cubic crystals were obtained in a yield of 56% (67.3 mg, 0.13 mmol). XRD quality crystals (block-type/transparent) were obtained from recrystallization in toluene. The final product showed a co-crystallized toluene molecule per unit cell (1/2 toluene per molecule). **^{1}H-NMR** (25°C, 500 MHz, C_6D_6): δ 7.02 (s, 2H, Ar-*H (Ag-Mesityl)*), δ 6.74 (s, 4H, Ar-*H (NHC-Mes)*), δ 6.08 (s, 2H, backbone C_2H_2), δ 2.42 (s, 6H, Ar-CH_3 (4–position) (*NHC)*), δ 2.34 (s, 3H, -CH_3 (4–position) *Ag-Mesityl)*), δ 2.11 (s, 6H, -CH_3 (2,6-position) *(Ag-Mesityl)*), δ 1.99 (s, 12H, -CH_3 (2,6-position) *(NHC)*). **^{13}C-NMR** (25°C, 125.7 MHz, C_6D_6): 190.6 (N-*C*-N, pseudo-*dd* ($^1J_{^{13}C\text{-}^{109}Ag}$ = 137 Hz; $^1J_{^{13}C\text{-}^{107}Ag}$ = 119 Hz)), 167.0 (Mesityl-C, d ($^1J_{^{13}C\text{-}^{107/109}Ag}$ = 187 Hz)) 138.8, 137.5, 135.9, 134.7, 132.6, 129.0, 125.3, 124.3, 121.1, 29.5, 21.3, 20.7, 17.4. **IR** (ATR-IR) [cm^{-1}] 3136/3111 (m, alkene C-H str.), 3020-2800 (m, C-H str.), 2729 (w, Mes C-H str.), 1612 (w, C=C str.), 1487 (s, arom. C-C str.), 1405 (s, C-H bend.), 1242 (s, C-N str.), 844/735/534 (s, alkene C-H bend.). **Elemental Analysis** C: 67.64% H: 6.81% N: 5.02% (Calc.: 67.80% / 6.64% / 5.27%) (including co-cryst. toluene).

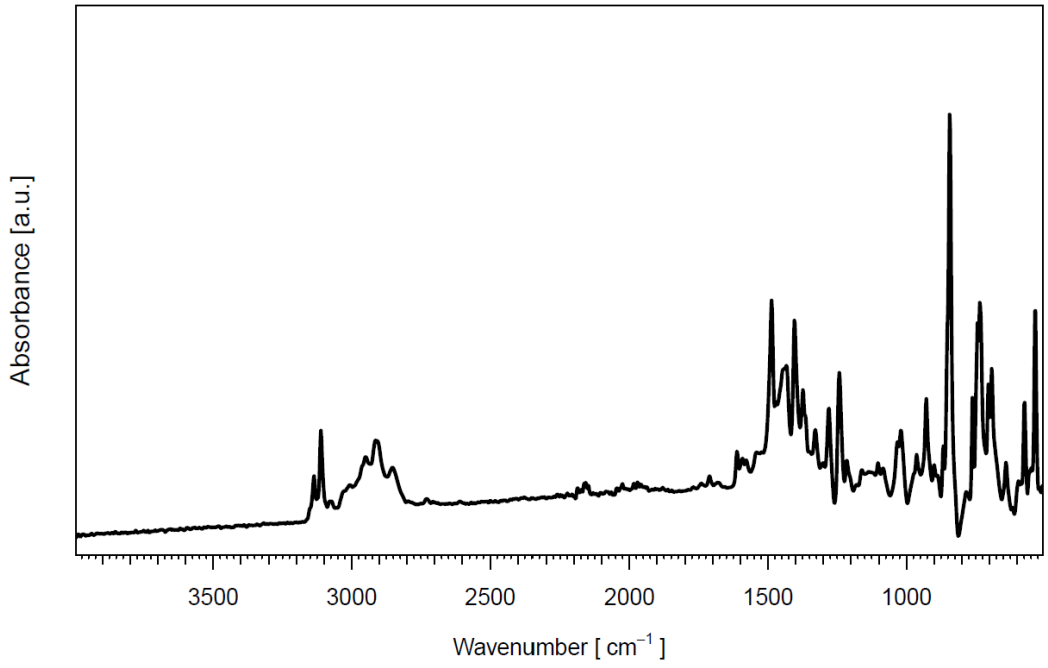

Figure S 31. ATR-IR spectrum of IMesAgMes (**B-Mes**) (264 scans)

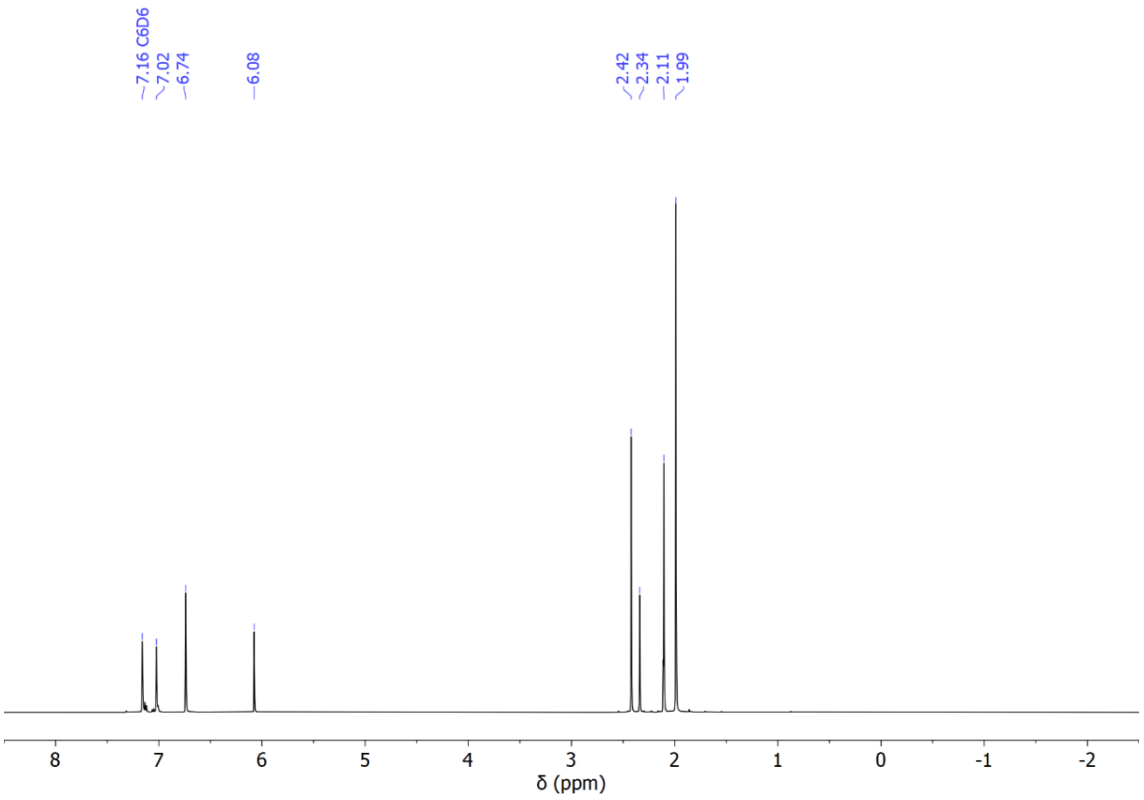

Figure S 32. ^{1}H NMR spectrum of IMesAgMes (**B-Mes**) recorded in C_6D_6 (500 MHz, 25°C).

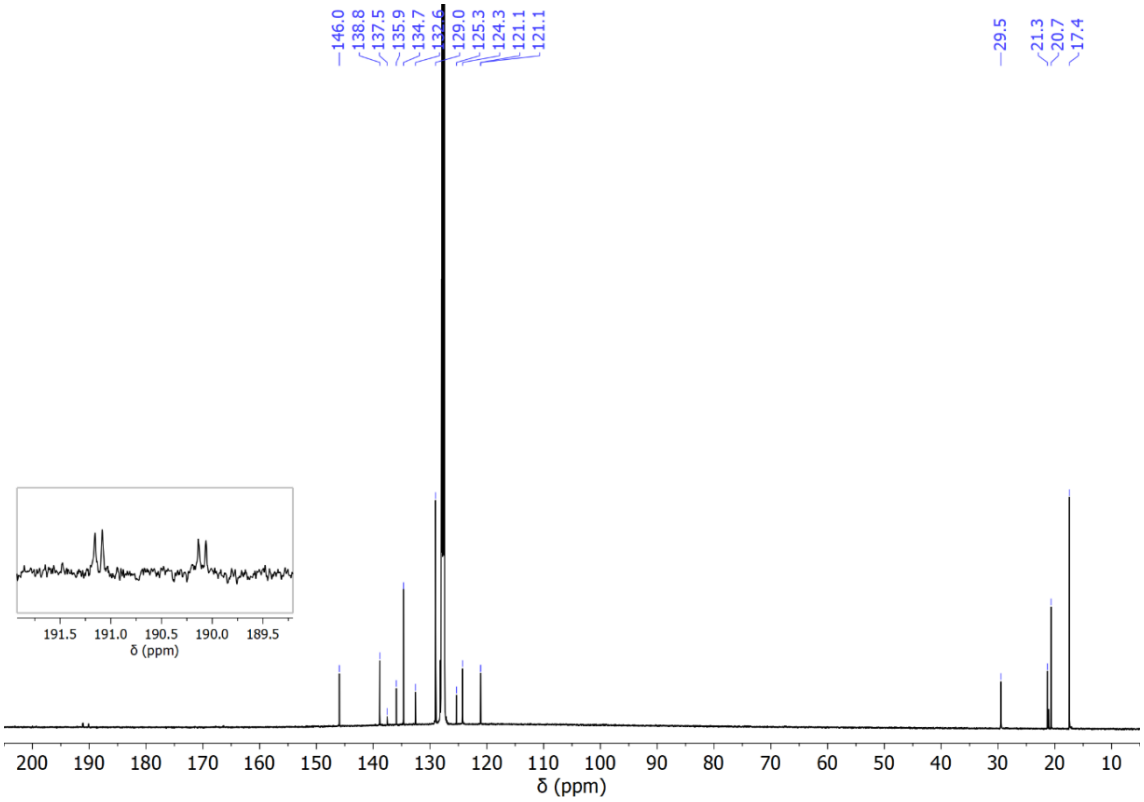

Figure S 33. ^{13}C NMR spectrum of IMesAgMes (**B-Mes**) recorded in C_6D_6 (125.7 MHz, 25°C). Zoomed region shown in inset shows coupling of carbene carbon to both isotopes of silver ($^{1}J_{^{13}C\text{-}^{109}Ag}$ = 137 Hz; $^{1}J_{^{13}C\text{-}^{107}Ag}$ = 119 Hz)

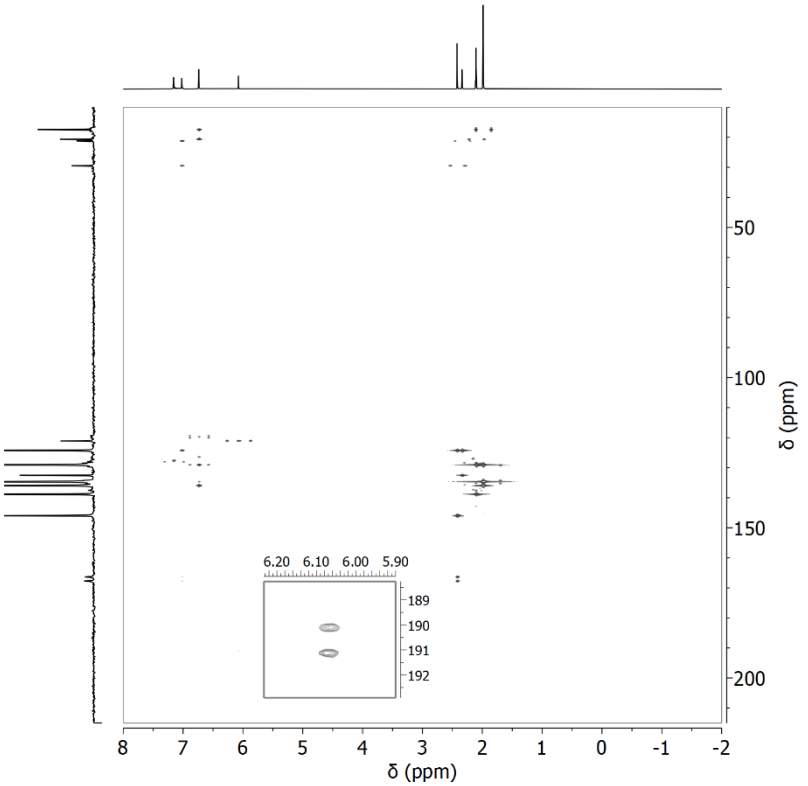

Figure S 34. IMesAgMes (**B-Mes**) ^{1}H-^{13}C HMBC (^{1}H: 500 MHz, ^{13}C: 125.7 MHz, C_6D_6, 298 K), inset shows region of interest containing carbene splitting.

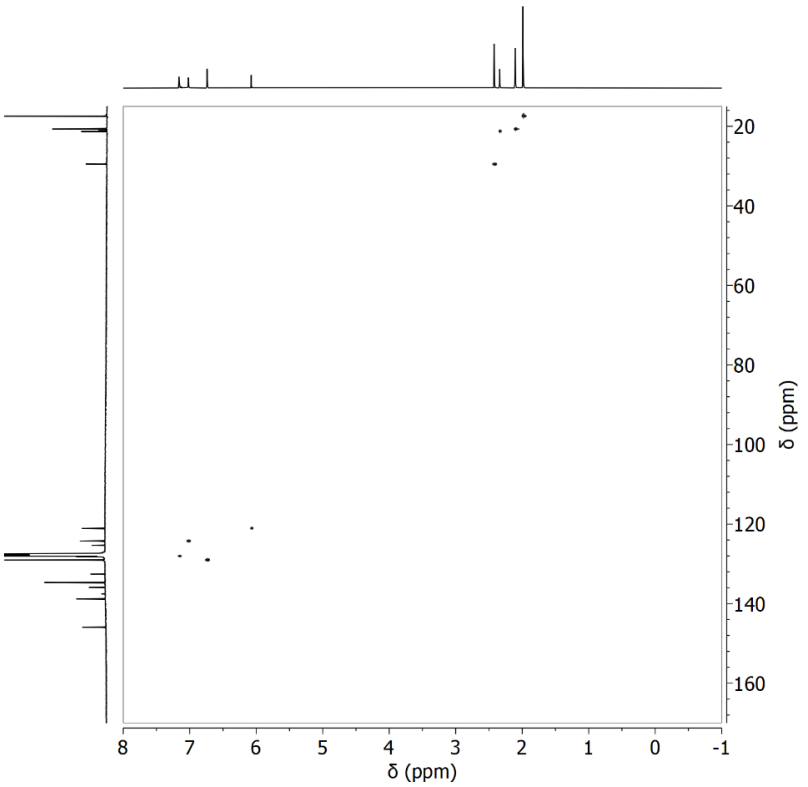

Figure S 35. IMesAgMes (**B-Mes**) ^{1}H-^{13}C HSQC (^{1}H: 500 MHz, ^{13}C: 125.7 MHz, C_6D_6, 298 K)

Synthesis of IMesAgOSi(O^{t}Bu)$_3$ (IMesAgOTBOS) (B-TBOS)

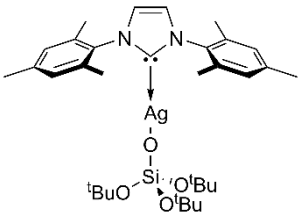

To an amber vial was added IMesAgCl (**B-Cl**) (98.7 mg, 0.22 mmol) followed by THF (ca. 5 mL). To the suspension was added NaOSi(O^{t}Bu)$_3$ (69.2 mg, 0.24 mmol) in THF (ca. 3mL). The mixture was stirred for 22 h. After filtering the reaction mixture through Celite® the solution was taken to dryness. The crude product was dissolved in toluene (ca. 5mL) for recrystallization in the freezer (-35°C) from which colorless/transparent cubic crystals were obtained in a yield of 70% (103.6 mg, 0.15 mmol). XRD quality crystals were obtained from recrystallisation in toluene. **^{1}H-NMR** (25°C, 500 MHz, C_6D_6): δ 6.67 (s, 4H, Ar-*H*), δ 5.98 (s, 2H, backbone C_2H_2), δ 2.10 (s, 6H, p-CH_3), δ 1.85 (s, 12H, o-CH_3), δ 1.54 (s, 27H, O-CH_3). **^{13}C-NMR** (25°C, 125.7 MHz, C_6D_6): 183.3 (N-*C*-N, pseudo-*dd* ($^1J_{^{13}C-^{109}Ag}$ = 253 Hz; $^1J_{^{13}C-^{107}Ag}$ = 220 Hz)), 139.0, 135.5, 134.3, 129.3, 121.6, 69.9, 32.1, 20.7, 17.2. **IR** (ATR-IR) [cm^{-1}] 3175/3130 (w, alkene C-H str.), 3000-2800 (m, C-H str.), 2733 (w, Mes C-H str.), 1487 (m, arom. C-C str.), 1357 (m, C-H bend.), 1234/1193 (m, C-O str.), 1000 (s, Si-O-C str.), 815/692 (m, Si-O str.). **Elemental Analysis** C: 58.64% H: 7.40% N: 4.14% (Calc.: 58.66% / 7.61% / 4.15%).

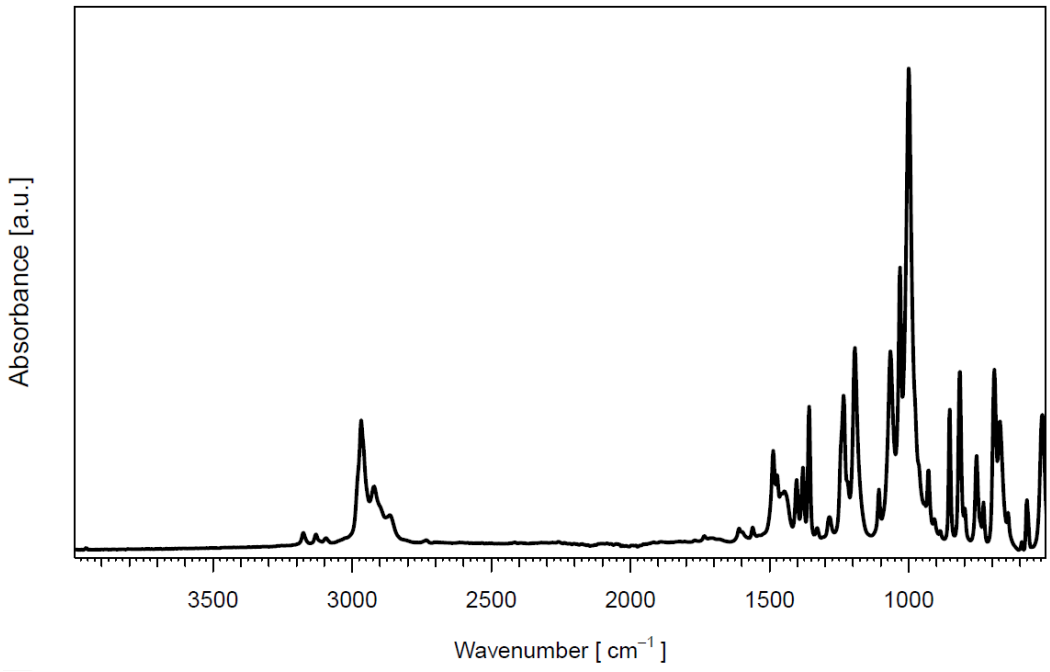

Figure S 36. ATR-IR spectrum of IMesAgOTBOS (**B-TBOS**) (264 scans)

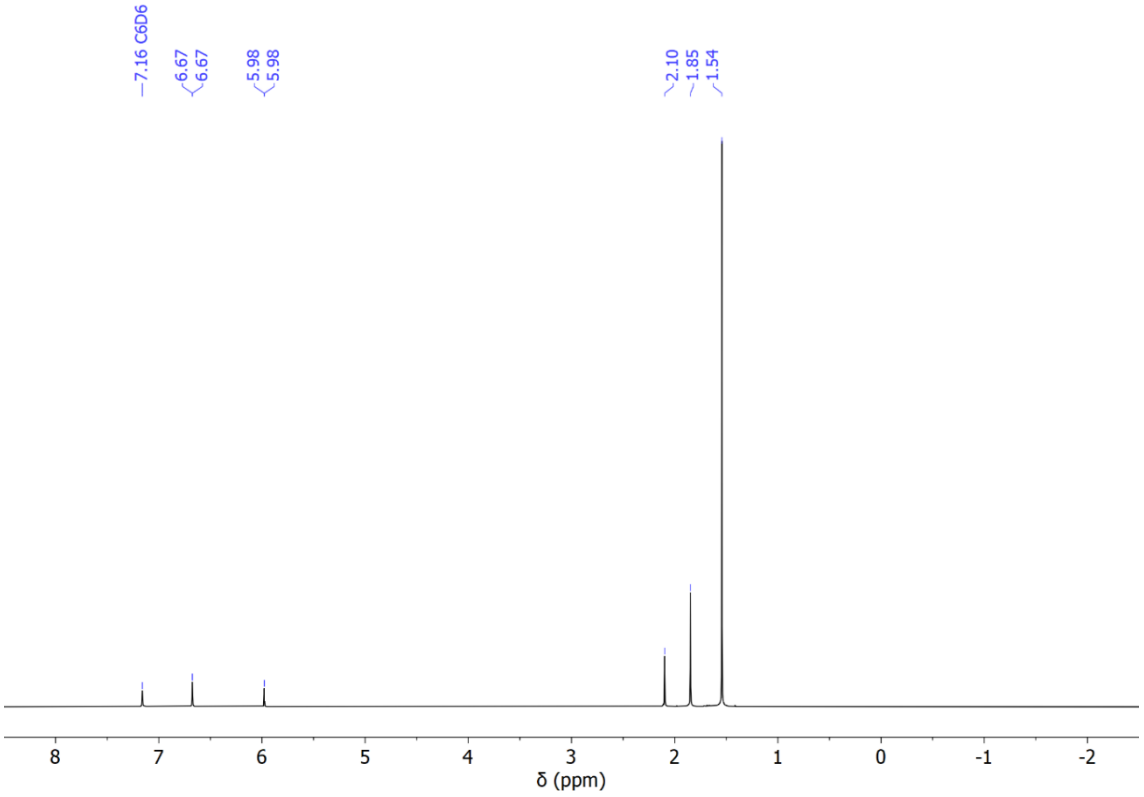

Figure S 37. ^{1}H NMR spectrum of IMesAgOTBOS (**B-TBOS**) recorded in C_6D_6 (500 MHz, 25°C).

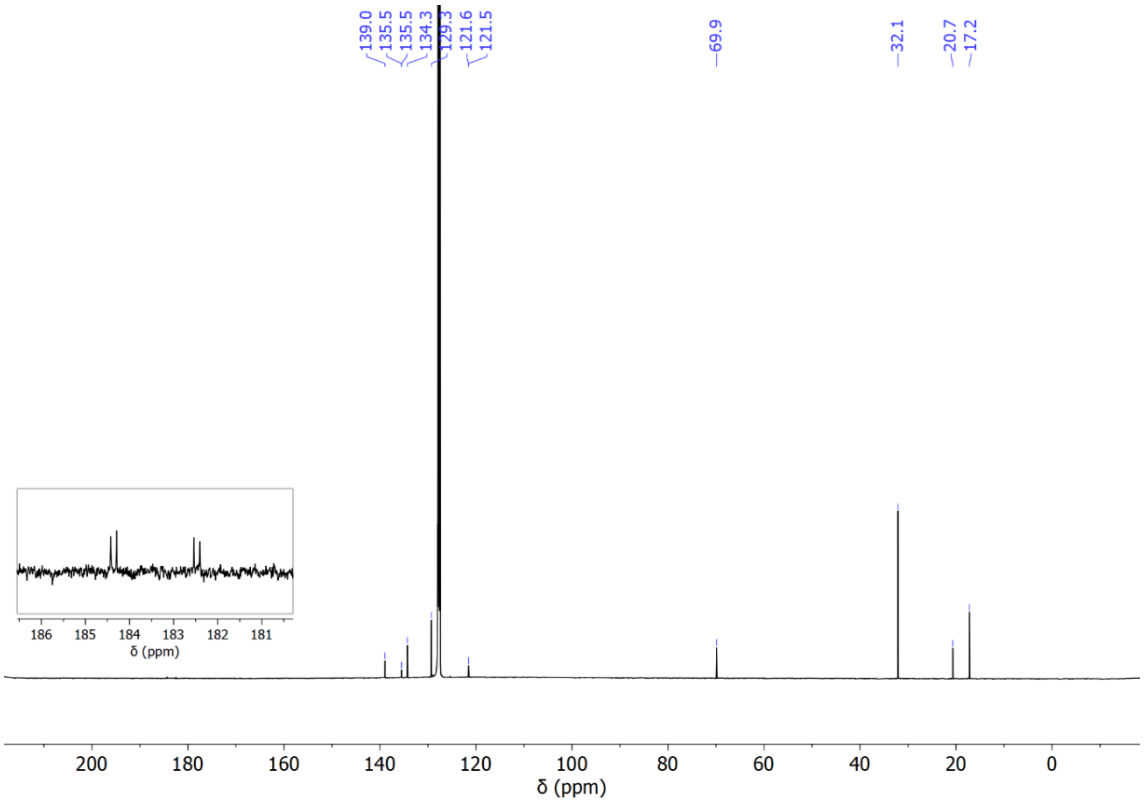

Figure S 38. ^{13}C NMR spectrum of IMesAgOTBOS (**B-TBOS**) recorded in C_6D_6 (125.7 MHz, 25°C). Zoomed region shown in inset shows coupling of carbene carbon to both isotopes of silver ($^{1}J_{^{13}C\text{-}^{109}Ag}$ = 253 Hz; $^{1}J_{^{13}C\text{-}^{107}Ag}$ = 220 Hz)

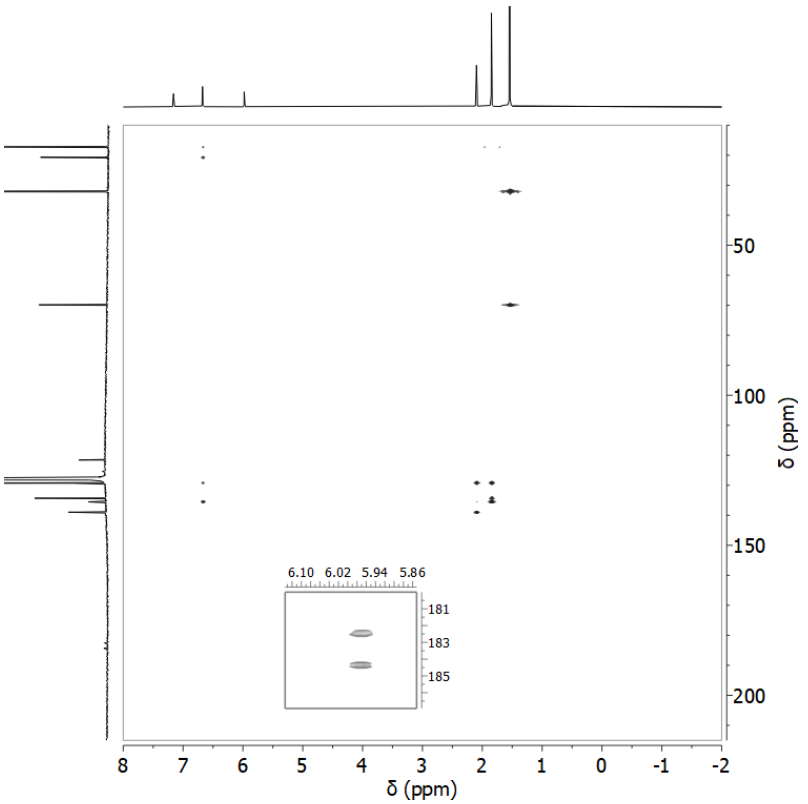

Figure S 39. IMesAgOTBOS (**B-TBOS**) ^{1}H-^{13}C HMBC (^{1}H: 500 MHz, ^{13}C: 125.7 MHz, C_6D_6, 298 K), inset shows region of interest containing carbene splitting.

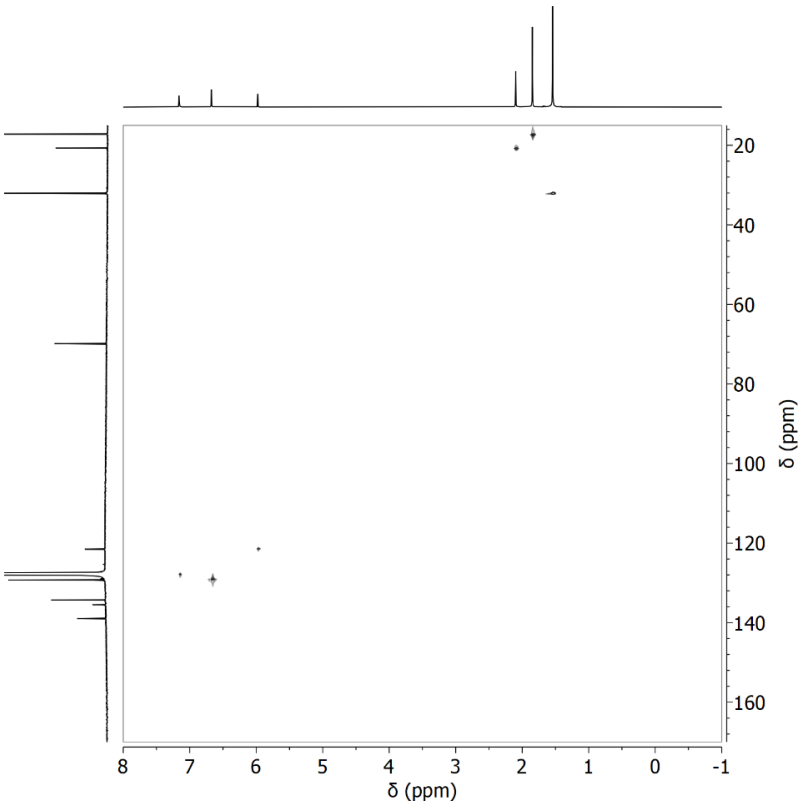

Figure S 40. IMesAgOTBOS (**B-TBOS**) ^{1}H-^{13}C HSQC (^{1}H: 500 MHz, ^{13}C: 125.7 MHz, C_6D_6, 298 K)

Preparation of Solid Supports

$SiO_{2\text{-}700}$: amorphous silicon dioxide partially dehydroxylated at 700 °C ($SiO_{2\text{-}700}$) was prepared according to literature procedure.[22] The Si-OH density was titrated to a value of 0.9 -OH nm^{-2} consistent with earlier reports. For calculations, the previously mentioned value is assumed. The preparation of the $SiO_{2\text{-}700}$ support is initiated via a calcination under static air at 500°C for 12h. The silica was allowed to return to room temperature and treated under high vacuum (10^{-5} mbar) at 500°C for 12 h (ramp: 5 °C min^{-1}) and then at 700 °C for 24 h (ramp: 1.7 °C min^{-1}).

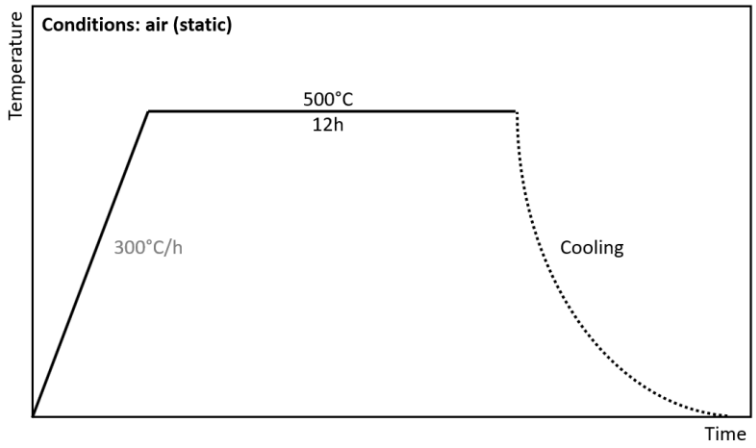

Figure S 41. Temperature profile for the calcination of SiO_2.

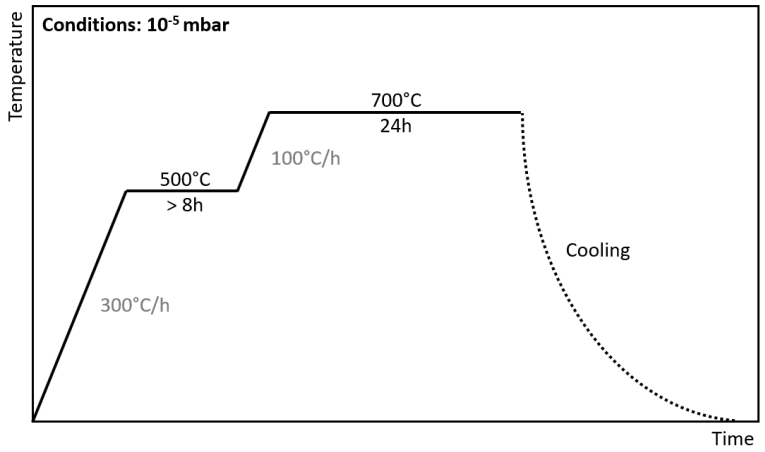

Figure S 42. Temperature profile for the high vacuum treatment of SiO_2 to form $SiO_{2\text{-}700}$.

γ-$Al_2O_{3\text{-}500}$: Gamma alumina partially dehydroxylated at 500 °C (γ-$Al_2O_{3\text{-}500}$) was prepared using an adapted literature procedure.[23] The compacted alumina powder was calcined in air at 500°C (5°C min^{-1}) for 4 h before being placed under high vacuum (10^{-5} mbar) for 12 h before being stored in an argon-filled glovebox. Reaction with dibenzyl magnesium results in liberation of 0.99 mmol toluene per gram of γ-$Al_2O_{3\text{-}500}$, consistent with the presence of 2.7 accessible OH nm^{-2}. Measured BET surface area: 216 $m^2\ g^{-1}$.

Preparation of HOSi(O^tBu)$_3$/γ-$Al_2O_{3\text{-}500}$: Prepared using an adapted literature procedure.[10] To a suspension of γ-$Al_2O_{3\text{-}500}$ (1.77 g, ca. 1.75 mmol –OH) in pentane (15 mL) was added a solution of HOSi(O^tBu)$_3$ (143 mg, 0.54 mmol) in pentane (8 mL). The resulting suspension was stirred at room temperature for 2 h before solvent was decanted, and the remaining solid was washed with pentane. The resulting solid was dried under vacuum and transferred to an argon-filled glovebox prior to further analysis.

Preparation of Si/γ-Al_2O_3: HOSi(O^tBu)$_3$/γ-$Al_2O_{3\text{-}500}$ was treated under high vacuum (10^{-5} mbar) at 300°C for 12 h (ramp: 5 °C min^{-1}). Elemental analysis: Measured BET surface area: 228 m^2 g^{-1}.

Grafting of SIMesAgMes (A-Mes) on various supports

Grafting of SIMesAgMes on $SiO_{2\text{-}700}$: To an amber 100 mL Schlenk was added $SiO_{2\text{-}700}$ (157 mg, 0.04 mmol OH) and 10 mL of benzene. To this was added SIMesAgMes (25.2 mg, 0.056 mmol) in a small amount of benzene and the reaction was stirred for 17 h. The silica was then washed with benzene (3 × 3 mL) and dried *in vacuo*. The completion of the reaction was checked by monitoring the produced mesitylene in NMR (liberation of approx. 0.047 mmol of Mesitylene observed (0.85 eq. per -OH)), showing near full conversion. Transmission IR indicates successful grafting (See Figure S 43 [Left]), as illustrated by the drop in intensity of the isolated –OH signal at 3747 cm^{-1} and the emergence of C-H stretching bands at approx. 3000 cm^{-1}. Elemental Analysis: Ag (2.75 wt%), C (6.92 wt%), H (0.70 wt%)

Grafting of SIMesAgMes on γ-$Al_2O_{3\text{-}500}$: To an amber 20 mL vial was added γ-$Al_2O_{3\text{-}500}$ (200 mg, 0.20 mmol OH) and 10 mL of benzene. To this was added SIMesAgMes (32 mg, 0.056 mmol) in benzene (4 mL) and the reaction was stirred for 17 h. The alumina was then washed with benzene (3 × 3 mL) and dried *in vacuo*. The completion of the reaction was checked by monitoring the produced mesitylene (0.048 mmol) in NMR, and only trace amounts of starting material, showing near full conversion. Transmission IR illustrates the emergence of C-H bending and stretching modes, as well as a reduction in intensity of the bands assigned to -OH at 3774 cm^{-1}, 3725 cm^{-1}, and 3726 cm^{-1}. Elemental Analysis: Ag (2.24 wt%), C (6.54 wt%), H (0.75 wt%)

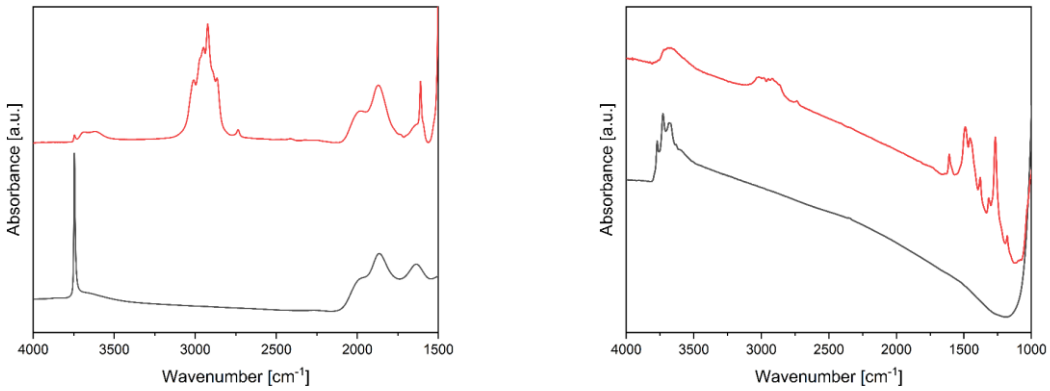

Figure S 43. [Left] Transmission IR of SIMesAgMes (**A-Mes**) grafted on silica (red) and unreacted $SiO_{2\text{-}700}$ (black) **[Right]** Transmission IR of SIMesAgMes (**A-Mes**) grafted on Alumina (red) and unreacted γ-$Al_2O_{3\text{-}500}$ (black).

Grafting of SIMesAgMes on Si/γ-$Al_2O_{3\text{-}500}$: To an amber 20 mL vial was added Si/γ-$Al_2O_{3\text{-}500}$ (203 mg) and 10 mL of benzene. To this was added SIMesAgMes (33 mg, 0.06 mmol) in benzene (4 mL) and the reaction was stirred for 2.5 h. The alumina was then washed with benzene (3 × 3 mL) and dried *in vacuo*. The completion of the reaction was checked by monitoring the produced mesitylene (0.048 mmol) in NMR, with the remaining starting material recovered. Transmission IR illustrates the emergence of C-H bending and stretching modes, as well as a reduction in intensity of the bands assigned to -OH at 3775 cm^{-1} and 3735 cm^{-1}. Elemental Analysis: Ag (1.55wt%), C (3.91 wt%), H (0.90 wt%)

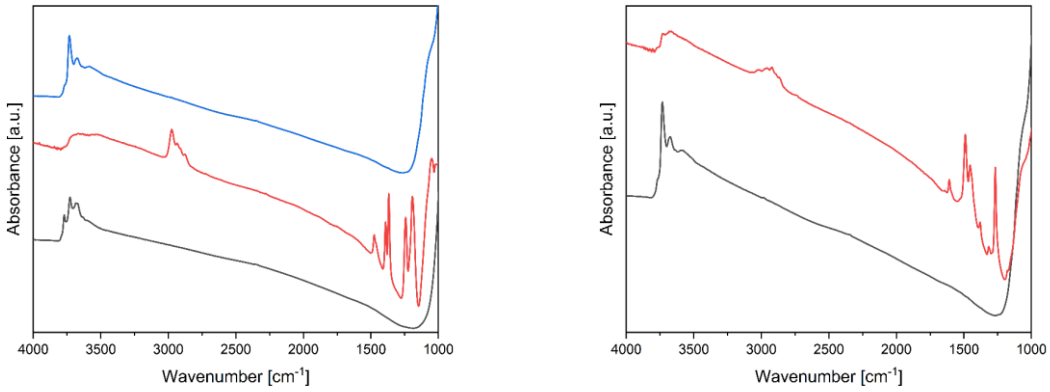

Figure S 44. [Left] Transmission IR of unreacted γ-$Al_2O_{3\text{-}500}$ (black), $HOSi(O^tBu)_3$/γ-$Al_2O_{3\text{-}500}$ (red) and Si/γ-$Al_2O_{3\text{-}500}$ (blue) **[Right]** Transmission IR of SIMesAgMes (**A-Mes**) grafted on Si/γ-$Al_2O_{3\text{-}500}$ (red) and unreacted Si/γ-$Al_2O_{3\text{-}500}$ (black).

S3 ^{109}Ag Solution-state NMR

Solution ^{109}Ag NMR data was collected as 2-dimensional spectra (^{1}H/^{109}Ag) using a gradient-enhanced HMQC sequence. The delay between pulses on X was set based on observed J-couplings from the corresponding ^{1}H spectrum. The determination of the isotropic chemical shift was performed from slices taken from the respective spectra. To ensure that signals were not folded or reflected, samples were measured with multiple carrier frequencies and spectral widths in the indirect dimension.

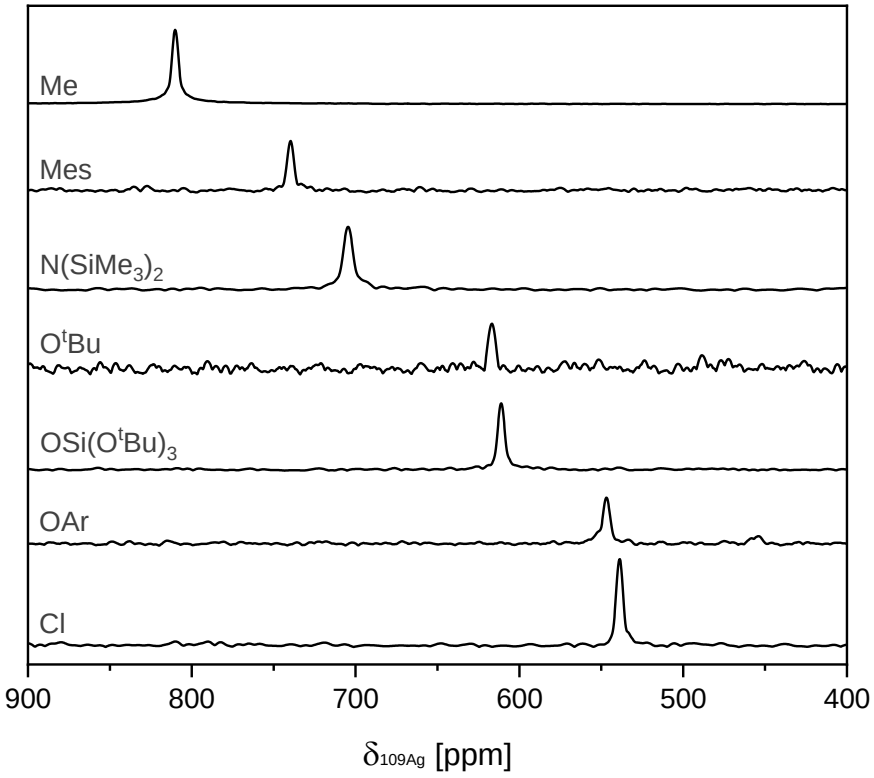

Figure S 45. Superimposed slices containing the ^{109}Ag signals for all saturated compounds: SIMesAgCl (**A-Cl**), SIMesAgOAr (**A-BHT**), SIMesAgOTBOS (**A-TBOS**), SIMesAgO^{t}Bu (**A-OtBu**), SIMesAgHMDS (**A-HMDS**), SIMesAgMes (**A-Mes**), SIMesAgMe (**A-Me**).

Table S 1. Experimental chemical shifts of ^{109}Ag, Carbene ^{13}C and the J couplings to the carbene C.

Compound	δ_{109Ag} [ppm]	$\delta_{13C,\ Carbene}$ [ppm]	$^{1}J_{13C\text{-}Ag}$ [Hz]
IMesAgCl (**B-Cl**)	548	183	-
IMesAgMes (**B-Mes**)	744	191	127
IMesAgOTBOS (**B-TBOS**)	617	183	237
SIMesAgCl (**A-Cl**)	539	208	217
SIMesAgMes (**A-Mes**)	740	214	122
SIMesAgO^{t}Bu (**A-OtBu**)	617	208	213
SIMesAgOTBOS (**A-TBOS**)	611	208	222
SIMesAgHMDS (**A-HMDS**)	705	209	190
SIMesAgMe (**A-Me**)	810	214	-
SIMesAgOAr (**A-BHT**)	547	207	240

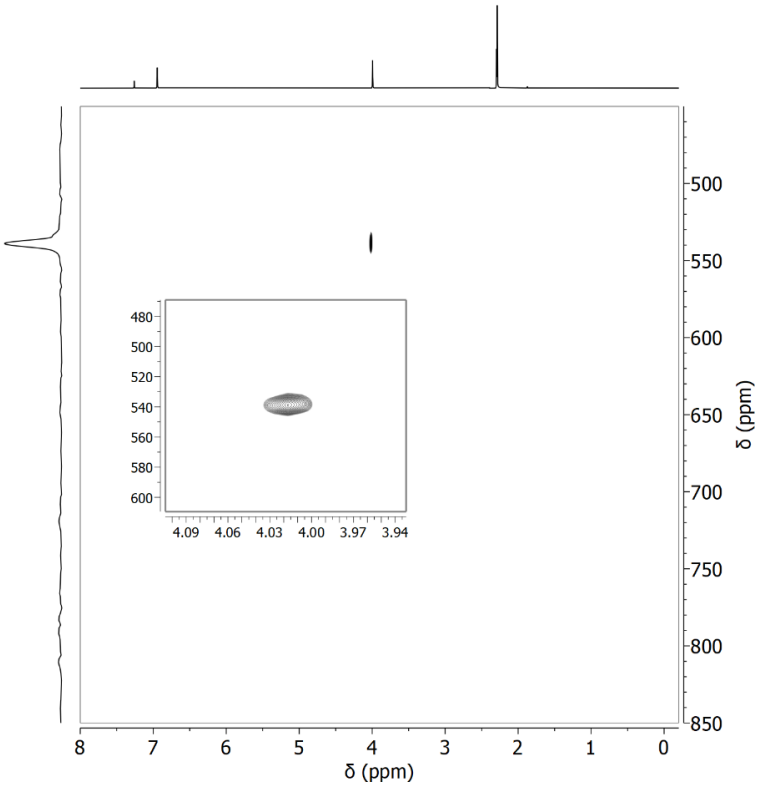

Figure S 46. SIMesAgCl (**A-Cl**) ^{1}H-^{109}Ag HMQC (^{1}H: 500.3 MHz, ^{109}Ag: 23.3 MHz, C_6D_6, 298 K), insets show the region of interest containing the silver/proton cross-peak.

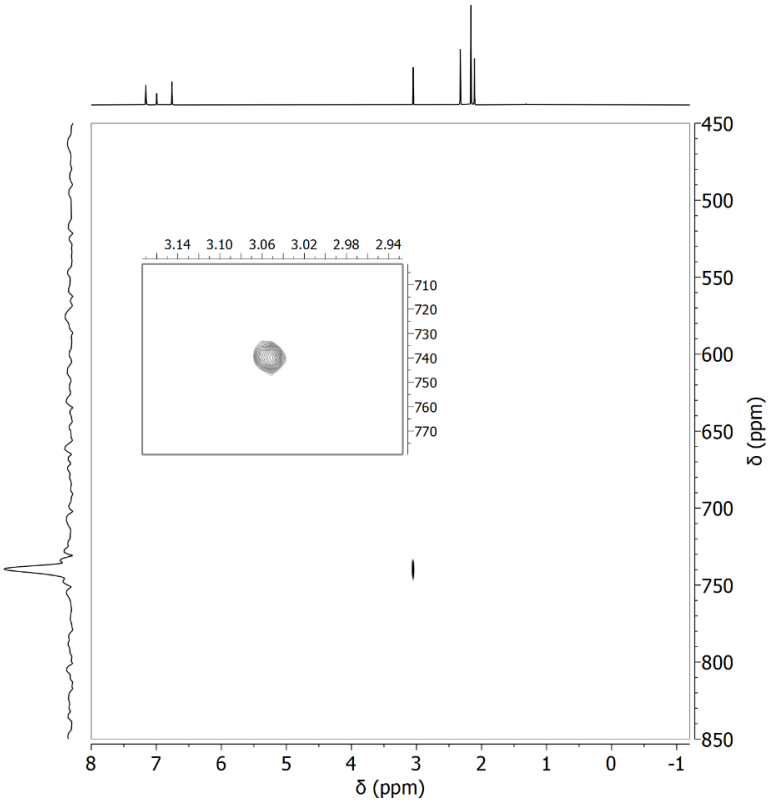

Figure S 47. SIMesAgMes (**A-Mes**) ^{1}H-^{109}Ag HMQC (^{1}H: 500.3 MHz, ^{109}Ag: 23.3 MHz, C_6D_6, 298 K), insets show the region of interest containing the silver/proton cross-peak.

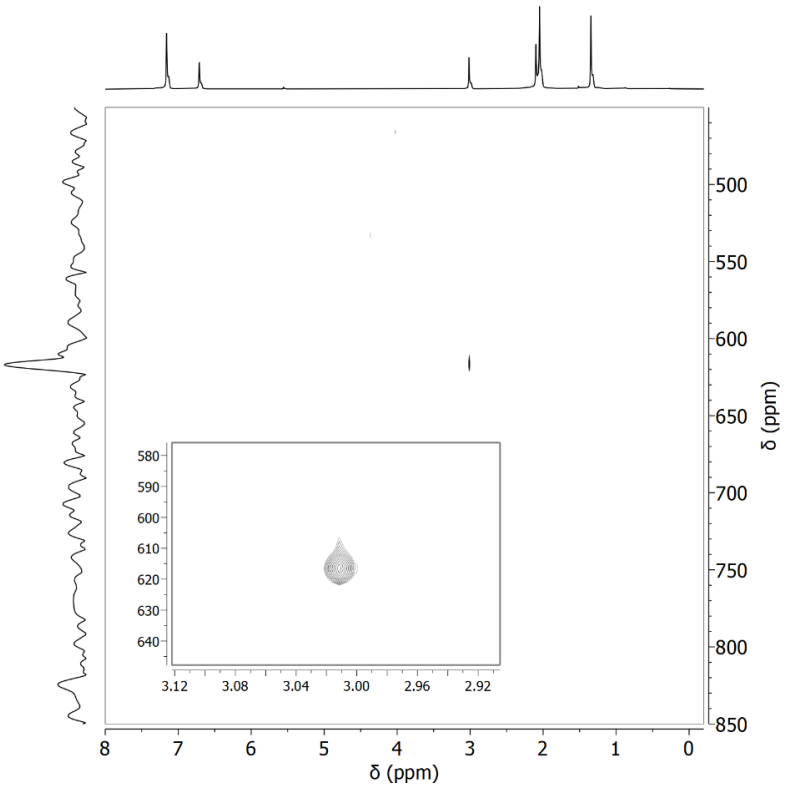

Figure S 48. SIMesAgO^{t}Bu (**A-OtBu**) ^{1}H-^{109}Ag HMQC (^{1}H: 500.3 MHz, ^{109}Ag: 23.3 MHz, C_6D_6, 298 K), insets show the region of interest containing the silver/proton cross-peak.

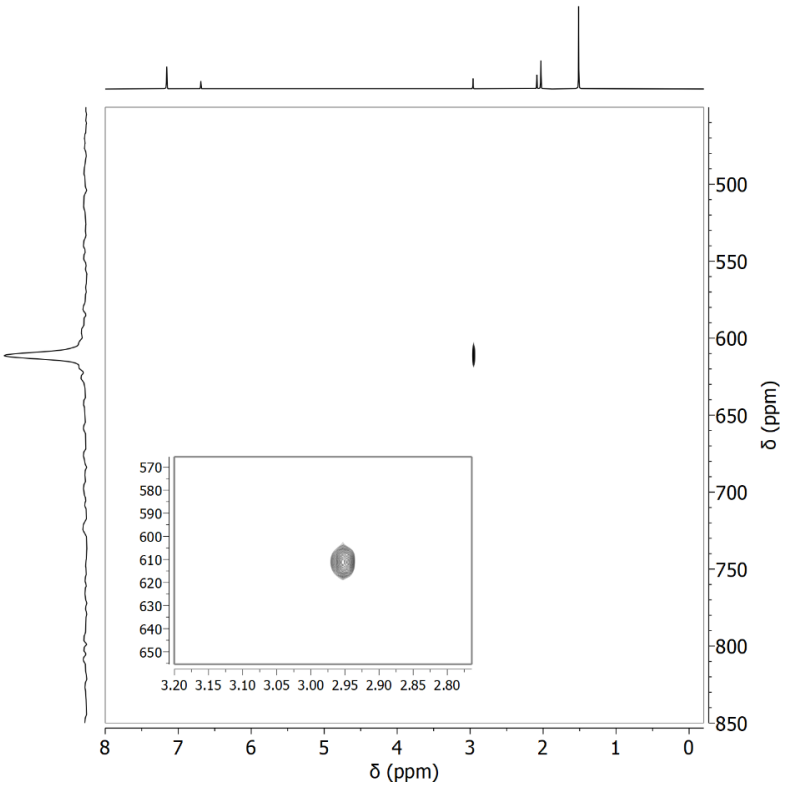

Figure S 49. SIMesAgOTBOS (**A-TBOS**) ^{1}H-^{109}Ag HMQC (^{1}H: 500.3 MHz, ^{109}Ag: 23.3 MHz, C_6D_6, 298 K), insets show the region of interest containing the silver/proton cross-peak.

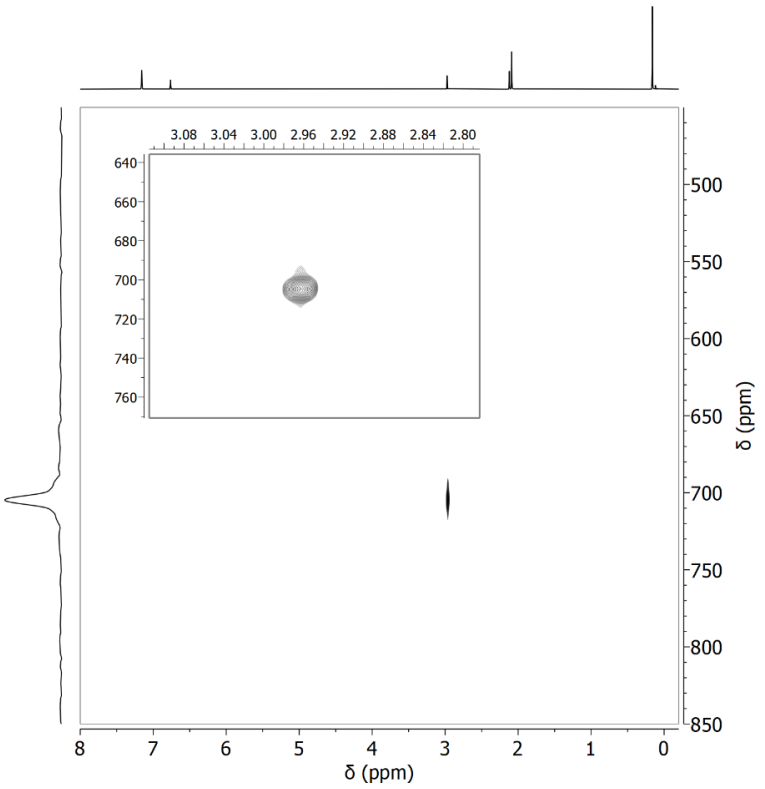

Figure S 50. SIMesAgHMDS (**A-HMDS**) ^{1}H-^{109}Ag HMQC (^{1}H: 500.3 MHz, ^{109}Ag: 23.3 MHz, C_6D_6, 298 K), insets show the region of interest containing the silver/proton cross-peak.

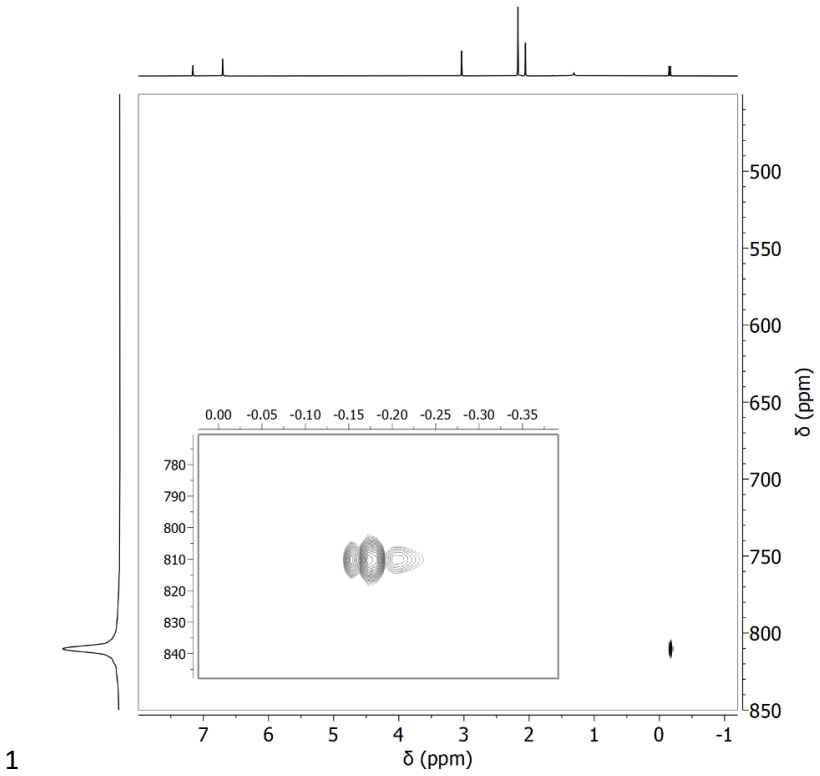

1

Figure S 51. SIMesAgMe (**A-Me**) ^{1}H-^{109}Ag HMQC (^{1}H: 500.3 MHz, ^{109}Ag: 23.3 MHz, C_6D_6, 298 K), insets show the region of interest containing the silver/proton cross-peak.

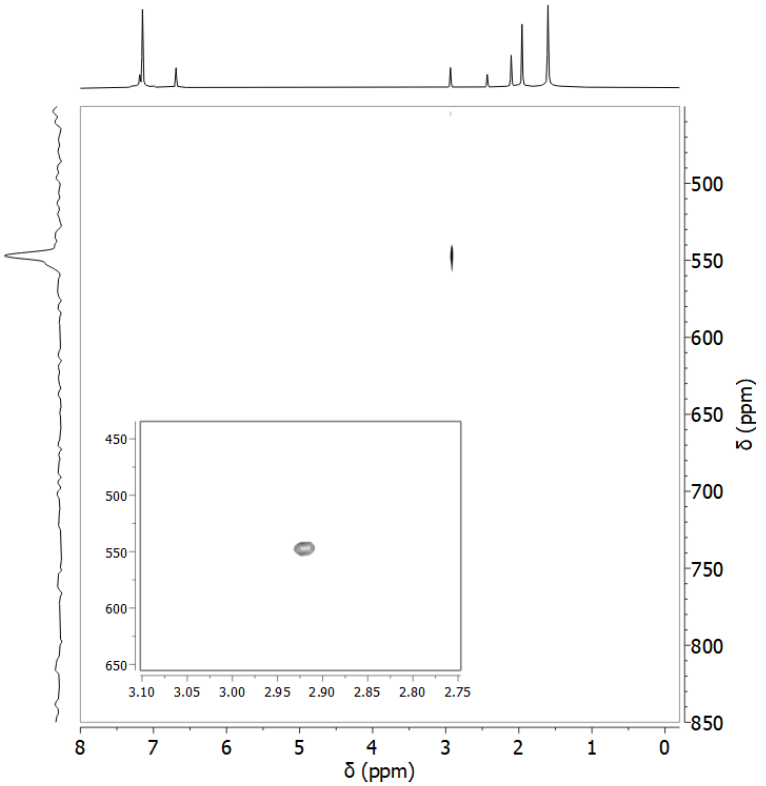

Figure S 52. SIMesAgOAr (**A-BHT**) ^{1}H-^{109}Ag HMQC (^{1}H: 500.3 MHz, ^{109}Ag: 23.3 MHz, C_6D_6, 298 K), insets show the region of interest containing the silver/proton cross-peak.

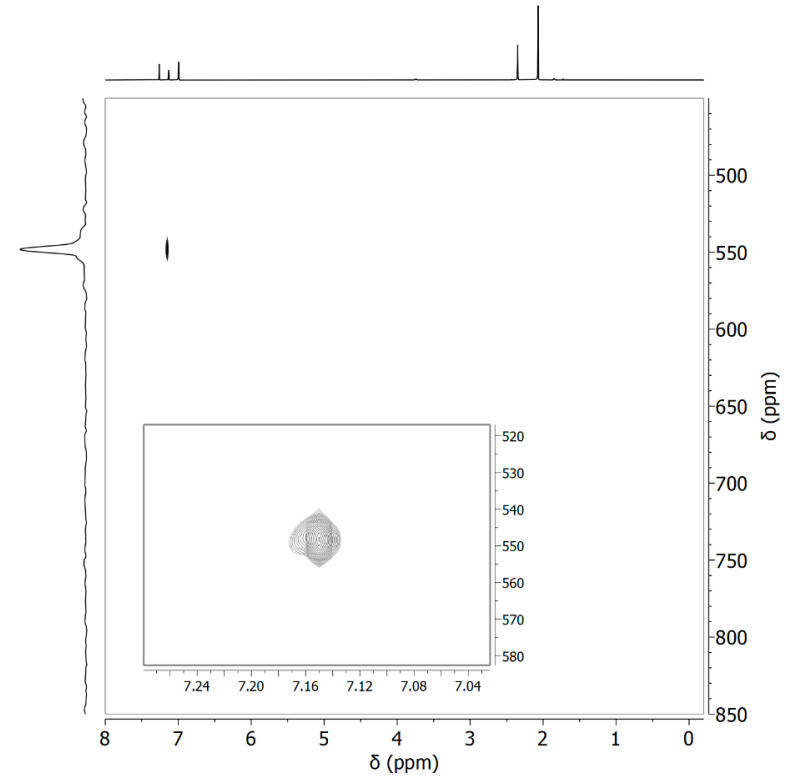

Figure S 53. IMesAgCl (**B-Cl**) ^{1}H-^{109}Ag HMQC (^{1}H: 500.3 MHz, ^{109}Ag: 23.3 MHz, C_6D_6, 298 K), insets show the region of interest containing the silver/proton cross-peak.

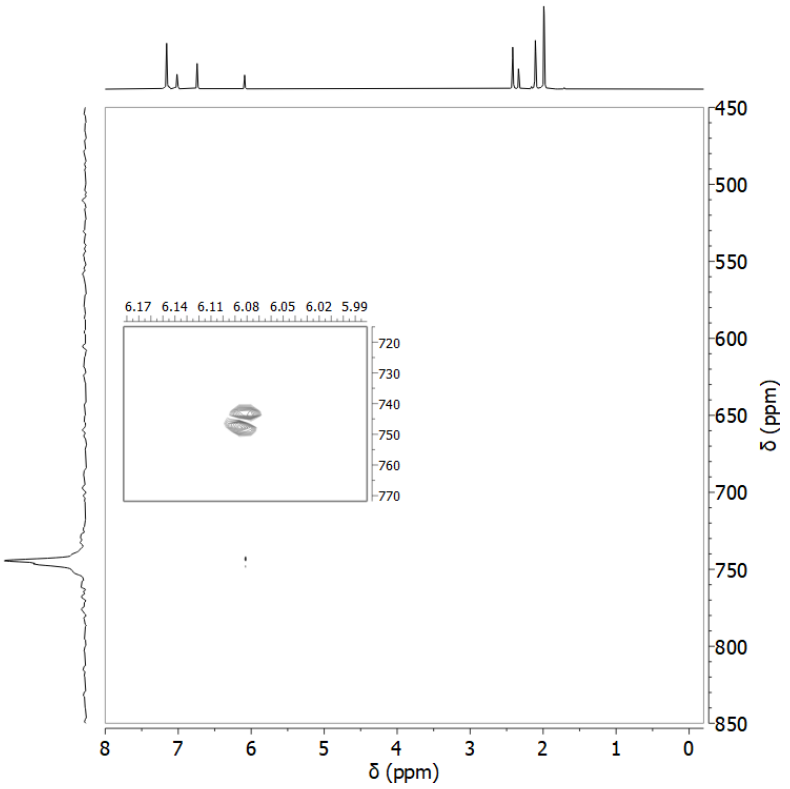

Figure S 54. IMesAgMes (**B-Mes**) ^{1}H-^{109}Ag HMQC (^{1}H: 500.3 MHz, ^{109}Ag: 23.3 MHz, C_6D_6, 298 K), insets show the region of interest containing the silver/proton cross-peak.

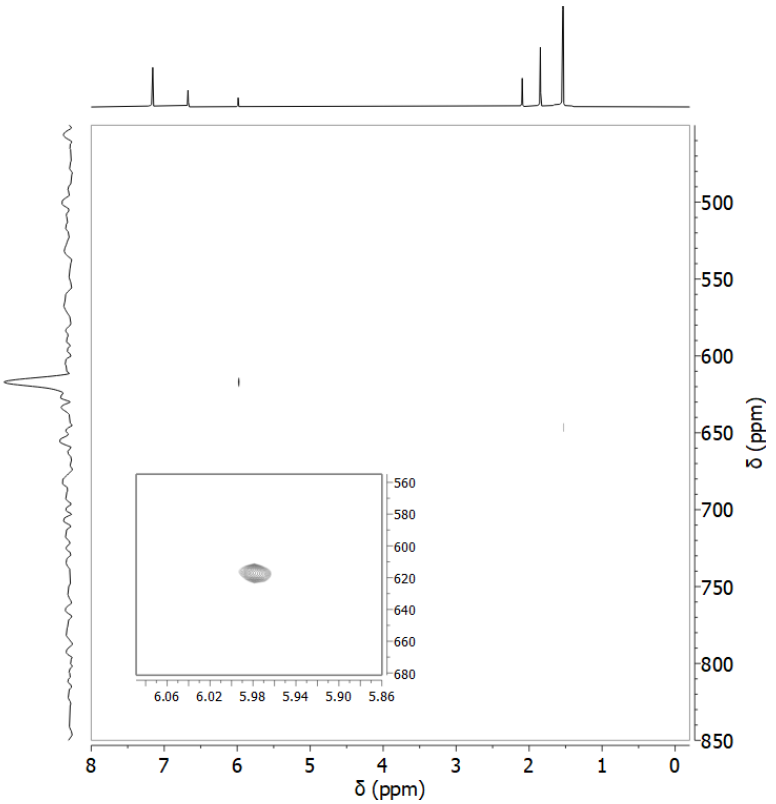

Figure S 55. IMesAgOTBOS (**B-TBOS**) ^{1}H-^{109}Ag HMQC (^{1}H: 500.3 MHz, ^{109}Ag: 23.3 MHz, C_6D_6, 298 K), insets show the region of interest containing the silver/proton cross-peak.

S4 Solid-State-NMR

^{109}Ag Solid-state NMR

Table S 2. Parameters for the fits of ^{109}Ag solid state NMR spectra of the grafted materials.

Compound	δ_{iso} [ppm]	Ω [ppm]	κ	width
SIMesAg-SiO_2	569	1368	0.26	60.2
SIMesAg-Al_2O_3	598	1393	0.26	58.5
SIMesAg- Si/Al_2O_3 (1st species)	549	1453	0.26	44.7
SIMesAg- Si/Al_2O_3 (2nd species)	584	1458	0.26	35.4

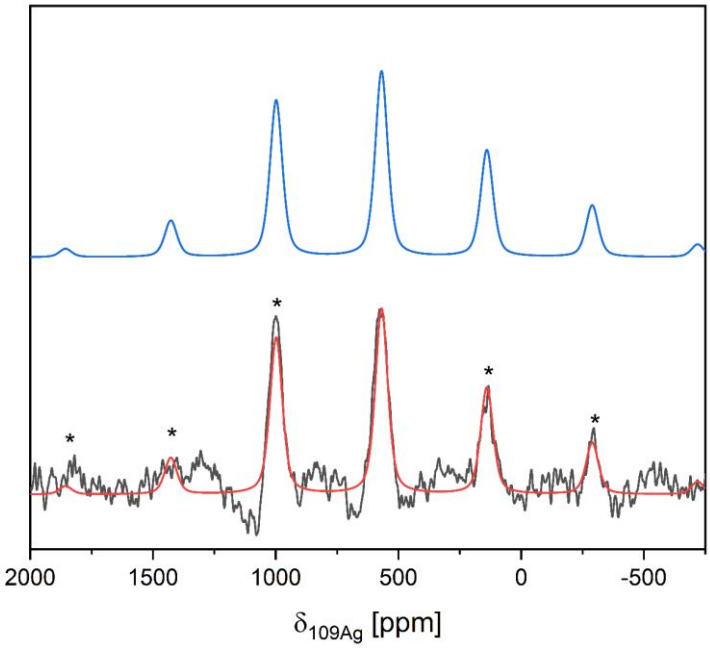

Figure S 56. SS-NMR of **(SIMes)Ag@SiO_2** (8kHz). [Bottom] Spectrum and overlayed fit. [Top] Fitted spectrum. Spinning sidebands are indicated with asterisk. Expt details: 77k scans, d1 = 1.8 seconds (expt time: 40 hours, ε_H= 16

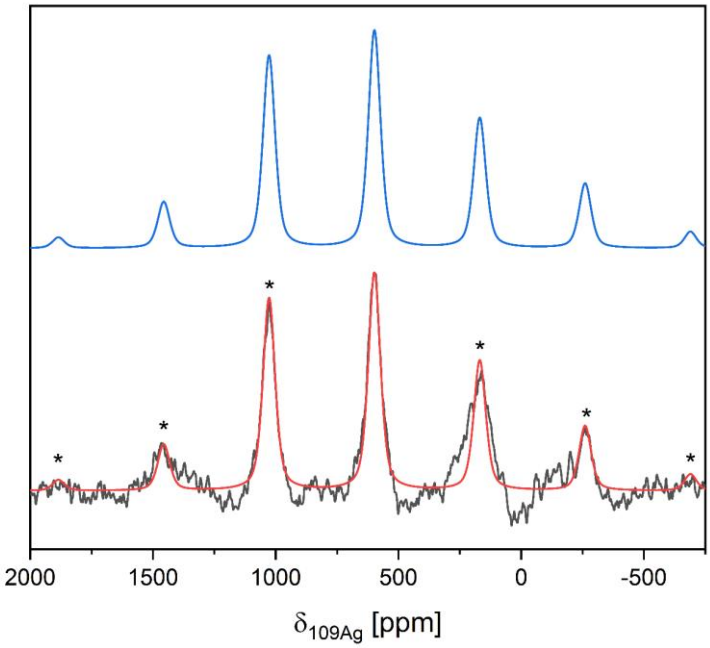

Figure S 57. SS-NMR of **(SIMes)Ag@γ-Al_2O_3** (8kHz). [Bottom] Spectrum and overlayed fit. [Top] Fitted spectrum. Spinning sidebands are indicated with asterisk. Expt details: 86k scans, d1 = 1.7 seconds expt time: 40 hours, ε_H= 16

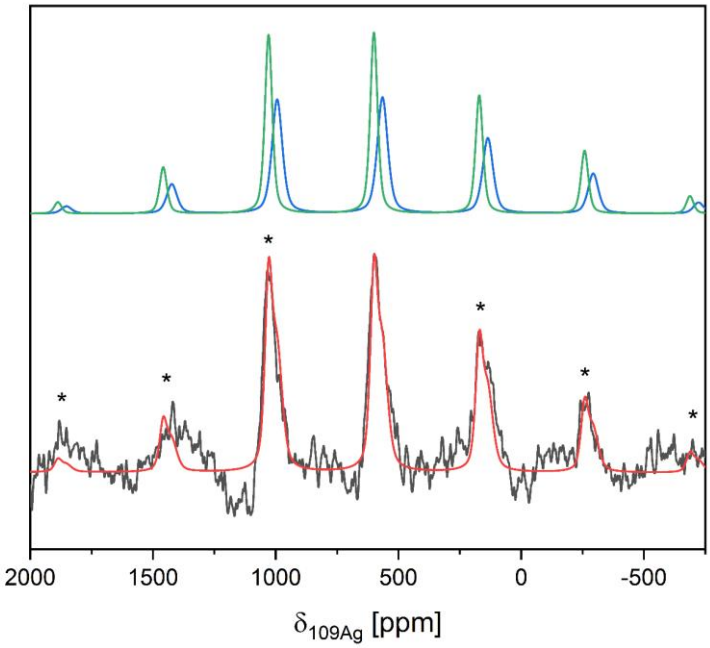

Figure S 58. SS-NMR of **(SIMes)Ag@Si/γ-Al_2O_3** (8kHz). [Bottom] Spectrum and composite fit. [Top] Decomposed fit. Spinning sidebands are indicated with asterisks. Expt details: 226k scans, d1 = 1.9 seconds (expt time: 5 days, ε_H= 9

^{29}Si-NMR of oxide materials

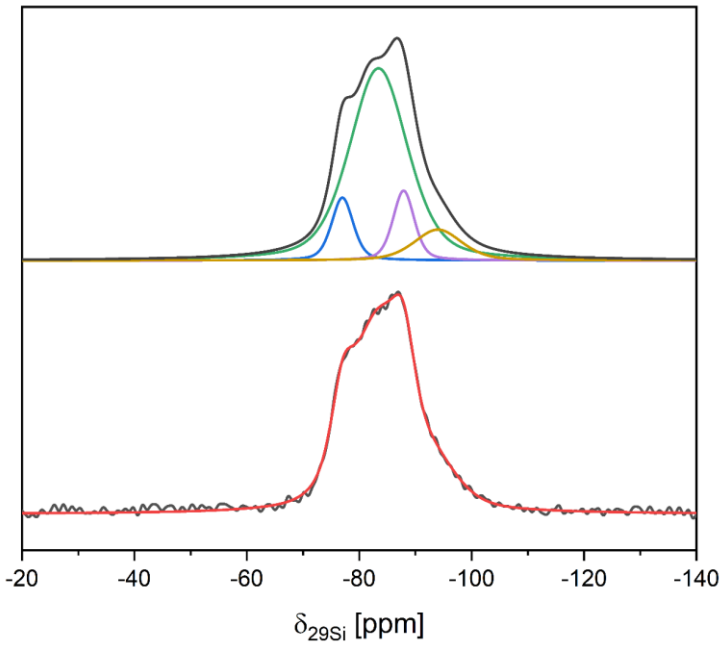

Figure S 59. DNP-enhanced ^{29}Si-NMR spectrum of Si/Al_2O_3 with fit. Expt details: 5848 scans, d1 = 9.75 seconds (expt time: 16 hours), S/N = 40, MAS = 10 kHz, T = 109 K, ε_H= 16.

Site	1a	2	3	4
δ_{iso} / ppm	-77	-83	-88	-94
Area	9	72	10	9

While the measurement shown is not quantitative in nature (due to the use of CP/DNP) it is possible to draw qualitative conclusions on the basis of this spectrum and the earlier literature.[10, 11] For the fit used, 4 separate sites are modelled. The sum of the sites shown reproduce the experimental lineshape well, with peaks centred at -77, -83, -88 and -94 ppm fitted. Notably, the dominant peaks at higher chemical shift are indicative of Si atoms bound through multiple O-Al or O-H linkages (i.e. $Q^n(x\text{Al})$ sites where n ≤ 3, and Al ≤ 1). More generally, this suggests that in this material the Si that are introduced during the synthesis are well-dispersed in nature and interact intimately with the Al_2O_3 surface. Moreover, the absence of observed peaks below -90 ppm indicate that only a small fraction of Q_4(2Al), Q_4(1Al), Q_4(0Al), Q3(0Al) or Q_2(0Al) can be present in the material.[24, 25]

^{15}N-NMR of pyridine-adsorbed oxide materials

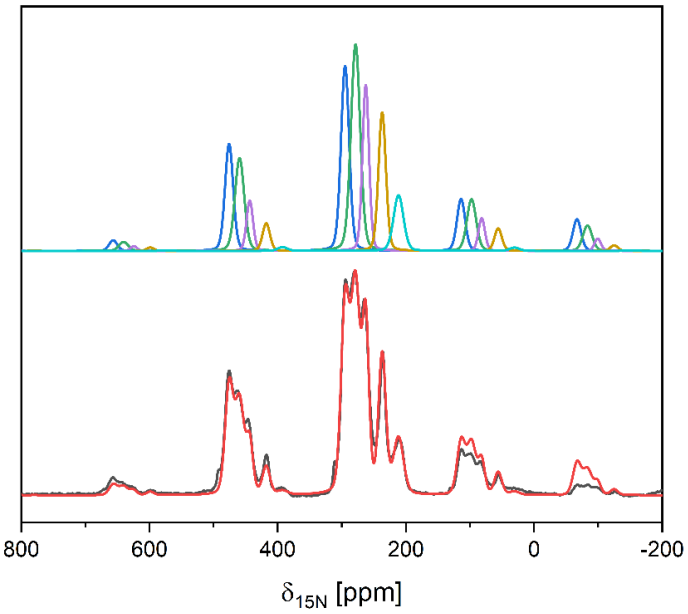

Figure S 60. Full spectrum (^{15}N-py)/Si/γ-Al_2O_3: 11 kHz 2048 scans, d1 = 5 seconds (expt time: 3 hours), T = 114 K, S/N 180, ε_H= 14

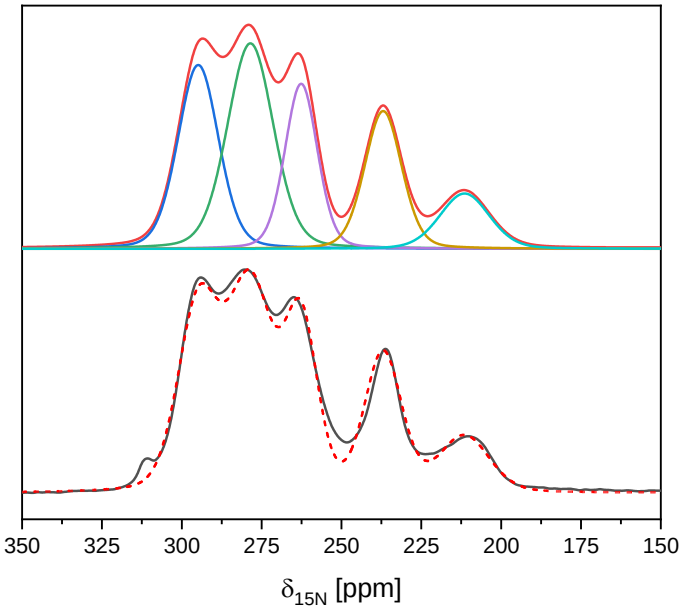

Figure S 61. Zoom of region containing isotropic signals for (^{15}N-py)/Si/γ-Al_2O_3: 11 kHz 2048 scans, d1 = 5 seconds (expt time: 3 hours), T = 114 K, S/N 180, ε_H= 14

Table S 3. Fitted parameters for (^{15}N-py)/Si/γ-Al_2O_3 used for fit depicted in **Figure S 61**

Site	1a	1b	1c	2	3
δ_{iso} / ppm	295	279	263	237	211
Ω / ppm	414	402	357	320	175
κ	0.95	0.69	0.55	0.27	0.27
Assignment	*Py Adsorbed on Al_2O_3*	*Py Adsorbed on Al_2O_3*	*Py Adsorbed on Al_2O_3*	*Lewis acid*	*Pyridinium (Brønsted acid)*

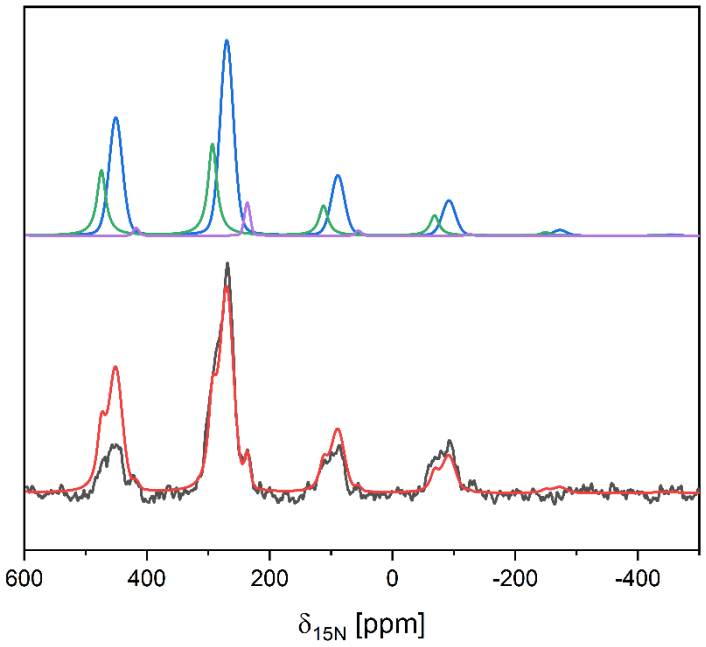

Figure S 62. (^{15}N-py)/(SIMes)Ag/Si/γ-Al_2O_3: 11 kHz, 2048 scans, d1 = 1.8 seconds (expt time: 1 hour), T = 112 K, S/N 30, ε_H= 8

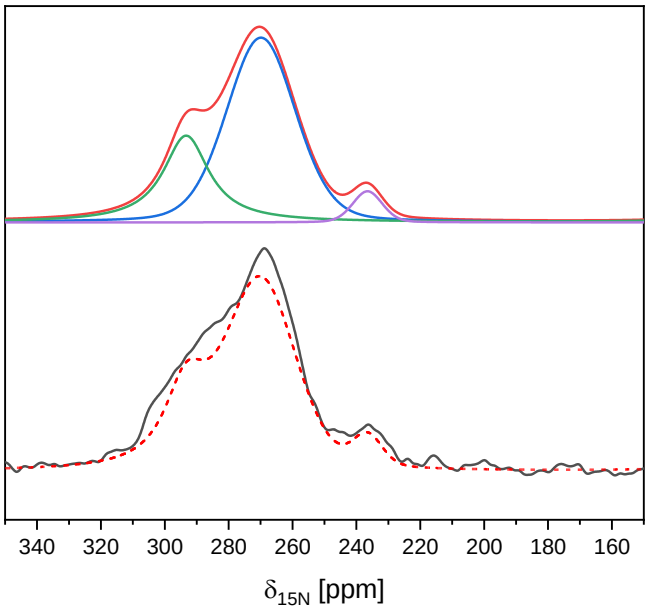

Figure S 63. Zoom of region containing isotropic signals for (^{15}N-py)/(SIMes)Ag/Si/γ-Al_2O_3: 11 kHz, 2048 scans, d1 = 1.8 seconds (expt time: 1 hour), T = 112 K, S/N 30, ε_H= 8

Table S 2. Fitted parameters for (^{15}N-py)/(SIMes)Ag/Si/γ-Al_2O_3 used for fit depicted in **Figure S 63**

Site	**1a**	**2**	**3**
δ_{iso} / ppm	293	270	237
Ω / ppm	460	451	309
κ	0.85	0.69	0.69
Assignment	*Py Adsorbed on Al_2O_3*	*Py Adsorbed on Al_2O_3*	*Lewis acid*

DNP-enhanced ^{15}N NMR spectroscopy of adsorbed ^{15}N-enriched pyridine (^{15}N-py) on Si/γ-Al_2O_3 (**Figure S 60**, **Figure S 61**) gives rises to five signals with distinct isotropic chemical shift (295, 279, 263, 237 and 211 ppm – Table 1), indicating the presence of pyridine interacting with hydroxyl groups on Al_2O_3 (δ_{iso} = 295, 279 and 263ppm), pyridine bound to strong Lewis acidic Al sites (Al_{LA}) (δ_{iso} = 237 ppm) and pyridinium (δ_{iso} = 211 ppm), associated with the presence of Brønsted acidic sites that arise from silanols interacting directly with adjacent Al sites, Al-(μ^2-OH)-Si. The isotropic chemical shift of peaks at 295, 279, 263 and 237 ppm are consistent with the chemical shifts reported for γ-Al_2O_3.[13] The emergence of a 5th peak at 211 ppm is consistent with the formation of pyridinium,[15, 26, 27] suggesting that strong Brønsted acid sites are present in this material - consistent with earlier reports for silicated

alumina materials. Analysis of the corresponding grafted sample ((^{15}N-py)/(SIMes)Ag/Si/γ-Al_2O_3, **Figure S 62**) results in a different line shape. The most notable difference before and after grafting of (SIMes)Ag(Mes), is the absence of a resolved peak at 211 ppm, which is presumably due to the facile reactivity of the strong Brønsted acid site with the Ag-C bond of (SIMes)Ag(Mes). It is also notable that the overall profile of the region assigned to pyridine interacting with hydroxyl groups on Al_2O_3. Overall, the observations are consistent with observations from IR spectroscopy, where selective grafting is inferred based on the disappearance of peaks at 3775 cm^{-1} and 3735 cm^{-1} (**Figure S 44**).

^{13}C-NMR of (SIMes)Ag@Al_2O_3

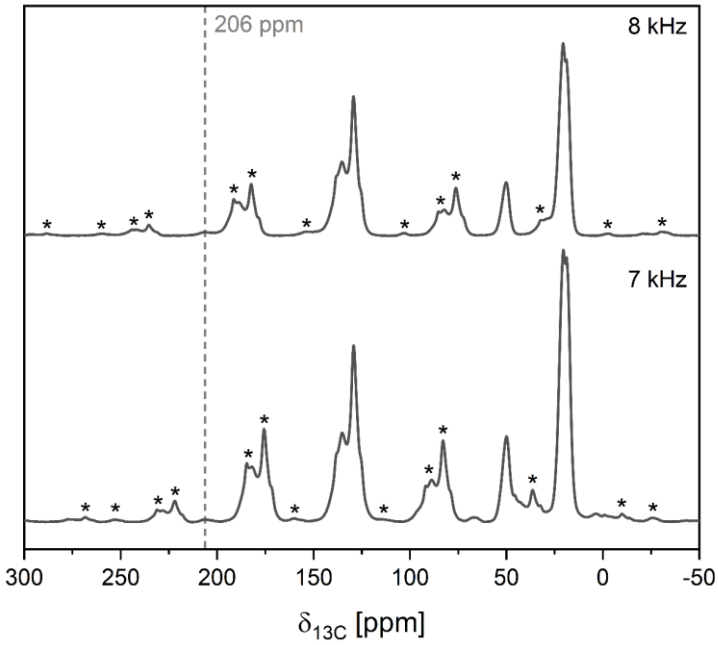

Figure S 64. DNP-enhanced ^{13}C NMR of (SIMes)Ag@Al_2O_3. 7 kHz MAS: 32768 scans, d1 = 2.5 seconds (expt time: 23 hours), T = 111 K, S/N ca. 1250. 8 kHz MAS: 21712 scans, d1 = 2.5 seconds (expt time: 15 hours), T = 111 K, S/N ca. 1100. $\varepsilon_H \approx 7$.

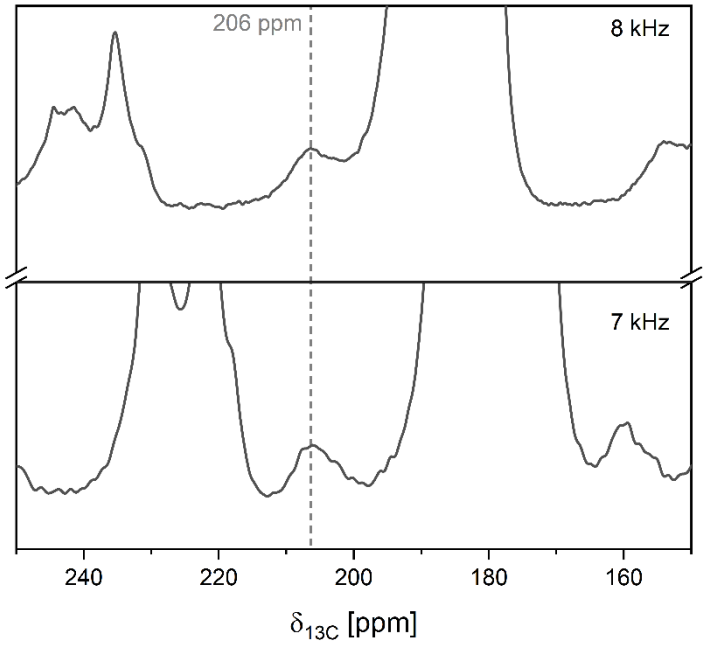

Figure S 65. Zoom of DNP-enhanced ^{13}C NMR of (SIMes)Ag@Al_2O_3. 7 kHz MAS: 32768 scans, d1 = 2.5 seconds (expt time: 23 hours), T = 111 K, S/N ca. 1250. 8 kHz MAS: 21712 scans, d1 = 2.5 seconds (expt time: 15 hours), T = 111 K, S/N ca. 1100. $\varepsilon_H \approx 7$.

The retention of the peak at 206 ppm in ^{13}C indicates the presence of (SIMes)Ag-O linkage and retention of (SIMes)Ag fragment. Measurement at multiple spinning speeds confirms that this signal is an isotropic signal. Notably, no resonances associated with either the free carbene (244 ppm) or the corresponding imidazolinium salts (ca. 160 ppm) are observed. In combination with analysis of washings during grafting, this ^{13}C NMR measurement provides evidence that the mode of reactivity for (SIMes)AgMes with oxides is through protonolysis of the Ag-Mes bond.[28-30]

S5 XRD Studies

Crystal Structures

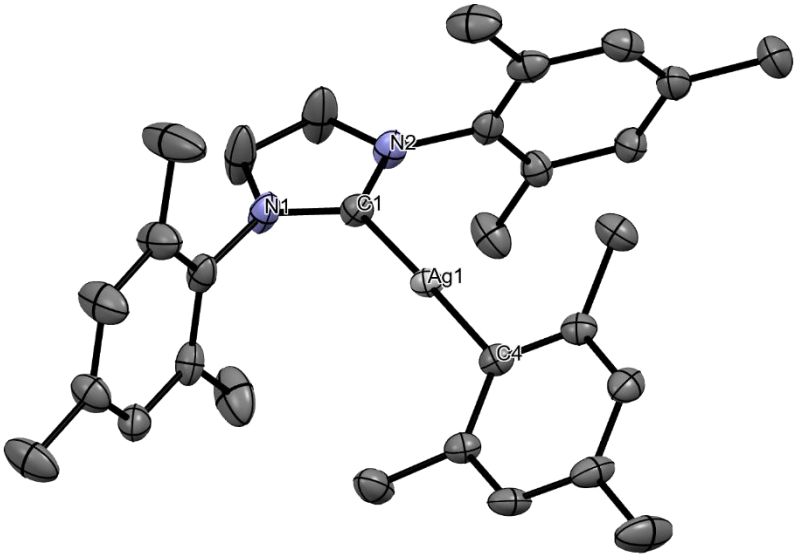

Figure S 66. Crystal structure for IMesAgMes (**B-Mes**). Ellipsoids shown at 50% probability, hydrogens omitted for clarity. (Co-crystallized Toluene omitted for clarity)

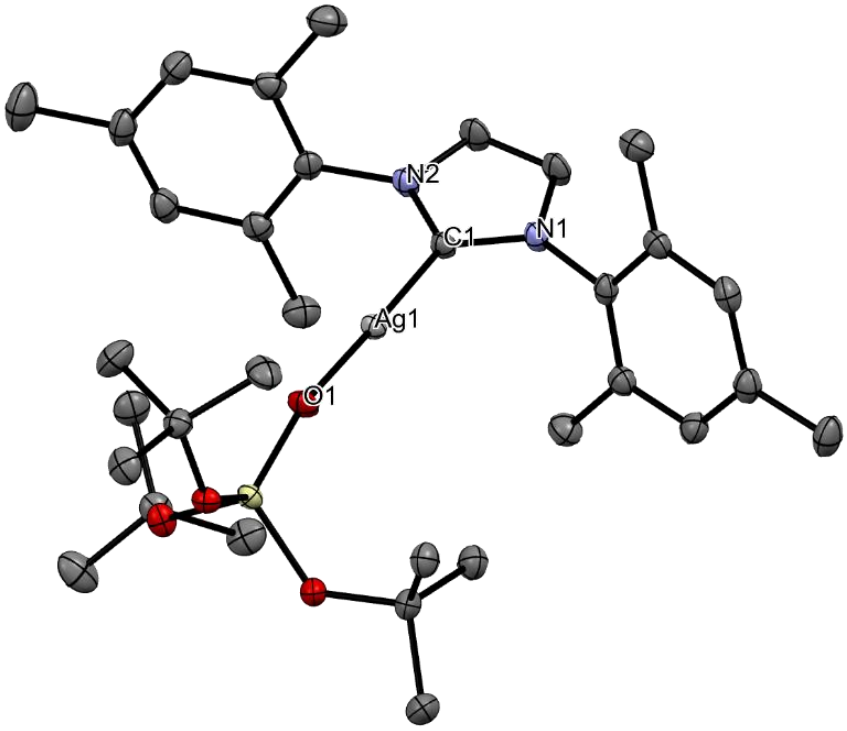

Figure S 67. Crystal structure for IMesAgOTBOS (**B-TBOS**). Ellipsoids shown at 50% probability, hydrogens omitted for clarity.

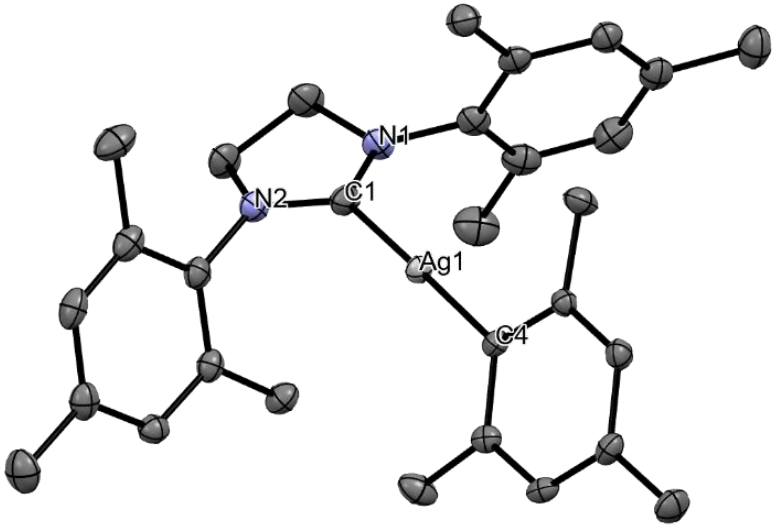

Figure S 68. Crystal structure for SIMesAgMes (**A-Mes**). Ellipsoids shown at 50% probability, hydrogens omitted for clarity.

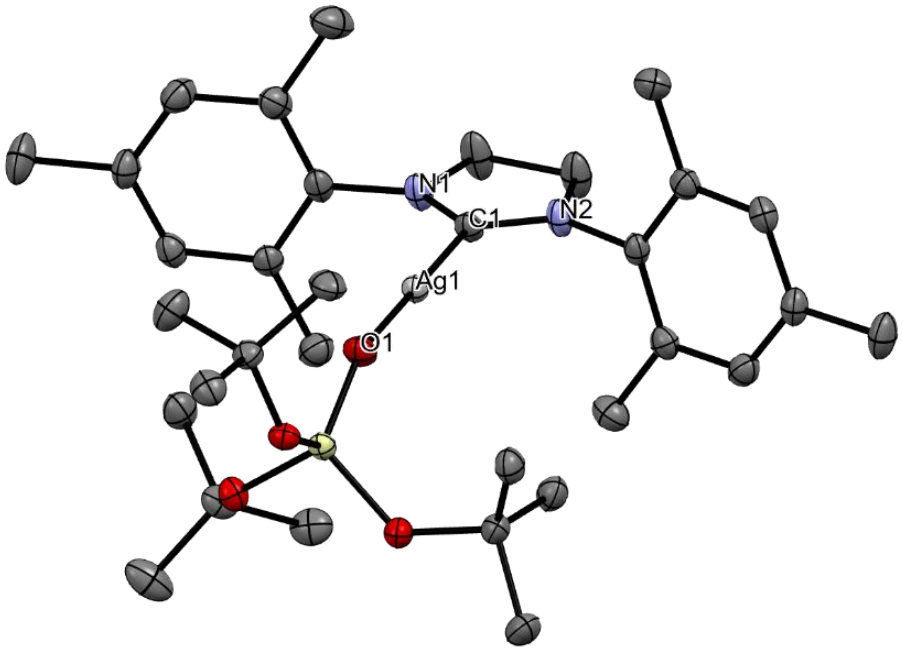

Figure S 69. Crystal structure for SIMesAgOTBOS (**A-TBOS**). Ellipsoids shown at 50% probability, hydrogens omitted for clarity.

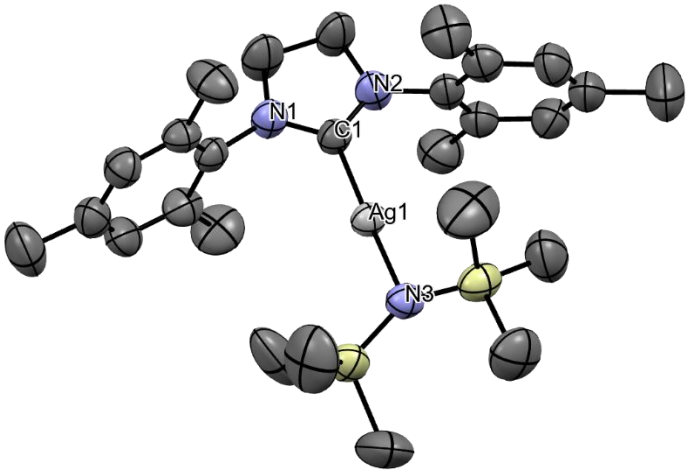

Figure S 70. Crystal structure for SIMesAgHMDS (**A-HMDS**). Ellipsoids shown at 50% probability, hydrogens omitted for clarity.

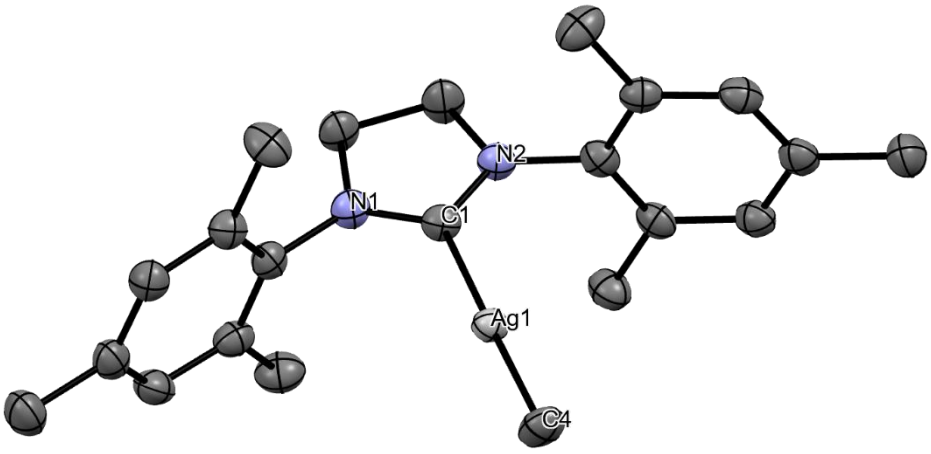

Figure S 71. Crystal structure for SIMesAgMe (**A-Me**). Ellipsoids shown at 50% probability, hydrogens omitted for clarity.

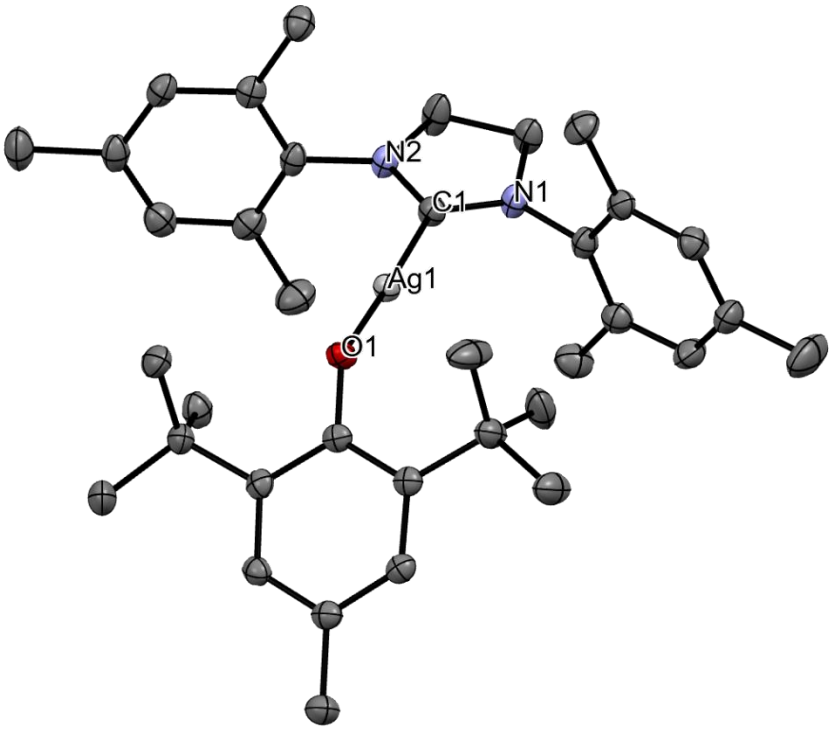

Figure S 72. Crystal structure for SIMesAgOAr (**A-BHT**). Ellipsoids shown at 50% probability, hydrogens omitted for clarity.

Table S 4. Important angles and distances in the synthesized compounds. IMesAgCl and SIMesAgCl structures are obtained from literature.[19, 20]

Compound	∡ X-Ag-C [°]	∡ N-C-N [°]	Δ NHC-Ag [Å]	Δ X-Ag [Å]
IMesAgCl (**B-Cl**)[19]	180	104.44	2.056	2.314
IMesAgMes (**B-Mes**)	178.02	104.03	2.087	2.097
IMesAgOTBOS (**B-TBOS**)	178.27	103.98	2.041	2.021
SIMesAgCl (**A-Cl**)[20]	173.69	108.51	2.083	2.336
SIMesAgMes (**A-Mes**)	176.76	107.98	2.107	2.096
SIMesAgOTBOS (**A-TBOS**)	178.86	108.34	2.051	2.025
SIMesAgHMDS (**A-HMDS**)	178.57	108.13	2.049	2.06
SIMesAgMe (**A-Me**)	179.48	108.24	2.087	2.088
SIMesAgOAr (**A-BHT**)	175.6	108.6	2.046	2.041

XRD Reports

The following pages contain detailed crystallographic information on the newly synthesized molecules.

IMesAgMes (B-Mes)

Table 1 Crystal data and structure refinement for IMesAgMes (B-Mes).

Identification code	IMesAgMes (B-Mes)
Empirical formula	$C_{33.5}H_{39}AgN_2$
Formula weight	577.53
Temperature/K	100.15
Crystal system	triclinic
Space group	P-1
a/Å	10.12120(10)
b/Å	11.2160(2)
c/Å	14.9017(2)
α/°	109.2690(10)
β/°	90.0610(10)
γ/°	109.0160(10)
Volume/Å^3	1498.50(4)
Z	2
ρ_{calc}g/cm^3	1.280
μ/mm^{-1}	5.550
F(000)	602.0
Crystal size/mm^3	0.3 × 0.25 × 0.15
Radiation	CuKα (λ = 1.54184)
2Θ range for data collection/°	6.33 to 159.254
Index ranges	-12 ≤ h ≤ 12, -13 ≤ k ≤ 14, -18 ≤ l ≤ 17
Reflections collected	40595
Independent reflections	5930 [R_{int} = 0.0385, R_{sigma} = 0.0184]
Data/restraints/parameters	5930/136/388
Goodness-of-fit on F^2	1.098
Final R indexes [I>=2σ (I)]	R_1 = 0.0259, wR_2 = 0.0715
Final R indexes [all data]	R_1 = 0.0260, wR_2 = 0.0716
Largest diff. peak/hole / e Å^{-3}	0.61/-0.63

IMesAgOTBOS (B-TBOS)

Table 1 Crystal data and structure refinement for IMesAgOTBOS (B-TBOS).

Identification code	IMesAgOTBOS (B-TBOS)
Empirical formula	$C_{33}H_{51}AgN_2O_4Si$
Formula weight	675.72
Temperature/K	100.00(10)
Crystal system	monoclinic
Space group	$P2_1/n$
a/Å	11.1581(2)
b/Å	16.6129(2)
c/Å	19.1762(3)
α/°	90
β/°	104.952(2)
γ/°	90
Volume/Å^3	3434.31(10)
Z	4
ρ_{calc}g/cm^3	1.307
μ/mm^{-1}	0.658
F(000)	1424.0
Crystal size/mm^3	0.2 × 0.2 × 0.2
Radiation	Mo Kα (λ = 0.71073)
2Θ range for data collection/°	3.292 to 59.15
Index ranges	-15 ≤ h ≤ 15, -23 ≤ k ≤ 23, -26 ≤ l ≤ 26
Reflections collected	143474
Independent reflections	9629 [R_{int} = 0.0757, R_{sigma} = 0.0337]
Data/restraints/parameters	9629/0/385
Goodness-of-fit on F^2	1.190
Final R indexes [I>=2σ (I)]	R_1 = 0.0380, wR_2 = 0.0857
Final R indexes [all data]	R_1 = 0.0485, wR_2 = 0.0900
Largest diff. peak/hole / e Å^{-3}	1.13/-1.80

SIMesAgMes (A-Mes)

Table 1 Crystal data and structure refinement for SIMesAgMes (A-Mes).

Identification code	SIMesAgMes (A-Mes)
Empirical formula	$C_{30}H_{37}AgN_2$
Formula weight	533.48
Temperature/K	100.1(3)
Crystal system	orthorhombic
Space group	Pbca
a/Å	15.7456(3)
b/Å	16.8545(4)
c/Å	19.8172(5)
α/°	90
β/°	90
γ/°	90
Volume/Å^3	5259.2(2)
Z	8
ρ_{calc}g/cm^3	1.348
μ/mm^{-1}	6.277
F(000)	2224.0
Crystal size/mm^3	0.1 × 0.1 × 0.05
Radiation	Cu Kα (λ = 1.54184)
2Θ range for data collection/°	8.888 to 160.404
Index ranges	-20 ≤ h ≤ 17, -21 ≤ k ≤ 21, -12 ≤ l ≤ 25
Reflections collected	27606
Independent reflections	5617 [R_{int} = 0.0273, R_{sigma} = 0.0206]
Data/restraints/parameters	5617/0/308
Goodness-of-fit on F^2	1.088
Final R indexes [I>=2σ (I)]	R_1 = 0.0372, wR_2 = 0.1024
Final R indexes [all data]	R_1 = 0.0384, wR_2 = 0.1035
Largest diff. peak/hole / e Å^{-3}	2.79/-0.71

SIMesAgOTBOS (A-TBOS)

Table 1 Crystal data and structure refinement for SIMesAgOTBOS (A-TBOS).

Identification code	SIMesAgOTBOS (A-TBOS)
Empirical formula	$C_{33}H_{53}AgN_2O_4Si$
Formula weight	677.73
Temperature/K	100.00(10)
Crystal system	monoclinic
Space group	$P2_1/n$
a/Å	11.1099(2)
b/Å	16.5691(2)
c/Å	19.2966(3)
α/°	90
β/°	104.487(2)
γ/°	90
Volume/Å^3	3439.20(10)
Z	4
ρ_{calc}g/cm^3	1.309
μ/mm^{-1}	5.319
F(000)	1432.0
Crystal size/mm^3	0.2 × 0.2 × 0.2
Radiation	Cu Kα (λ = 1.54184)
2Θ range for data collection/°	7.13 to 161.59
Index ranges	-14 ≤ h ≤ 13, -21 ≤ k ≤ 21, -24 ≤ l ≤ 24
Reflections collected	71442
Independent reflections	7488 [R_{int} = 0.0353, R_{sigma} = 0.0168]
Data/restraints/parameters	7488/0/386
Goodness-of-fit on F^2	1.129
Final R indexes [I>=2σ (I)]	R_1 = 0.0298, wR_2 = 0.0850
Final R indexes [all data]	R_1 = 0.0300, wR_2 = 0.0852
Largest diff. peak/hole / e Å^{-3}	0.88/-0.65

SIMesAgHMDS (A-HMDS)

Table 1 Crystal data and structure refinement for SIMesAgHMDS (A-HMDS).

Identification code	SIMesAgHMDS (A-HMDS)
Empirical formula	$C_{27}H_{44}AgN_3Si_2$
Formula weight	574.70
Temperature/K	100.00
Crystal system	orthorhombic
Space group	Fdd2
a/Å	20.852(4)
b/Å	44.031(12)
c/Å	13.785(4)
α/°	90
β/°	90
γ/°	90
Volume/Å^3	12656(6)
Z	16
ρ_{calc}g/cm^3	1.206
μ/mm^{-1}	0.730
F(000)	4832.0
Crystal size/mm^3	0.15 × 0.1 × 0.1
Radiation	MoKα (λ = 0.71073)
2Θ range for data collection/°	4.5 to 50.054
Index ranges	-24 ≤ h ≤ 24, -52 ≤ k ≤ 52, -16 ≤ l ≤ 16
Reflections collected	100378
Independent reflections	5586 [R_{int} = 0.0715, R_{sigma} = 0.0269]
Data/restraints/parameters	5586/1/310
Goodness-of-fit on F^2	1.096
Final R indexes [I>=2σ (I)]	R_1 = 0.0329, wR_2 = 0.0623
Final R indexes [all data]	R_1 = 0.0373, wR_2 = 0.0642
Largest diff. peak/hole / e Å^{-3}	0.23/-0.32
Flack parameter	0.009(11)

SIMesAgMe (A-Me)

Table 1 Crystal data and structure refinement for SIMesAgMe (A-Me).

Identification code	SIMesAgMe (A-Me)
Empirical formula	$C_{22}H_{29}AgN_2$
Formula weight	429.34
Temperature/K	100.00(10)
Crystal system	monoclinic
Space group	$P2_1/n$
a/Å	17.3928(6)
b/Å	14.3855(4)
c/Å	17.9551(6)
α/°	90
β/°	112.995(4)
γ/°	90
Volume/Å^3	4135.5(3)
Z	8
ρ_{calc}g/cm^3	1.379
μ/mm^{-1}	7.843
F(000)	1776.0
Crystal size/mm^3	0.2 × 0.15 × 0.1
Radiation	Cu Kα (λ = 1.54184)
2Θ range for data collection/°	6 to 156.1
Index ranges	-22 ≤ h ≤ 21, -18 ≤ k ≤ 16, -22 ≤ l ≤ 21
Reflections collected	64187
Independent reflections	8667 [R_{int} = 0.0356, R_{sigma} = 0.0170]
Data/restraints/parameters	8667/0/466
Goodness-of-fit on F^2	1.113
Final R indexes [I>=2σ (I)]	R_1 = 0.0320, wR_2 = 0.0877
Final R indexes [all data]	R_1 = 0.0330, wR_2 = 0.0884
Largest diff. peak/hole / e Å^{-3}	0.71/-1.12

SIMesAgOAr (A-BHT)

Table 1 Crystal data and structure refinement for SIMesAgOAr (A-BHT).

Identification code	SIMesAgOAr (A-BHT)
Empirical formula	$C_{36}H_{49}AgN_2O$
Formula weight	633.64
Temperature/K	100.01(10)
Crystal system	monoclinic
Space group	$P2_1/c$
a/Å	10.6810(2)
b/Å	13.7656(2)
c/Å	22.8895(4)
α/°	90
β/°	93.6160(10)
γ/°	90
Volume/Å^3	3358.75(10)
Z	4
ρ_{calc}g/cm^3	1.253
μ/mm^{-1}	5.016
F(000)	1336.0
Crystal size/mm^3	0.2 × 0.1 × 0.1
Radiation	Cu Kα (λ = 1.54184)
2Θ range for data collection/°	7.498 to 161.108
Index ranges	-13 ≤ h ≤ 13, -17 ≤ k ≤ 16, -29 ≤ l ≤ 29
Reflections collected	97033
Independent reflections	7368 [R_{int} = 0.0344, R_{sigma} = 0.0144]
Data/restraints/parameters	7368/0/375
Goodness-of-fit on F^2	1.147
Final R indexes [I>=2σ (I)]	R_1 = 0.0262, wR_2 = 0.0737
Final R indexes [all data]	R_1 = 0.0266, wR_2 = 0.0740
Largest diff. peak/hole / e Å^{-3}	0.50/-0.51

S6 Calculation of Gas Phase Acidities

Calculation Principles

The Calculation of Gas Phase Acidities was performed via very trivial energetic comparisons. The Gas Phase Acidity is defined as the ΔH of the following reaction:[31]

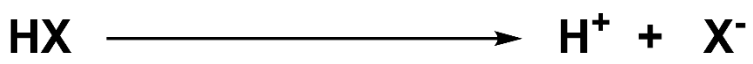

Figure S 73. Gas phase deprotonation reaction of general compounds (HX)

DFT calculations were performed on the ETH Euler cluster using Gaussian 09.[8] The determination of semi-accurate gas phase acidities was performed by calculating the energy difference between the single point energy of the X-anion and the HX-adduct (The proton single point energy was left out at this point, for it to be corrected later.). The structure optimization, as well as the calculation of single point energies of adducts and anions was performed using the B3LYP hybrid functional[32] and the DEF2TZVP basis set.[33, 34]

Table S 5. Calculated single point energies for all HX/X^- pairs including their energy differences. ΔH_{exp} represents literature values (obtained by calculating the energy difference of HX and $X^- + H^+$ from Thermodynamic data)[35], while ΔH_{corr} is obtained when energy correcting the calculated values. pK_a values were obtained from literature (where possible).[36, 37] Italic pK_a values represent values approximated from closely related structures.[37, 38]

HX	E(HX) [Hartree]	$E(X^-)$ [Hartree]	ΔE_{calc} [Hartree]	ΔH_{calc} [kcal/mol]	ΔH_{exp} [kcal/mol]	ΔH_{corr} [kcal/mol]	pK_a [H_2O]
ACE	-229.187	-228.627	0.5603352	351.61	346.39	344.32	-
PRP	-116.710	-116.084	0.6260449	392.84	382.08	380.53	-
BEN	-232.356	-231.697	0.6585308	413.22	399.32	398.44	43[37]
BHT	**-661.612**	**-661.057**	**0.555205**	**348.39**	**-**	**341.49**	***9.95*[37]**
DMA	-135.230	-134.580	0.649359	407.47	393.23	393.38	-
ETH	-155.109	-154.490	0.6192954	388.60	390.23	376.81	-
HCL	**-460.835**	**-460.288**	**0.5468005**	**343.11**	**332.26**	**336.86**	**-5.9[36]**
HMD	**-874.191**	**-873.601**	**0.5903624**	**370.45**	**355.88**	**360.87**	**26[37]**
MES	**-350.366**	**-349.709**	**0.6570067**	**412.27**	**-**	**397.60**	***43*[37]**
MET	**-40.539**	**-39.839**	**0.6996534**	**439.03**	**414.57**	**421.10**	**48[37]**
OTB	**-233.792**	**-233.176**	**0.6159256**	**386.49**	**374.51**	**374.96**	**17[37]**
PHE	-307.613	-307.043	0.570089	357.73	347.81	349.70	9.95[37]
TTS	**-1065.185**	**-1064.614**	**0.5713535**	**358.52**	**-**	**350.39**	***12*[38]**
TTB	-531.659	-531.067	0.5915185	371.17	-	361.51	-
HTB	-829.510	-828.946	0.5637125	353.72	-	346.18	-
TMS	-485.282	-484.692	0.5898517	370.13	359.86	360.59	-
TOL	-271.693	-271.067	0.6253804	392.42	381.34	380.17	-
MEO	-115.778	-115.152	0.6263565	393.66	381.32	381.26	-
HNO	-281.0179	-280.488	0.5303015	332.769	-	327.79	-

The correction of the calculated gas phase acidity data was performed by correlating experimentally known gas phase acidities with the calculated values. Experimental values were calculated as the result of the energy difference of the enthalpies of formation of the reaction partners (including ΔH_f of the proton) (See **Table S 5**). The resulting linear correlation between experimental and calculated values allows for the interpolation of calculated values onto the trend line, which results in energy corrected values (accounting for the exclusion of the single point energy of a proton and possible inaccuracies in DFT calculations).

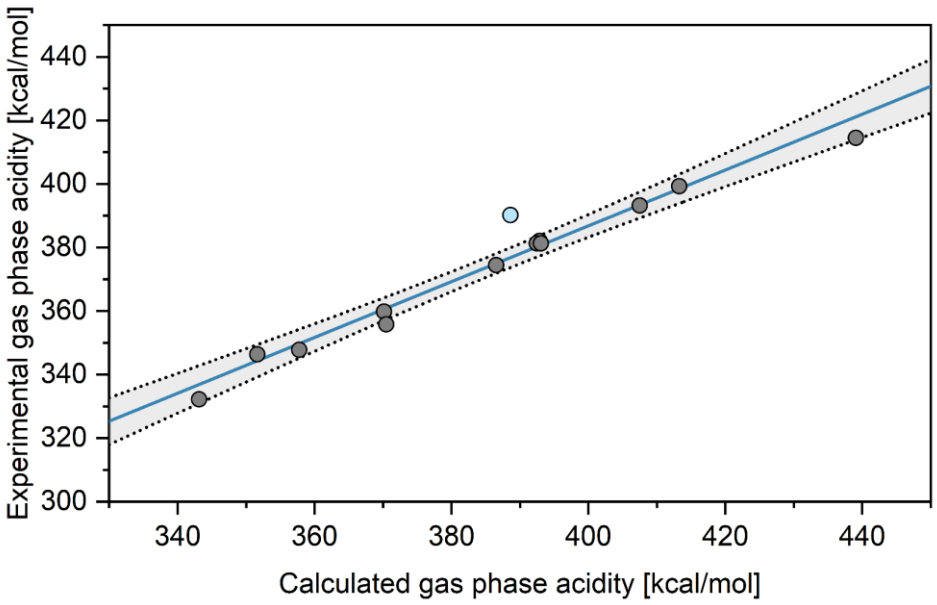

Figure S 74. Correlation of ΔH_{calc} and ΔH_{exp}. grey dots represent the data points with known experimental values (used for the linear regression). The blue spot represents ethanol, which is the only significant outlier. The linear correlation was then used to interpolate values for unknown gas phase acidities. (R^2=0.955)

Optimized Structures

Acetic Acid (ACE)

C	-1.36932	0.04992	-0.00000
C	0.13026	-0.14115	0.00000
H	-1.85653	-0.92053	0.00000
H	-1.68192	0.61109	-0.88358
H	-1.68192	0.61110	0.88358
O	0.68545	-1.19985	-0.00000
O	0.86103	1.00794	0.00000
H	0.28281	1.78099	-0.00000

Acetic Acid Anion

C	-1.34943	-0.04983	-0.00000
C	0.21289	0.00126	-0.00000
H	-1.72147	-1.07662	-0.00002
H	-1.73190	0.47709	-0.87964
H	-1.73189	0.47706	0.87967
O	0.80098	-1.10382	0.00000
O	0.69957	1.15555	0.00000

Propyne (PRP)

C	1.23601	-0.00000	-0.00000
C	-0.21808	0.00000	0.00000
H	1.62583	0.74279	-0.69890
H	1.62583	-0.97666	-0.29383
H	1.62583	0.23386	0.99272
C	-1.41759	0.00000	0.00000
H	-2.47951	-0.00002	-0.00001

Propyne Anion

C	1.12951	-0.00000	0.00000
C	-0.33491	0.00001	-0.00000
H	1.55581	-0.33927	0.95678
H	1.55581	0.99823	-0.18457
H	1.55581	-0.65896	-0.77220
C	-1.57250	-0.00000	0.00000

Benzene (BEN)

C	-0.00000	1.39049	-0.00000
C	-1.20419	0.69525	-0.00000
C	-1.20419	-0.69524	0.00000
C	0.00000	-1.39049	0.00000
C	1.20419	-0.69525	0.00000
C	1.20419	0.69524	-0.00000
H	2.14172	1.23652	-0.00000

H	0.00000	2.47305	-0.00000
H	-2.14172	1.23653	-0.00000
H	-2.14172	-1.23652	0.00000
H	-0.00000	-2.47305	0.00000
H	2.14172	-1.23653	0.00000

Benzene Anion

C	0.10211	-1.38787	0.00000
C	-1.13842	-0.74255	0.00000
C	-1.19924	0.64958	0.00000
C	0.00000	1.35918	0.00000
C	1.21824	0.67270	0.00000
C	1.35843	-0.73580	0.00000
H	0.07247	-2.48276	0.00000
H	-2.06327	-1.32113	0.00000
H	-2.15430	1.16689	0.00000
H	-0.02066	2.44991	0.00000
H	2.11910	1.29568	0.00000

Butylhydroxytoluene (BHT)

C	-1.24215	0.16353	-0.00000
C	-1.20186	1.55312	0.00001
C	-0.01094	2.27159	0.00001
C	1.17894	1.56179	0.00001
C	1.22278	0.16620	-0.00000
C	-0.00706	-0.51519	-0.00001
C	-2.58235	-0.59047	0.00000
C	-0.02370	3.77723	-0.00001
H	-0.53956	4.17153	0.87912
H	-0.53898	4.17150	-0.87950
H	0.98938	4.18034	0.00031
C	2.57524	-0.57284	0.00000
H	-2.12780	2.10875	0.00002

H	2.10112	2.12235	0.00002
O	-0.06781	-1.88816	-0.00002
H	0.81944	-2.25216	-0.00002
C	-3.77857	0.37281	0.00001
H	-3.79065	1.01044	0.88551
H	-4.70132	-0.20929	0.00001
H	-3.79065	1.01045	-0.88548
C	-2.70518	-1.46304	1.26516
H	-2.64703	-0.84184	2.16135
H	-1.92219	-2.21409	1.31664
H	-3.67191	-1.97203	1.27032
C	-2.70519	-1.46303	-1.26517
H	-2.64704	-0.84182	-2.16135
H	-3.67191	-1.97201	-1.27033
H	-1.92220	-2.21407	-1.31666
C	3.76186	0.40370	0.00001
H	3.76290	1.04074	-0.88487
H	4.69250	-0.16579	0.00001
H	3.76290	1.04073	0.88491
C	2.73228	-1.43273	-1.27431
H	2.68436	-0.79690	-2.15921
H	1.96834	-2.20056	-1.40083
H	3.70095	-1.93651	-1.26762
C	2.73227	-1.43274	1.27430
H	2.68434	-0.79692	2.15922
H	3.70094	-1.93653	1.26761
H	1.96833	-2.20057	1.40081

Butylhydroxytoluene Anion

C	-1.23217	0.16520	-0.00190
C	-1.18994	1.55248	0.01178
C	-0.00000	2.27818	0.01612

C	1.18994	1.55248	0.01178
C	1.23217	0.16520	-0.00191
C	0.00000	-0.59761	-0.01404
C	-2.56669	-0.59020	0.00260
C	-0.00000	3.78420	-0.02079
H	-0.88214	4.19585	0.47901
H	0.00004	4.18494	-1.04397
H	0.88208	4.19587	0.47908
C	2.56669	-0.59020	0.00259
H	-2.11701	2.11460	0.02144
H	2.11701	2.11460	0.02145
O	-0.00000	-1.87602	-0.02670
C	-3.78226	0.34620	0.01879
H	-3.79466	0.98033	0.90838
H	-4.69839	-0.25141	0.02092
H	-3.80768	0.99403	-0.86060
C	-2.65375	-1.48664	1.25405
H	-2.64096	-0.87221	2.15851
H	-1.80344	-2.16499	1.27574
H	-3.58418	-2.06629	1.24780
C	-2.67251	-1.46730	-1.26108
H	-2.67287	-0.83907	-2.15611
H	-3.60300	-2.04679	-1.24990
H	-1.82272	-2.14517	-1.30574
C	3.78226	0.34620	0.01879
H	3.80770	0.99402	-0.86061
H	4.69839	-0.25141	0.02096
H	3.79464	0.98036	0.90837
C	2.67252	-1.46731	-1.26107
H	2.67287	-0.83909	-2.15612
H	1.82275	-2.14519	-1.30573

H	3.60302	-2.04678	-1.24989
C	2.65375	-1.48663	1.25405
H	2.64094	-0.87220	2.15851
H	3.58418	-2.06627	1.24781
H	1.80344	-2.16498	1.27574

Dimethylamine (DMA)

N	-0.00000	0.56197	-0.14699
C	-1.21211	-0.22226	0.02005
H	-2.08568	0.42630	-0.05686
H	-1.26485	-0.76430	0.97905
H	-1.27712	-0.96414	-0.77971
C	1.21211	-0.22226	0.02005
H	0.00000	1.33766	0.50329
H	1.27714	-0.96412	-0.77974
H	1.26483	-0.76433	0.97904
H	2.08568	0.42631	-0.05682

Dimethylamine Anion

N	0.00000	0.65386	0.00000
C	-1.14467	-0.16362	-0.00000
H	-2.07042	0.43518	-0.00000
H	-1.23625	-0.87097	0.88605
H	-1.23625	-0.87097	-0.88605
C	1.14467	-0.16362	0.00000
H	1.23625	-0.87097	-0.88605
H	1.23625	-0.87097	0.88605
H	2.07042	0.43518	0.00000

Ethanol (ETH)

C	-1.21164	-0.24125	-0.02204
C	0.07943	0.55662	0.04714
H	-1.27319	-0.95924	0.80063
H	-1.27189	-0.79253	-0.96160

H	-2.07877	0.41966	0.04963
O	1.23976	-0.25593	-0.10665
H	0.12691	1.12245	0.98621
H	0.12462	1.27823	-0.76972
H	1.24749	-0.91339	0.59746

Ethanol Anion

C	-1.17861	-0.20329	0.00000
C	0.22366	0.48222	0.00000
H	-1.27020	-0.84409	0.88468
H	-1.27020	-0.84410	-0.88468
H	-2.00605	0.52651	-0.00000
O	1.23919	-0.36393	0.00000
H	0.18130	1.19977	0.88868
H	0.18130	1.19977	-0.88868

Hydrochloric Acid (HCL)

Cl	0.00000	0.00000	0.07122
H	0.00000	0.00000	-1.21082

Hydrochloric Acid Anion

Cl	0.00000	0.00000	0.00000

Hexamethyldisilazane (HMD)

N	-0.00000	0.00006	0.80360
Si	1.58090	0.00852	0.08670
Si	-1.58090	-0.00852	0.08670
H	-0.00000	0.00013	1.81407
C	2.08212	-1.70302	-0.50097
H	2.08361	-2.41443	0.32816
H	3.08294	-1.69672	-0.94058
H	1.38825	-2.07757	-1.25642
C	2.79457	0.59371	1.39198
H	2.78243	-0.06257	2.26614

H	2.55700	1.60564	1.72735
H	3.81543	0.60047	1.00304
C	1.60026	1.17185	-1.38622
H	0.88611	0.86576	-2.15378
H	2.58917	1.18921	-1.85084
H	1.34992	2.19102	-1.08519
C	-2.08213	1.70295	-0.50119
H	-1.38828	2.07740	-1.25671
H	-2.08360	2.41447	0.32785
H	-3.08296	1.69660	-0.94077
C	-2.79459	-0.59354	1.39204
H	-2.78243	0.06284	2.26613
H	-2.55705	-1.60544	1.72753
H	-3.81544	-0.60031	1.00309
C	-1.60023	-1.17202	-1.38608
H	-0.88601	-0.86604	-2.15363
H	-2.58911	-1.18939	-1.85077
H	-1.34995	-2.19116	-1.08491

Hexamethyldisilazane Anion

N	-0.00000	0.00001	0.54796
Si	1.57613	0.00000	0.09214
Si	-1.57613	0.00000	0.09215
C	2.11713	-1.50796	-0.95144
H	1.91596	-2.43559	-0.40764
H	3.18292	-1.48594	-1.20569
H	1.54731	-1.54730	-1.88475
C	2.76238	-0.00003	1.58450
H	2.58531	-0.88180	2.20724
H	2.58533	0.88172	2.20727
H	3.81575	-0.00004	1.28357
C	2.11716	1.50799	-0.95139

H	1.54733	1.54738	-1.88469
H	3.18295	1.48595	-1.20565
H	1.91602	2.43560	-0.40755
C	-2.11715	1.50797	-0.95142
H	-1.54732	1.54733	-1.88473
H	-1.91600	2.43559	-0.40761
H	-3.18294	1.48594	-1.20568
C	-2.76238	0.00001	1.58449
H	-2.58532	0.88177	2.20725
H	-2.58532	-0.88175	2.20726
H	-3.81575	0.00000	1.28357
C	-2.11714	-1.50798	-0.95141
H	-1.54731	-1.54735	-1.88471
H	-3.18293	-1.48596	-1.20567
H	-1.91598	-2.43560	-0.40758

Methanol (MEO)

C	-0.66538	-0.02018	0.00000
O	0.74817	0.12220	0.00000
H	-1.02839	-0.54433	0.89116
H	-1.02839	-0.54433	-0.89116
H	-1.08301	0.98566	0.00000
H	1.14670	-0.75350	0.00000

Methanol Anion

C	-0.53087	0.00001	0.00000
O	0.78956	0.00000	-0.00000
H	-1.04377	1.02201	-0.07962
H	-1.04372	-0.44208	0.92490
H	-1.04374	-0.57999	-0.84528

Mesitylene (MES)

C	0.99955	-0.98450	0.00000
C	-0.34893	-1.33989	0.00000

C	-1.35384	-0.37740	0.00000
C	-0.98728	0.96821	-0.00000
C	0.34870	1.35640	-0.00000
C	1.33105	0.36679	-0.00000
C	2.07694	-2.03600	0.00000
H	1.65125	-3.03937	-0.00000
H	2.71882	-1.94337	0.87928
H	2.71882	-1.94337	-0.87928
C	-2.80649	-0.77138	0.00000
H	-2.92306	-1.85507	0.00000
H	-3.32209	-0.37772	-0.87924
H	-3.32210	-0.37772	0.87923
C	0.73403	2.81160	-0.00000
H	-0.14599	3.45464	0.00000
H	1.33281	3.06108	-0.87922
H	1.33282	3.06108	0.87921
H	2.37654	0.65744	-0.00000
H	-0.61990	-2.38967	0.00000
H	-1.76028	1.72908	-0.00000

Mesitylene Anion

C	-1.21877	-0.68445	0.00000
C	-1.15338	0.71650	0.00000
C	0.07191	1.37751	0.00000
C	1.22357	0.59107	-0.00000
C	1.14027	-0.80609	-0.00000
C	-0.08090	-1.51426	-0.00000
C	-2.59034	-1.33511	0.00000
H	-3.40554	-0.60119	0.00000
H	-2.70740	-1.98077	0.87559
H	-2.70740	-1.98077	-0.87558

C	0.15431	2.88329	0.00000
H	-0.84478	3.32738	0.00000
H	0.68492	3.26611	-0.87953
H	0.68492	3.26611	0.87952
C	2.43386	-1.59983	-0.00000
H	3.32328	-0.95795	0.00000
H	2.47998	-2.25452	-0.87544
H	2.47997	-2.25453	0.87544
H	-2.06752	1.31232	0.00000
H	2.19639	1.08603	-0.00000

Methane (MET)

C	0.00000	-0.00000	0.00000
H	-0.71935	-0.36032	0.73423
H	0.61490	-0.83071	-0.34384
H	0.63568	0.75782	0.45608
H	-0.53123	0.43321	-0.84648

Methane Anion

C	0.00000	0.00000	0.00000
H	1.06549	-0.19588	0.00000
H	-0.36311	1.02068	0.00000
H	-0.70238	-0.82480	0.00000

Tert-Butanol (OTB)

O	-0.03370	-0.00003	1.45158
C	0.00599	-0.00000	0.01286
H	-0.95672	0.00002	1.72933
C	-0.68064	1.25881	-0.51748
H	-0.62871	1.30759	-1.60694
H	-0.20424	2.14934	-0.10611
H	-1.73635	1.27146	-0.23337
C	-0.68103	-1.25857	-0.51755
H	-1.73675	-1.27090	-0.23344

H	-0.20491	-2.14927	-0.10622
H	-0.62911	-1.30731	-1.60700
C	1.48782	-0.00022	-0.34026
H	1.97387	0.88367	0.07404
H	1.62609	-0.00020	-1.42232
H	1.97359	-0.88430	0.07397

Tert-Butanol Anion

O	0.00002	-0.00005	-1.48317
C	-0.00001	-0.00001	-0.15126
C	1.27229	-0.70414	0.43440
H	1.30275	-1.73124	0.05892
H	1.31430	-0.72723	1.53388
H	2.15874	-0.18461	0.05871
C	-1.24598	-0.74972	0.43438
H	-1.23929	-1.77721	0.05876
H	-2.15068	-0.26256	0.05881
H	-1.28703	-0.77447	1.53387
C	-0.02632	1.45391	0.43433
H	0.84798	1.99381	0.05886
H	-0.02736	1.50184	1.53382
H	-0.91944	1.96187	0.05860

Phenol (PHE)

C	-1.18299	-1.15959	0.00000
C	0.02222	-1.84988	0.00000
C	1.21624	-1.13494	0.00000
C	1.21263	0.25212	0.00000
C	0.00000	0.93616	0.00000
C	-1.19995	0.23011	0.00000
O	0.04693	2.30151	0.00000
H	-0.84955	2.65488	0.00000
H	-2.14308	0.76561	0.00000

H	-2.11998	-1.70160	0.00000
H	0.03234	-2.93135	0.00000
H	2.16185	-1.66189	0.00000
H	2.13413	0.81841	0.00000

Phenol Anion

C	1.19632	-1.09703	0.00000
C	0.00004	-1.82243	0.00000
C	-1.19629	-1.09707	0.00000
C	-1.20861	0.28599	0.00000
C	0.00000	1.07638	0.00000
C	1.20860	0.28605	0.00000
O	-0.00005	2.34043	0.00000
H	2.14861	0.82947	0.00000
H	2.14303	-1.63376	0.00000
H	0.00005	-2.90609	0.00000
H	-2.14297	-1.63386	0.00000
H	-2.14861	0.82942	0.00000

Tris-tert-Butoxysilanol (TTS)

Si	-0.05689	-0.02144	0.55330
O	0.74297	1.38107	0.74922
O	0.68385	-1.08629	-0.42320
O	-1.50185	0.31997	-0.10831
O	-0.16085	-0.69772	2.05114
H	-0.24961	-0.07841	2.78007
C	-2.70807	-0.45481	-0.24522
C	-2.38864	-1.93144	-0.47001
C	-3.43498	0.12637	-1.45348
H	-2.82527	0.01083	-2.35038
H	-3.62656	1.18929	-1.30177
H	-4.38838	-0.38001	-1.61265
C	-3.53178	-0.26817	1.02748

H	-2.99437	-0.66912	1.88738
H	-4.48961	-0.78541	0.94722
H	-3.72303	0.79203	1.19846
C	0.90905	2.51273	-0.12789
C	-0.30864	3.42156	0.02556
H	-1.21223	2.89571	-0.27979
H	-0.19799	4.31847	-0.58675
H	-0.41884	3.72592	1.06744
C	1.06156	2.05002	-1.57618
H	0.16465	1.53134	-1.91569
H	1.90923	1.37200	-1.67598
H	1.22759	2.90903	-2.22822
C	2.17601	3.21698	0.34583
H	2.07579	3.50689	1.39237
H	2.36490	4.11304	-0.24763
H	3.03558	2.55172	0.25520
C	1.85223	-1.90773	-0.23969
C	1.43475	-3.17574	0.50238
H	1.04791	-2.92717	1.49006
H	2.28518	-3.85030	0.61783
H	0.65474	-3.69553	-0.05544
C	2.92820	-1.15178	0.53832
H	3.82556	-1.76594	0.62933
H	2.58191	-0.90268	1.54157
H	3.19372	-0.22646	0.02691
C	2.34271	-2.23911	-1.64546
H	1.55599	-2.74282	-2.20802
H	3.21659	-2.89150	-1.60661
H	2.61307	-1.32590	-2.17711
H	-1.74824	-2.05675	-1.34212
H	-3.31192	-2.49156	-0.62716

H	-1.87709	-2.35603	0.39462

Tris-tert-Butoxysilanol Anion

Si	0.03514	-0.11008	-0.63801
O	-0.43444	1.48809	-0.79507
O	-1.00738	-0.75866	0.52292
O	1.45717	0.01709	0.25460
O	0.09762	-0.89432	-1.97477
C	2.51669	-0.92793	0.24146
C	1.98401	-2.34702	0.47110
C	3.45192	-0.52712	1.38382
H	2.91921	-0.57264	2.33588
H	3.80090	0.49692	1.23642
H	4.32057	-1.18925	1.43421
C	3.24634	-0.85343	-1.10440
H	2.53221	-1.06421	-1.90164
H	4.07375	-1.56885	-1.14396
H	3.64683	0.15232	-1.25259
C	-0.32911	2.59151	0.08189
C	1.07253	3.20195	-0.04682
H	1.81660	2.46547	0.25234
H	1.17460	4.09502	0.57725
H	1.25810	3.47664	-1.08712
C	-0.59786	2.20028	1.54031
H	0.13974	1.47510	1.88068
H	-1.58246	1.74244	1.63372
H	-0.55322	3.08417	2.18342
C	-1.38329	3.60109	-0.38283
H	-1.21242	3.85600	-1.43018
H	-1.35001	4.51645	0.21474
H	-2.37899	3.16181	-0.29847
C	-2.21142	-1.45070	0.23647

C	-1.88741	-2.83043	-0.34884
H	-1.30358	-2.69384	-1.25999
H	-2.80239	-3.38921	-0.56944
H	-1.29239	-3.40425	0.36560
C	-3.07774	-0.65743	-0.75036
H	-4.03179	-1.16452	-0.92246
H	-2.55169	-0.55539	-1.70010
H	-3.27634	0.34139	-0.35749
C	-2.94134	-1.59634	1.57366
H	-2.30546	-2.12642	2.28541
H	-3.87680	-2.15057	1.45663
H	-3.16643	-0.61096	1.98705
H	1.39890	-2.38147	1.39136
H	2.80883	-3.06179	0.54560
H	1.33811	-2.63342	-0.35882

Trifluoro-tert-Butanol (TTB)

C	0.76557	0.00399	-0.05075
C	1.31992	1.32781	0.45524
H	0.95507	2.15074	-0.15640
H	2.40672	1.30017	0.38869
H	1.03431	1.49828	1.49242
C	-0.77316	0.01540	0.03248
F	-1.20644	0.05861	1.30955
F	-1.29333	-1.10476	-0.52519
F	-1.31591	1.05992	-0.60980
C	1.31300	-1.18289	0.74031
H	1.06453	-1.10535	1.79815
H	2.39693	-1.19869	0.63359
H	0.91214	-2.12495	0.36323
O	1.12325	-0.08629	-1.42332
H	0.83360	-0.93964	-1.76792

Trifluoro-tert-Butanol Anion

C	0.81530	-0.00000	-0.19810
C	1.34752	1.26557	0.55478
H	0.96545	2.15779	0.05616
H	2.43418	1.25781	0.44789
H	1.09140	1.30684	1.62028
C	-0.73729	0.00000	0.00526
F	-1.15187	0.00002	1.32684
F	-1.34114	-1.08274	-0.54480
F	-1.34114	1.08272	-0.54483
C	1.34752	-1.26557	0.55478
H	1.09136	-1.30685	1.62028
H	2.43418	-1.25779	0.44794
H	0.96548	-2.15779	0.05615
O	1.11086	-0.00001	-1.48548

Hexafluoro-tert-Butanol (HTB)

C	-0.00410	0.60418	-0.11451
C	-1.29093	-0.24564	0.02139
F	-1.41163	-1.15549	-0.94665
F	-2.37215	0.54891	-0.02929
F	-1.31515	-0.88911	1.20271
C	1.27088	-0.27033	0.03467
F	1.44497	-0.71456	1.28816
F	2.34652	0.49332	-0.27353
F	1.28423	-1.32308	-0.78418
C	0.00495	1.71026	0.93842
H	-0.04715	1.30251	1.94587
H	-0.84742	2.36402	0.77004
H	0.92218	2.29196	0.84906
O	-0.04585	1.10742	-1.42767
H	0.66331	1.75150	-1.53840

Hexafluoro-tert-Butanol Anion

C	-0.00000	0.66031	-0.28748
C	-1.27462	-0.22224	0.01734
F	-1.38422	-1.29875	-0.78819
F	-2.40070	0.50789	-0.16995
F	-1.37289	-0.70885	1.29815
C	1.27462	-0.22224	0.01734
F	1.37290	-0.70884	1.29816
F	2.40070	0.50789	-0.16995
F	1.38422	-1.29875	-0.78819
C	-0.00000	1.81005	0.77402
H	0.00000	1.47307	1.81439
H	-0.88308	2.41966	0.58659
H	0.88308	2.41966	0.58659
O	-0.00000	1.06587	-1.52940

Trimethylsilanol (TMS)

Si	0.00669	-0.00000	0.03460
C	-0.91103	1.52871	-0.54366
H	-1.93305	1.55286	-0.15643
H	-0.97413	1.55885	-1.63448
H	-0.40608	2.43839	-0.21159
C	1.76369	-0.00007	-0.59181
H	2.30242	0.88266	-0.24143
H	1.79055	-0.00009	-1.68402
H	2.30241	-0.88278	-0.24137
C	-0.91111	-1.52870	-0.54358
H	-0.97421	-1.55887	-1.63440
H	-1.93313	-1.55281	-0.15634
H	-0.40620	-2.43839	-0.21148
O	0.14382	0.00005	1.69338
H	-0.66212	0.00009	2.21437

Trimethylsilanol Anion

Si	0.00000	-0.00003	0.22471
C	0.26124	1.71863	-0.59451
H	-0.52561	2.41220	-0.28042
H	0.25394	1.67178	-1.69012
H	1.21881	2.14690	-0.28072
C	1.35778	-1.08541	-0.59473
H	2.35183	-0.75061	-0.28073
H	1.32080	-1.05563	-1.69035
H	1.25005	-2.12884	-0.28096
C	-1.61890	-0.63299	-0.59487
H	-1.57465	-0.61579	-1.69046
H	-2.46864	-0.01792	-0.28105
H	-1.82614	-1.66125	-0.28091
O	-0.00014	-0.00022	1.78932

Toluene (TOL)

C	1.20517	-1.19277	0.00000
C	1.19780	0.19818	0.00000
C	0.00000	0.90991	0.00000
C	-1.19623	0.18953	0.00000
C	-1.19492	-1.19837	0.00000
C	0.00839	-1.89645	0.00000
H	2.14797	-1.72508	0.00000
H	2.13671	0.73903	0.00000
H	-2.13887	0.72475	0.00000
H	-2.13399	-1.73730	0.00000
C	-0.01330	2.41468	0.00000
H	0.99852	2.81973	0.00000
H	-0.53143	2.80467	0.87930
H	-0.53143	2.80467	-0.87930
H	0.01104	-2.97873	0.00000

Toluene Anion

C	-1.13512	-1.19507	-0.00000
C	0.24256	-1.20791	0.00002
C	1.03603	0.00001	0.00001
C	0.24256	1.20791	0.00002
C	-1.13512	1.19507	-0.00000
C	-1.87211	-0.00000	-0.00002
H	-1.66432	-2.14598	0.00001
H	0.76581	-2.16023	0.00005
H	0.76580	2.16024	0.00005
H	-1.66432	2.14598	0.00000
C	2.41955	-0.00000	-0.00003
H	2.98098	-0.92692	-0.00003
H	2.98099	0.92691	-0.00001
H	-2.95499	-0.00001	-0.00004

Nitric Acid (HNO)

N	-0.15178	0.03248	-0.00000
O	1.14660	-0.51983	0.00000
H	1.72068	0.26568	0.00000
O	-1.02308	-0.78000	0.00000
O	-0.20579	1.23819	0.00000

Nitric Acid Anion

N	0.00000	0.00000	-0.00000
O	0.82381	0.94859	-0.00000
O	-1.23340	0.23915	0.00000
O	0.40959	-1.18773	0.00000

S7 Chemical Shift Correlations

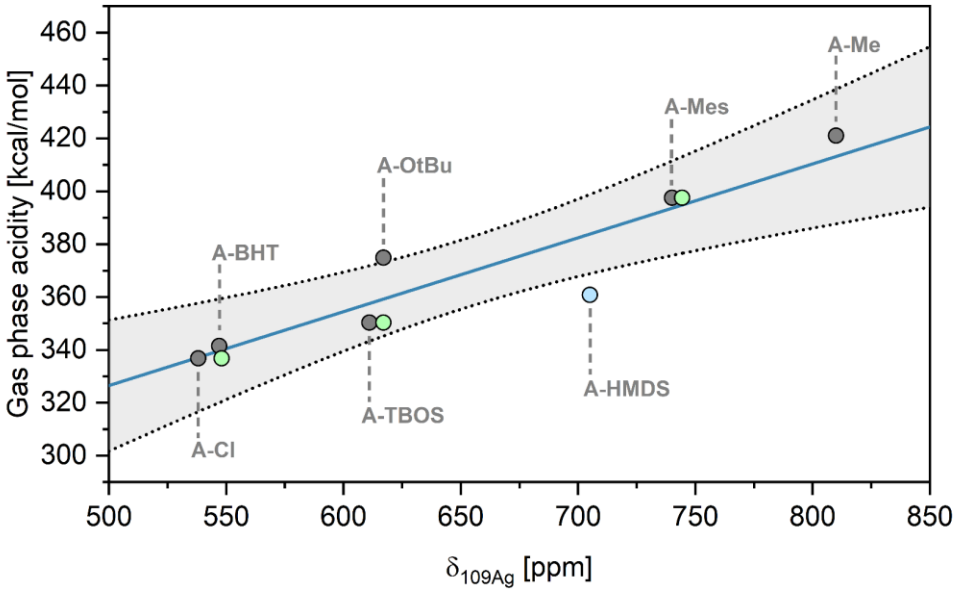

Figure S 75. Correlation of ΔH_{corr} to ^{109}Ag chemical shift. Grey dots represent the points that make up the correlation (saturated complexes SIMesAgX), while green dots show the unsaturated compounds (IMesAgX) for reference. A-HMDS is shown as a blue spot, which is the only significant oiutlier. (R^2=0.812)

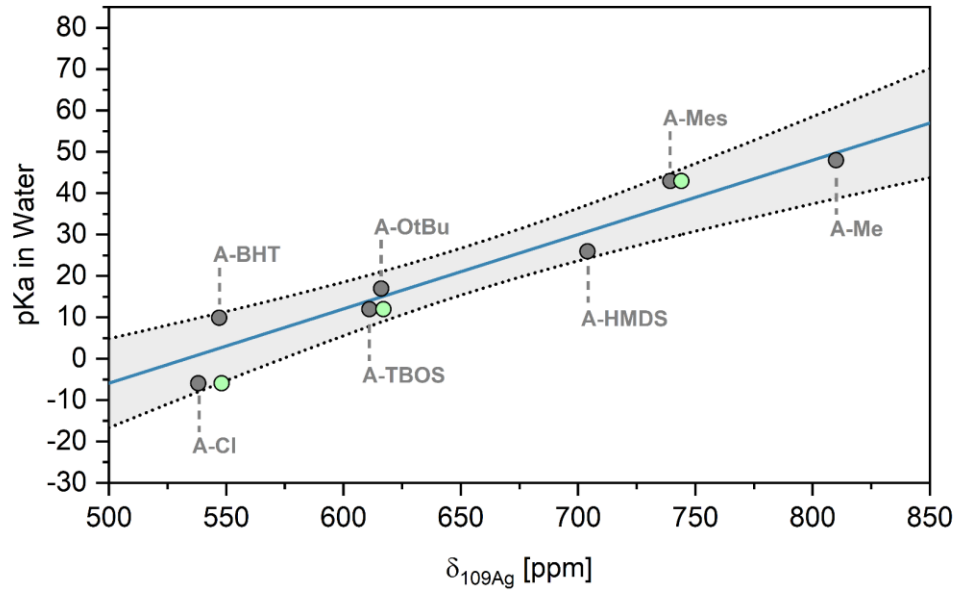

Figure S 76. Correlation of pKa (H_2O) to ^{109}Ag chemical shift. Grey dots represent the points that make up the correlation (saturated complexes SIMesAgX), while green dots show the unsaturated compounds (IMesAgX) for reference. (R^2=0.906)

References

1. J. Möbus, G. Kehr, C. G. Daniliuc, R. Fröhlich and G. Erker, *Dalton Trans.*, 2014, **43**, 632-638.
2. S. R. Docherty, N. Phongprueksathat, E. Lam, G. Noh, O. V. Safonova, A. Urakawa and C. Copéret, *JACS Au*, 2021, **1**, 450-458.
3. X. Bantreil and S. P. Nolan, *Nature Protocols*, 2011, **6**, 69-77.
4. G. R. Fulmer, A. J. M. Miller, N. H. Sherden, H. E. Gottlieb, A. Nudelman, B. M. Stoltz, J. E. Bercaw and K. I. Goldberg, *Organometallics*, 2010, **29**, 2176-2179.
5. O. V. Dolomanov, L. J. Bourhis, R. J. Gildea, J. A. K. Howard and H. Puschmann, *J. Appl. Crystallogr.*, 2009, **42**, 339-341.
6. G. Sheldrick, *Acta Crystallographica Section A*, 2015, **71**, 3-8.
7. G. Sheldrick, *Acta Crystallographica Section C*, 2015, **71**, 3-8.
8. G. W. T. M. J. Frisch, H. B. Schlegel, G. E. Scuseria, M. A. Robb, J. R. Cheeseman, G. Scalmani, V. Barone, G. A. Petersson, H. Nakatsuji, X. Li, M. Caricato, A. Marenich, J. Bloino, B. G. Janesko, R. Gomperts, B. Mennucci, H. P. Hratchian, J. V. Ortiz, A. F. Izmaylov, J. L. Sonnenberg, D. Williams-Young, F. Ding, F. Lipparini, F. Egidi, J. Goings, B. Peng, A. Petrone, T. Henderson, D. Ranasinghe, V. G. Zakrzewski, J. Gao, N. Rega, G. Zheng, W. Liang, M. Hada, M. Ehara, K. Toyota, R. Fukuda, J. Hasegawa, M. Ishida, T. Nakajima, Y. Honda, O. Kitao, H. Nakai, T. Vreven, K. Throssell, J. A. Montgomery, Jr., J. E. Peralta, F. Ogliaro, M. Bearpark, J. J. Heyd, E. Brothers, K. N. Kudin, V. N. Staroverov, T. Keith, R. Kobayashi, J. Normand, K. Raghavachari, A. Rendell, J. C. Burant, S. S. Iyengar, J. Tomasi, M. Cossi, J. M. Millam, M. Klene, C. Adamo, R. Cammi, J. W. Ochterski, R. L. Martin, K. Morokuma, O. Farkas, J. B. Foresman, and D. J. Fox, *Journal*, 2016, Gaussian 09.
9. S. Brunauer, P. H. Emmett and E. Teller, *J. Am. Chem. Soc.*, 1938, **60**, 309-319.
10. F. Héroguel, G. Siddiqi, M. D. Detwiler, D. Y. Zemlyanov, O. V. Safonova and C. Copéret, *J. Catal.*, 2015, **321**, 81-89.
11. A. G. M. Rankin, P. B. Webb, D. M. Dawson, J. Viger-Gravel, B. J. Walder, L. Emsley and S. E. Ashbrook, *J. Phys. Chem. C*, 2017, **121**, 22977-22984.
12. S. Büchele, A. Yakimov, S. M. Collins, A. Ruiz-Ferrando, Z. Chen, E. Willinger, D. M. Kepaptsoglou, Q. M. Ramasse, C. R. Müller, O. V. Safonova, N. López, C. Copéret, J. Pérez-Ramírez and S. Mitchell, *Small*, 2022, **18**, 2202080.
13. I. B. Moroz, K. Larmier, W.-C. Liao and C. Copéret, *J. Phys. Chem. C*, 2018, **122**, 10871-10882.
14. I. B. Moroz, A. Lund, M. Kaushik, L. Severy, D. Gajan, A. Fedorov, A. Lesage and C. Copéret, *ACS Catal.*, 2019, **9**, 7476-7485.
15. M. Kaushik, C. Leroy, Z. Chen, D. Gajan, E. Willinger, C. R. Müller, F. Fayon, D. Massiot, A. Fedorov, C. Copéret, A. Lesage and P. Florian, *Chem. Mater.*, 2021, **33**, 3335-3348.
16. G. H. Penner and W. Li, *Solid State Nucl. Magn. Reson.*, 2003, **23**, 168-173.
17. M. Paas, B. Wibbeling, R. Fröhlich and F. E. Hahn, *Eur. J. Inorg. Chem.*, 2006, **2006**, 158-162.
18. C. A. Citadelle, E. L. Nouy, F. Bisaro, A. M. Z. Slawin and C. S. J. Cazin, *Dalton Trans.*, 2010, **39**, 4489-4491.
19. T. Ramnial, C. D. Abernethy, M. D. Spicer, I. D. McKenzie, I. D. Gay and J. A. C. Clyburne, *Inorg. Chem.*, 2003, **42**, 1391-1393.
20. P. de Frémont, N. M. Scott, E. D. Stevens, T. Ramnial, O. C. Lightbody, C. L. B. Macdonald, J. A. C. Clyburne, C. D. Abernethy and S. P. Nolan, *Organometallics*, 2005, **24**, 6301-6309.
21. B. K. Tate, A. J. Jordan, J. Bacsa and J. P. Sadighi, *Organometallics*, 2017, **36**, 964-974.
22. C. Copéret, A. Comas-Vives, M. P. Conley, D. P. Estes, A. Fedorov, V. Mougel, H. Nagae, F. Núñez-Zarur and P. A. Zhizhko, *Chem. Rev.*, 2016, **116**, 323-421.
23. J. Meyet, A. Ashuiev, G. Noh, M. A. Newton, D. Klose, K. Searles, A. P. van Bavel, A. D. Horton, G. Jeschke, J. A. van Bokhoven and C. Copéret, *Angew. Chem. Int. Ed.*, 2021, **60**, 16200-16207.
24. S. Greiser, G. J. G. Gluth, P. Sturm and C. Jäger, *RSC Advances*, 2018, **8**, 40164-40171.

25. A. Dessombz, G. Coulibaly, B. Kirakoya, R. W. Ouedraogo, A. Lengani, S. Rouziere, R. Weil, L. Picaut, C. Bonhomme, F. Babonneau, D. Bazin and M. Daudon, *Comptes Rendus Chimie*, 2016, **19**, 1573-1579.
26. W. Jiang, L. Lumata, W. Chen, S. Zhang, Z. Kovacs, A. D. Sherry and C. Khemtong, *Scientific Reports*, 2015, **5**, 9104.
27. W. R. Gunther, V. K. Michaelis, R. G. Griffin and Y. Román-Leshkov, *J. Phys. Chem. C*, 2016, **120**, 28533-28544.
28. A. J. Arduengo, R. Krafczyk, R. Schmutzler, H. A. Craig, J. R. Goerlich, W. J. Marshall and M. Unverzagt, *Tetrahedron*, 1999, **55**, 14523-14534.
29. O. Back, M. Henry-Ellinger, C. D. Martin, D. Martin and G. Bertrand, *Angew. Chem. Int. Ed.*, 2013, **52**, 2939-2943.
30. N. Kaeffer, D. Mance and C. Copéret, *Angew. Chem. Int. Ed.*, 2020, **59**, 19999-20007.
31. I. A. Topol, G. J. Tawa, R. A. Caldwell, M. A. Eissenstat and S. K. Burt, *J. Phys. Chem. A*, 2000, **104**, 9619-9624.
32. P. J. Stephens, F. J. Devlin, C. F. Chabalowski and M. J. Frisch, *The Journal of Physical Chemistry*, 1994, **98**, 11623-11627.
33. F. Weigend, *Physical Chemistry Chemical Physics*, 2006, **8**, 1057-1065.
34. F. Weigend and R. Ahlrichs, *Physical Chemistry Chemical Physics*, 2005, **7**, 3297-3305.
35. B. Ruscic, Bross, D. H., Active Thermodynamical Tables (ATcT) values based on ver. 1.122r of the Thermochemical Network, https://atct.anl.gov).
36. A. Trummal, L. Lipping, I. Kaljurand, I. A. Koppel and I. Leito, *J. Phys. Chem. A*, 2016, **120**, 3663-3669.
37. F. G. Bordwell, *Acc. Chem. Res.*, 1988, **21**, 456-463.
38. D. J. Belton, O. Deschaume and C. C. Perry, *FEBS J.*, 2012, **279**, 1710-1720.